UNIVERSITÉ DU QUÉBEC À TROIS-RIVIÈRES

DISTRIBUTION DES NUCLÉOÏDES ET RÔLE DE LA FISSION MITOCHONDRIALE DANS SA RÉGULATION

ROLE OF MITOCHONDRIAL FISSION IN THE REGULATION OF NUCLEOID DISTRIBUTION

THÉSE PRÉSENTÉE
COMME EXIGENCE PARTIELLE DU
DOCTORAT EN BIOLOGIE CELLULAIRE ET MOLÉCULAIRE

PAR
HEMA SARANYA ILAMATHI

MAI 2022

UNIVERSITÉ DU QUÉBEC À TROIS-RIVIÈRES

DOCTORAT EN BIOLOGIE CELLULAIRE ET MOLÉCULAIRE (PH. D.)

Direction de recherche :

Marc Germain	Directeur de recherche

Jury d'évaluation de la thèse :

Marc Germain	Directeur de recherche
Patrick Narbonne	Président de jury
Geneviève Pépin	Évaluateur interne
Mireille Khacho	Évaluatrice externe

Thèse soutenue le 11 juillet 2022

I dedicate my thesis to my mother, father,
family, and friends

ACKNOWLEDGEMENTS

I would like to express my sincere gratitude to Professor Marc Germain for his enormous support in my PhD work. His excellence in mentorship really helped me to sharpen my abilities and explore new skills. He not only appreciated my strengths but helped me to work on my weak points. His positive nature and strong guidance gave me the confidence to handle different hurdles in my PhD work. I really appreciate all his time and efforts throughout my PhD. I feel fortunate to have been trained under him in my early research career. “Thank you sincerely from the bottom of my heart, Marc, for your profound belief in my abilities and for giving me this most memorable opportunity in my life! You are my inspiration for an ideal mentor!”

I would like to thank all our collaborators Dr Matthew A. Lines, Dr Timothy E. Shutt, and other authors of our papers, for their valuable contributions in my PhD work. Especially, I would like to thank Mathieu Ouellet for his collaborative work to develop an automated computational tool. Also, I would like to thank my summer intern, Justine Desrochers-Goyette, for all her contributions in my PhD research work.

I would like to express my sincere gratitude to my friends and colleagues Dr. Kiran Todkar, Priya Gatti, Sara Benhammouda and Anjali Vishwakarma for all their collaborative research works and scientific contributions we worked together. Along with them, I would like to thank Pamela, Gerald, Julie, Lilia, Lydia Amari and Joseph for making these five years most memorable with a lot of science and fun activities. Also, my sincere thanks to other labs in UQTR for sharing research equipment and resources.

I’m extremely thankful to the Queen Elizabeth II Scholarship (QES) and Fond de recherche – nature et technologies (FRQNT) scholarship programs. Their financial assistance helped me to focus better on science.

I would like to thank my friends Marion, Melanie for their sincere support and encouragements. I especially appreciate their strong motivation and assistance in presenting my work in French during MT180 (2022). In addition to them, I would like to express my gratitude to Karima and Cassandra (from SAE, UQTR) for their relentless support for MT180.

I cannot begin to express my thanks to my family (Father, Shalini, Sundar chithappa, Gana akka, Abi, Anna, Maggie) for all their patience, support, motivation, and care. My special thanks to my mother for her unconditional love and persistent motivation to live a meaningful life. I dedicate my PhD thesis to my beloved mother.

Finally, and most importantly, I would like to thank all my friends for their unparalleled support. My special thanks to my friends in Trois-Rivieres for all those fun-filled moments and for making me feel at home here. I'm extremely grateful to Amita and Priya for their unconditional support, love, and care at home. Also, I would like to thank Jennifer for her valuable advice and care.

My sincere thanks to all my well-wishers!

RÉSUMÉ

Les mitochondries sont des organites à multiples facettes importantes pour le maintien de l'homéostasie cellulaire. Les mitochondries fusionnent dynamiquement et se séparent par un processus appelé dynamique mitochondriale. La fusion et la fission des mitochondries réorganise le réseau mitochondrial en fonction des besoins énergétiques cellulaires. Les mitochondries ont leur propre génome qui code pour des gènes nécessaires à la production d'énergie. Le génome mitochondrial est emballé dans des complexes ADN-protéine appelés nucléoïdes. Cependant, la fonction mitochondriale, y compris la maintenance de l'ADNmt, est régulée par des gènes codés au niveau nucléaire. Des défauts dans ces gènes de maintenance de l'ADNmt entraînent des maladies mitochondriales incurables. Particulièrement, la dynamique mitochondriale, en plus de son rôle dans la régulation du réseau de mitochondries, est essentielle pour la maintenance de l'ADNmt. Par exemple, un défaut de fusion affecte à la fois le nombre de copies et l'intégrité de l'ADNmt, alors qu'un défaut de fission provoque un élargissement des nucléoïdes et une diminution du nombre de nucléoïdes, bien que le mécanisme sous-jacent soit mal compris. De plus, on ne sait pas si ces altérations affectent la distribution des nucléoïdes dans les réseaux mitochondriaux. Dans mon travail de thèse, nous abordons le rôle de la fission dans la distribution des nucléoïdes.

À ce jour, il n'existe pas d'outil automatisé pour mesurer la distribution des nucléoïdes dans les réseaux mitochondriaux. Ainsi, dans un premier temps, nous avons développé un outil automatisé, Mitomate tracker, qui mesure la distribution probable des nucléoïdes au sein des réseaux mitochondriaux. À l'aide de cet outil, nous avons déterminé que les nucléoïdes ne sont pas distribués de manière aléatoire au sein des réseaux mitochondriaux et qu'ils maintiennent une certaine distance par rapport aux nucléoïdes voisins. Un défaut dans les protéines de fission MYH14 ou DRP1 affecte la distribution des nucléoïdes au sein des réseaux mitochondriaux. Cette altération de la distribution est principalement associée à des modifications des caractéristiques des nucléoïdes et de la structure du réseau mitochondrial.

La perte de protéines de fission est connue pour affecter la structure du réseau mitochondrial. Cependant, le mécanisme par lequel la fission régule les caractéristiques des nucléoïdes n'est pas défini. Des études antérieures ont démontré que la réplication de l'ADNmt se produit au niveau des sites de contact entre les tubules du réticulum endoplasmique (RE) et les mitochondries. Un défaut dans DRP1 provoque un élargissement des nucléoïdes dans la région périnucléaire, région qui est généralement caractérisés par des feuillets de RE. Ici, nous avons démontré que les feuilles de RE interagissent avec les mitochondries aux sites de fission. Une bonne régulation de l'interaction entre les feuilles de RE et les mitochondries est essentielle pour la réplication de l'ADNmt et la distribution des nucléoïdes. L'altération de la structure des feuilles de RE a entraîné une interaction accrue avec les mitochondries, notamment aux sites de nucléoïdes élargis chez les mutants DRP1. La modulation des feuilles de RE dans le mutant DRP1 a permis la redistribution appropriée des nucléoïdes. Nos travaux ont donc

permis de caractériser la distribution des nucléoïdes dans les réseaux mitochondriaux et d'identifier le rôle des feuillets de RE dans la distribution des nucléoïdes. Ainsi, notre travail fournit une compréhension approfondie du processus de maintenance de l'ADNmt et de la distribution des nucléoïdes, dont l'échec pourrait contribuer au développement de maladies mitochondriales incurables.

Mots-clés : Fission, ADNmt, nucléoïdes, DRP1, feuillets RE, mitochondries.

ABSTRACT

Mitochondria are multi-faceted organelles important for maintaining cellular homeostasis. Mitochondria dynamically fuse or divide by a process called mitochondrial dynamics. Mitochondrial fusion and fission reorganize mitochondrial networks depending on cellular energy demands. Mitochondria have their own genome that encodes essential genes necessary for energy production. This genome is packed into DNA-protein complexes called nucleoids. However, mitochondrial function including mtDNA maintenance is regulated by nuclear-encoded genes. Defects in mtDNA maintenance gene result in incurable mitochondrial diseases. Especially, mitochondrial dynamics in addition to role in network regulation, is essential for mtDNA maintenance. For instance, fusion defects affect both mtDNA copy number and integrity while loss or defect in fission causes nucleoid enlargement and a decline in nucleoids number, although the mechanism behind this is poorly understood. Further, whether these alterations affect nucleoid distribution within mitochondrial networks is unknown. In my PhD work, we addressed the role of fission in nucleoid distribution.

Till date, there are no automated tools to measure nucleoid distribution within mitochondrial networks. So, initially, we developed an automated tool, Mitomate tracker, that measures the probable distribution of nucleoids within mitochondrial networks. Using this tool, we identified that nucleoids are not randomly distributed within networks, maintaining a certain distance from their neighboring nucleoids. Defect in fission proteins (MYH14, DRP1) affect the nucleoid distribution pattern within mitochondrial networks. This alteration in distribution is mainly associated with changes in nucleoid features and mitochondrial network structure in fission mutants.

Loss of fission proteins is known to affect mitochondrial network structure. However, the mechanism of fission-mediated regulation of nucleoid features is undefined. Previous studies demonstrated that mtDNA replication occurs at endoplasmic reticulum (ER) tubule-mitochondria contact sites followed by DRP1 mediated fission of newly divided daughter mitochondria. Defects in DRP1 cause nucleoid enlargement in the perinuclear region, which are typically characterized by ER sheets. Here we demonstrated that ER sheets interact with mitochondria at fission sites. Proper regulation of ER sheets-mitochondria interaction is critical for mtDNA replication and nucleoid distribution. Alteration in ER sheet structure resulted in increased interaction with mitochondria, notably at the sites of enlarged nucleoid in DRP1 mutants. Modulating ER sheets in DRP1 mutant rescued enlarged nucleoids, which are basically clusters of mtDNA, by properly redistributing them. Altogether our work identified the nucleoid distribution pattern within mitochondrial network and the role of ER sheets-mitochondrial contact in nucleoid distribution in fission mutants. Thus, our work provides in-depth understanding on the process of mtDNA maintenance and nucleoid distribution, failure of which could contribute to the development of incurable mitochondrial diseases.

Mots-clés : Fission, mtDNA, nucleoids, DRP1, ER sheets, mitochondria.

TABLE OF CONTENTS

LIST OF FIGURES AND TABLE

Figure **Page**

Table

LIST OF ABBREVIATIONS AND ACRONYMS

AMFR	Autocrine Motility Factor Receptor
ANOVA	Analysis of Variance
Arf1	ADP-Ribosylation Factor-1
ATAD3	ATPase Family AAA-Domain-Containing Protein
ATL	Atlastin
ATP	Adenosine Triphosphate
ATP5a	ATP Synthase Alpha Subunit 1
BSE	Bundle Signaling Element
CAMK1	Calcium/Calmodulin-Dependent Proteinase Kinase-1
CC	Coiled Coil
CDK1	Cyclin-Dependent Kinase 1
CLIMP63	Cytoskeleton-Linking Membrane Protein Of 63kda
CNX	Calnexin
Ctrl	Control
Cyb5	Cytochrome B5
DIC	Differential Interference Contrast
DMEM	Dulbecco's Modified Eagle's Medium
DNA	Deoxyribonucleic Acid
Dnm	Dynamin
DP1	Deleted in Polyposis 1
DRP1	Dynamin Related Protein 1
EdU	5-Ethynyl-2′-Deoxyuridine
ELC	Essential Light Chain

ER	Endoplasmic Reticulum
ERK 1/2	Extracellular-Signal-Regulated Kinase 1/2
ERMCS	ER Tubules-Mitochondria Contact Sites
ETC	Electron Transport Chain
FBS	Fetal Bovine Serum
FIS1	Mitochondrial Fission 1 Protein
GAP	GTPase-Accelerating Proteins
GED	GTPase Effector Domain
GFP	Green Fluorescent Protein
GSK 3β	Glycogen Synthase Kinase 3β
HC	Heavy Chain
HFs	Human Fibroblasts
HR	Heptad Repeat
IMM	Inner Mitochondrial Membrane
IMS	Intermembrane Space
INF2	Inverted Formin-2
IP_3R	Inositol 1,4,5-Trisphosphate Receptor
IRP	Independent Random Process
KD	Knockdown
KIF5B	Kinesin 5B
KO	Knockout
LHON	Leber's Hereditary Optic Neuropathy
Lnp	Lunapark
LONP1	Lon Peptidase1
mCh	mCherry

MCU	Mitochondrial Ca^{2+} Uniporter
MD	Middle Domain
MDT	Mitochondrial Dynamic Tubulation
MEFs	Mouse Embryonic Fibroblasts
MELAS	Mitochondrial Encephalomyopathy, Lactic Acidosis, Stroke-Like Episodes
MERF	Myoclonus Epilepsy and Ragged Red Fibers
MFF	Mitochondrial Fission Factor
MFNs	Mitofusins
MICOS	Mitochondrial Contact Site and Cristae Organizing System
MiD	Mitochondrial Dynamics Protein
MMP	Mitochondrial Membrane Potential
mtDNA	Mitochondrial DNA
mTORC2	Mammalian Target of Rapamycin Complex 2
MTS	Mitochondrial Targeting Sequence
mtSSB	Mitochondrial Single-Stranded DNA-Binding
Myo	Myosin
NAD+	Nicotinamide Adenine Dinucleotide (+)
nDNA	Nuclear DNA
NMII	Non-Muscle Myosin Protein II
nndist	Nearest Neighbor Distance
NTD	Nucleotidyl Transferase Domain
OMM	Outer Mitochondrial Membrane
OPA1	Optic Atrophy Protein 1
OXPHOS	Oxidative Phosphorylation
PC	Phosphotidylcholine

pcf	Pair Correlation Function
PE	Phosphotidylethanolamine
PI4KIIIβ	Phosphatidylinositol 4-Kinase IIIβ
PK	Protein Kinase
PLA	Proximity Ligation Assay
POLRMT	Mitochondrial RNA Polymerase
POLγ	DNA Polymerase γ
PR	Proline-Rich Domain
PS	Phosphatidylserine
RLC	Regulatory Light Chain
RNA	Ribonucleic Acid
ROS	Reactive Oxygen Species
RR	Repeat Region
RRBP1	Ribosome Binding Protein 1
rRNA	Ribosomal RNA
RT	Room Temperature
RTN	Reticulon
SD	Standard Deviation
SENP5	Sentrin/ SUMO Specific Protease 5
siRNA	Small Interfering RNA
SYNJ2BP	Synaptojanin-2-Binding Protein
TAC	Tip Attachment Complex
TEM	Transmission Electron Microscope
TFAM	Transcription Factor A
TGN	Trans-Golgi Network

TM domain	Transmembrane Domain
TMRM	Tetramethylrhodamine, Methyl Ester
TOM20	Translocase of Outer Membrane 20
TOP3A	Topoisomerase 3 Alpha
tRNA	Transfer RNA
VDAC	Voltage Dependent Anion-Selective Channel

CHAPTER I

INTRODUCTION

Over 1.5 billion years ago, it is believed that proto-eukaryotic cells engulfed aerobic bacteria that eventually developed a symbiotic relationship with the host cell. Finally, they transformed into an integral organelle of the cell called mitochondria (1). During this evolutionary transformation, a vast majority of the bacterial genome was transferred to nuclear DNA (nDNA). However, mitochondria still retained a fraction of its genome called mitochondrial DNA (mtDNA) which is essential for its proper function (2).

Mitochondria are commonly known for their role in energy production. Beyond its popular tagline of being "the powerhouse of the cell", mitochondria are a metabolic hub that generate precursors necessary for the biosynthesis of macromolecules such as glucose, amino acids, fatty acids, and nucleotides (3, 4). In addition, mitochondria control redox balance, clearance of metabolic waste products such as ammonia and hydrogen sulfide (4). At times of stress, mitochondria act as a signaling hub and activate nuclear gene expression through signaling molecules (reactive oxygen species (ROS), calcium, ATP, and NAD^+ flux) (4-6). Due to their multifaceted role, mitochondria influence cell fate through controlling cellular differentiation and apoptosis (cell death) pathways (7-9).

1.1 Structure and function of mitochondria

Mitochondria are double-membraned organelles with four functionally distinct compartments, namely, the outer mitochondrial membrane (OMM), the intermembrane space (IMS), the inner mitochondrial membrane (IMM) and the matrix. The OMM is characterized by proteins involved in different functions such as import of mitochondrial proteins and metabolites, mitochondrial shaping, and transport proteins. The IMM is a highly impermeable structure that contain specific proteins necessary for the transport of

ions, metabolites, and proteins into the mitochondrial matrix. The IMM contains invaginations called cristae that constitute a hub for electron transport chain (ETC) proteins and are the principal site of energy production (ATP) through oxidative phosphorylation (OXPHOS). The IMS is an intermediate aqueous zone between the OMM and the IMM that is enriched with the H^+ ions necessary to regulate mitochondrial respiration and energy production. In addition, the IMS has different antioxidant systems to detoxify some of the ROS molecules generated during mitochondrial respiration. Finally, the mitochondrial matrix is a large aqueous compartment of mitochondria and a hub for metabolic enzymes necessary for the synthesis of biomolecules (glucose, amino acids, fatty acids, nucleic acids). The mitochondrial genome (mtDNA) is present within the mitochondrial matrix (Figure 1.1) (10, 11).

Mitochondria are primarily known for their role in energy production. By utilizing the nutrients that are absorbed from the food, mitochondria generate energy in the form of ATP to support the cellular functions. Nutrients are initially metabolized through mitochondrial citric acid cycle that generates electron-rich reducing equivalents (NADH, $FADH_2$). Intermediates for citric acid cycle are supplied by glucose, amino acids, and fatty acids. ETC protein complexes (I to IV) oxidize NADH, $FADH_2$ to release electrons and pump H^+ ions into the IMS. Finally, the F_0F_1 ATP synthase (complex V) pumps back electrons into the matrix to generate the force necessary for ATP synthesis. Besides, mitochondria are metabolic hubs of the cell. They generate intermediates necessary for the biosynthesis of glucose, amino acids, fatty acids, cholesterol, iron and heme (4). In addition, mitochondria act as a signaling organelle during cell stress and release their content (e.g mtDNA) to activate the expression of innate immune response genes. These signaling molecules are called mitochondrial damage associated molecular patterns.

1.2 mtDNA-nucleoids organization

mtDNA varies in shape (circular, linear) and size (16 kbp in mammals – 150 kbp in fungi) across different species. Mammalian cells have a circular mtDNA encoding

37 genes, including 13 ETC protein subunits, 2 ribosomal RNA (rRNA), and 22 transfer RNA (tRNA). Unlike nuclear DNA, mitochondrial DNA is present in ~100-1000 copies per cell. mtDNA is compactly packed into nucleo-protein complexes called nucleoids to protect the genome from any oxidative damage (12).

Each nucleoid contains a number of mtDNA copies packed by multi-layer protein complexes that are involved in mtDNA replication, transcription, and translation. Generally, in mammalian cells each nucleoid has on an average 1-2 mtDNA molecules compactly packed by transcription factor A (TFAM) (13, 14). More than 1000 TFAM proteins bind around mtDNA and form the nucleoid core (13) (Figure 1.1). High level of TFAM is bound to mtDNA to protect it from damage. On the other hand, actively replicating mtDNA has less TFAM protein (15) (Figure 1.1). In addition to TFAM, other proteins are associated with mtDNA, and they are classified as core and peripheral region proteins based on their association with mtDNA. Besides TFAM, proteins regulating mtDNA replication and transcription are present in the core region closely associated with mtDNA. The peripheral region of a nucleoid includes proteins involved in RNA processing and translation. In addition, there are several proteins of unknown function in the peripheral region of a nucleoid.

1.2.1 mtDNA replication and gene expression

Unlike nDNA, mtDNA lacks introns (non-coding region) except for a small segment (~1kb) called the D-loop. This non-coding region docks mtDNA to the IMM along with other proteins such as the ATPase family AAA-domain-containing protein (ATAD3), mitochondrial single-stranded DNA-binding protein (mtSSB), mitochondrial AAA protease Lon peptidase1 (LONP1) and TFAM (16). In addition, the D-loop regulates mtDNA replication and transcription. mtDNA replication is mediated by mtDNA polymerase γ (POLγ) with the help of two other proteins, the mitochondrial helicase TWINKLE and mtSSB, which are present at the replication fork (17, 18). mtDNA has two replication origins, the heavy strand (OriH) and the light strand (OriL) (Figure 1.1). Different models of mtDNA replication have been proposed so far (19-22). The most

widely accepted model is the strand displacement model (23, 24), in which POLγ is recruited on OriH and primers for DNA synthesis are generated by mitochondrial RNA polymerase (POLRMT). The leading strand is synthesized using the parental L-strand as a template. TWINKLE unwinds double-stranded mtDNA along the replication fork and mtSSB binds to ssDNA to protect it from nuclease activity. Once the replication fork reaches OriL, a stem-loop structure is formed to facilitate primer synthesis by POLRMT. The lagging strand is then synthesized using the parental H-strand as a template. Finally, newly synthesized mtDNA is separated by human type IA topoisomerase 3α (TOP3A) (25).

mtDNA transcription follows mtDNA replication (26). mtDNA transcripts are synthesized by POLRMT with the help of transcription initiation factors TFAM and TFB2M. As mtDNA lacks introns, polycistronic mRNA is generated at the end of transcription, which is further processed by the endoribonucleases RNaseP and ElaC Ribonuclease Z 2. Newly synthesized transcripts are further modified in RNA granules (27, 28). Finally, mtDNA transcripts are translated into proteins by mitochondrial ribosomes and are directly embedded in the IMM (29).

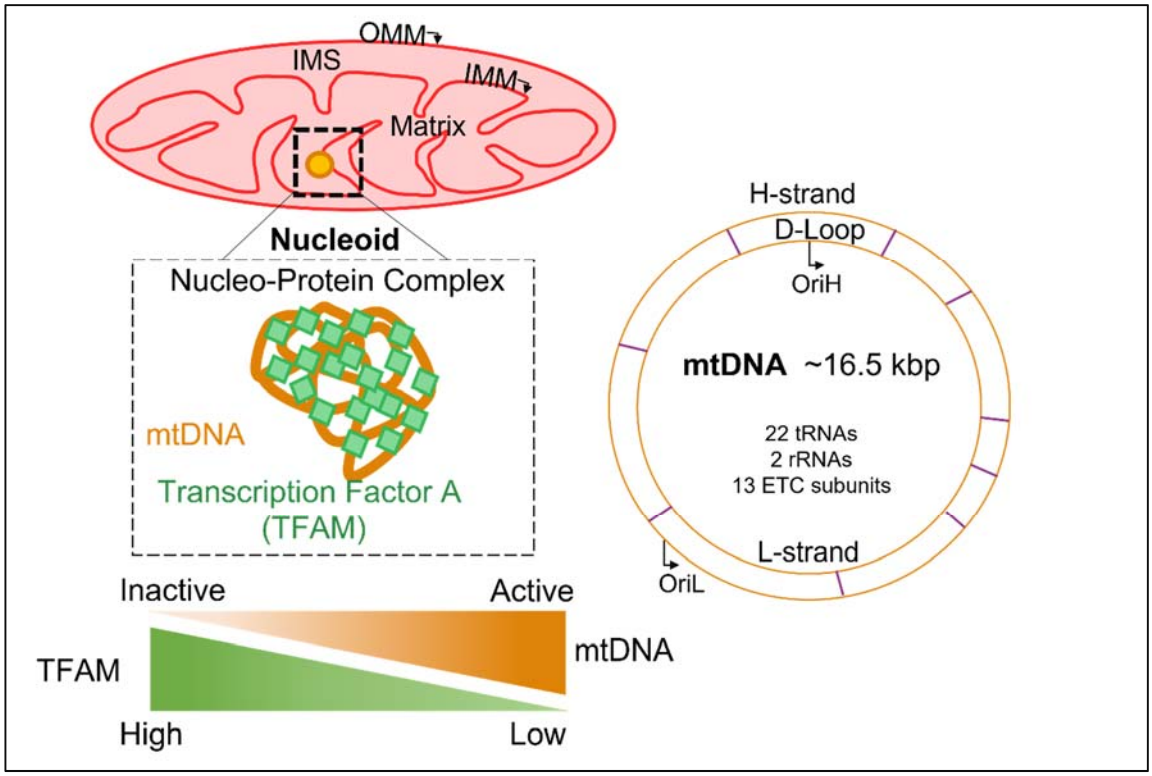

Figure 1.1 Mitochondria and mtDNA organization.
Mitochondria are double-membrane organelles with four different compartments (OMM, IMS, IMM, matrix). Mitochondria have their own genome (mtDNA) that is compactly packed into a nucleo-protein complex called nucleoid. TFAM is mainly involved in mtDNA packaging. mtDNA bound TFAM load decides the active status of mtDNA by modulating its replication and gene expression.

1.2.2 Nucleoid distribution

Nucleoids maintain a certain distance from each other within mitochondrial networks, although their global distribution pattern is poorly understood. A limited number of studies have attempted to understand inter-nucleoid distances, either manually or using tailored program code. A study in yeast cells suggested that nucleoids maintain a distance of approximately 800 nm from their neighboring nucleoids (30). On the other hand, in mammalian cells, nucleoids are proposed to be separated at equidistance from each other (10, 31). However, the overall distribution pattern of nucleoids within a complex mitochondrial network structures is yet to be addressed. Further, the process regulating nucleoid distribution is poorly understood. Studies have reported that nucleoids

move within mitochondrial networks, which could influence nucleoid distribution. This trafficking is suggested to be regulated by direct/indirect association of nucleoids with the cytoskeletal network (10, 32, 33).

Nucleoids in the mitochondrial matrix are linked to microtubules in the cytoplasm through adaptor proteins on mitochondrial membranes (10). Microtubules carry mitochondria toward plus-end/anterograde or minus-end/retrograde direction with the help of the microtubule motor proteins kinesin-1 and dyneins, respectively. Microtubules are especially important for proper nucleoid distribution within peripheral mitochondrial networks. The microtubule motor protein kinesin 5B (KIF5B) indirectly connects with nucleoids through Miro1 (OMM) and the mitochondrial contact site and cristae organizing system (MICOS, in the IMM). KIF5B binds to the mitochondrial membrane and pulls mitochondria in the anterograde direction. This process is called mitochondrial dynamic tubulation (MDT). During this process, KIF5B actively transports nucleoids (33). Thus, microtubules are essential for active transport of nucleoids containing mitochondria to the peripheral regions of the cell.

In addition to microtubules, actin filaments are proposed to be involved in nucleoid transport. There is a mitochondrial fraction of β-actin and its motor protein, non-muscle myosin protein II A (NMIIA) associated with mtDNA. Defects in these proteins affect mtDNA maintenance (34). In fact, actin is proposed to distribute mtDNA through MDT formation independent of mitochondrial fission and fusion machinery in yeast (30). Further, mitochondrial actin could be necessary to provide structural support for mtDNA and transport them within mitochondrial networks. Altogether, these studies suggest that cytoskeletal networks (microtubules, actin) are involved in nucleoid trafficking and distribution within the mitochondrial network.

1.3 Mitochondrial Dynamics

Mitochondria are social organelles that dynamically connect with each other and form a complex network within the cell (Figure 1.2). Mitochondrial dynamics is essential

for proper mitochondrial maintenance and to regulate mitochondrial metabolism. For example, the mitochondrial network is modified as an adaption to cellular differentiation. During stem cell differentiation, mitochondria adapt an interconnected network structure to switch to OXPHOS metabolism, though there are a few exceptions (35-37). Mitochondrial dynamics are also essential for proper mitochondrial distribution across the cell. For example, proper mitochondrial dynamics are important to facilitate the transport of mitochondria from the soma to axonal terminals in neuronal cells or to the leading edge of invading cells such as lymphocytes (38, 39). Furthermore, mitochondrial dynamics are important for mitochondrial quality control, a mechanism by which damaged mitochondria are eliminated (40).

In addition to mitochondrial dynamics, mitochondrial network structure is modulated by the cytoskeleton and interorganelle contact sites. Altogether, these factors influence the shape and distribution of the mitochondrial network within the cell.

1.3.1 Fission and fusion shape mitochondrial network

Mitochondrial dynamics involving mitochondrial membrane fusion and fission regularly changes network structure depending on cellular metabolic demands. This dynamic process is regulated by GTPase proteins. Most proteins involved in mitochondrial dynamics are conserved across eukaryotic species. however, mammalian systems have evolved a more sophisticated system (Table 1.1). These variations could be essential to modulate the mitochondrial network structure in different cell types.

Table 1.1 Fission and fusion proteins in higher eukaryotes.

	Mammals	Yeast	*Caenorhabditis elegans*	*Drosophila melanogaster*
Fusion protein	MFN 1/2	Fzo1p	FZO-1	FZO / Marf
	?	Ugo1		
	OPA1	Mgm1p	EAT-3	OPA1
Fission protein	DRP1	Dnm1	DRP-1	Drp1
	FIS1	Fis	FIS-1/2	Fis
	?	Mdv1	?	?
	MFF	?	?	Dme1
	MID49	?	?	?
	MID51	?	?	?

Mitochondrial fusion is regulated by Mitofusins (MFN 1/2) and Optic atrophy protein (OPA1) in the OMM and the IMM, respectively. On the other hand, fission is regulated by the cytosolic GTPase Dynamin related protein 1 (DRP1), which is recruited onto the OMM by the fission receptors: mitochondrial fission factor (MFF), mitochondrial fission 1 protein (FIS1), and mitochondrial dynamics protein of 49 and 51 kDa (MiD49/51). Mitochondrial dynamics regularly alter the mitochondrial network and cristae structure to adapt to cellular metabolic needs. Generally, mitochondrial dynamics alters the length of mitochondrial tubules, resulting in short/ fragmented, long/tubular, and intermediate mitochondrial phenotypes (Figure 1.2). In addition to changes in length, our lab has demonstrated that mitochondria also alter their connectivity/ branching depending on metabolic cues (41).

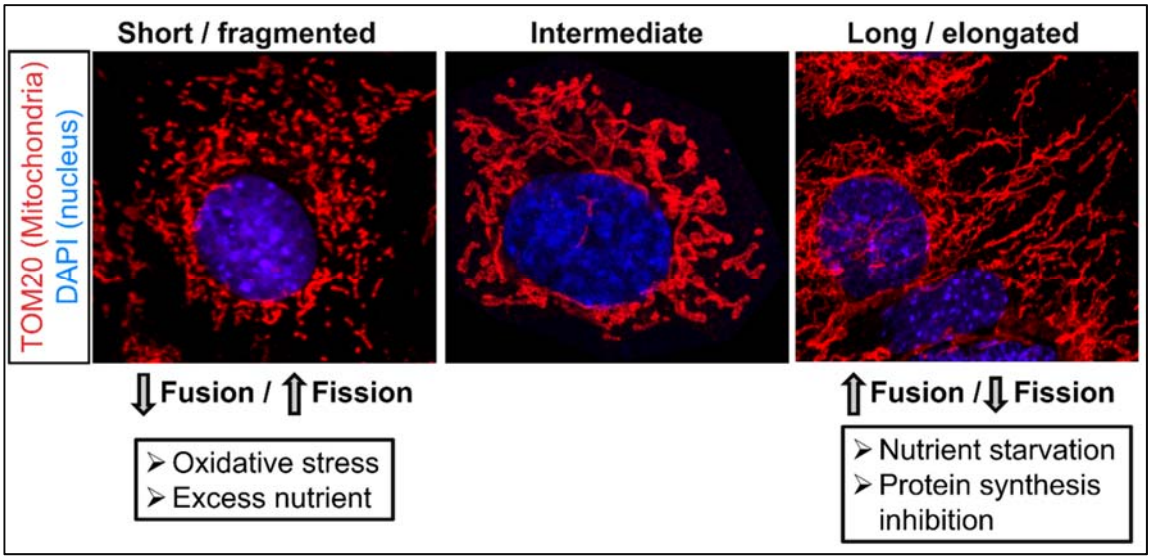

Figure 1.2 Mitochondrial form and function.
Mitochondrial networks are modified by mitochondrial fission and fusion, resulting in different network shapes. Mitochondria adopt a distinct network structure depending on the stress condition (mentioned in the box).

Mitochondrial fission and fusion are essential for proper mitochondrial function. Under physiological conditions, mitochondrial networks are modulated by the balance between fission and fusion. However, an excess or depletion of mitochondrial fission and fusion impairs the shape of the mitochondrial network. For example, excess of mitochondrial fission or loss of mitochondrial fusion results in short, fragmented mitochondria (42, 43). Similarly, an excess of fusion or loss of fission results in a highly fused mitochondrial network (44-46) (Figure 1.2). It is speculated that mitochondrial networks are modified to meet cellular metabolic demands. For instance, to meet cellular energy demands during starvation, mitochondria adapt an elongated network structure (44, 45). Some studies have shown that mitochondria hyperfuse in response to acute stress inducing agents (e.g., actinomycin D, cycloheximide treatment, oxidized glutathione), a phenomenon called stress induced hyperfusion (47-49). On the other hand, excessive stress (e.g., ROS, fatty acid) activates mitochondrial fragmentation (50, 51) (Figure 1.2). This compromises the integrity of mitochondrial structure, resulting in the release of proteins involved in the activation of apoptosis (cytochrome c, Smac/Diablo) (52, 53). However, lower mitochondrial bioenergetics cannot be directly correlated to fragmented networks in all scenarios. Overall, mitochondrial network structure is modulated

depending on the balance between fission and fusion proteins. Hence, mitochondrial network is proposed to be undisturbed when fission and fusion proteins are simultaneously depleted in the cell. However, genetic ablation of fission (DRP1) and fusion (MFN 1/2) protein in adult mouse heart resulted in premature senescence of cardiomyocytes. This suggest that mitochondrial dynamics is highly essential for proper functioning of the cell. Further studies are necessary to identify the link between mitochondrial form and function.

1.3.2 The Cytoskeleton transports mitochondria and shapes mitochondrial networks

Mitochondrial network shape is also influenced by the cellular cytoskeletal network. These transport cables run across the cell and help in the transportation of mitochondria to meet local energy demands. Cellular cytoskeletal systems include microtubules, actin /microfilaments, and intermediate filaments. These cytoskeletal networks are also essential for the docking of mitochondria at the cellular periphery. For instance, cytoskeletal networks transport and anchor mitochondria onto the neuronal dendrites for synapse formation. Generally, different cues such as ATP/ADP ratio and calcium levels activate and determine the direction of mitochondrial movement (54-57).

Microtubules are the major trafficking cables for mitochondrial transportation. Microtubule adaptor proteins Miro and TRAK, connect mitochondria to motor proteins (kinesin, dyneins). Each of these adaptors exists in two different isoforms: Miro1 and Miro2, TRAK1 and TRAK2. The mitochondrial transmembrane protein Miro1 interacts with the TRAK2 protein, and they preferentially transport mitochondria in a retrograde direction (58, 59). On the other hand, TRAK1 can bidirectionally transport mitochondria (59). Some studies suggest that TRAK can regulate mitochondrial movement independently of Miro proteins (58). Besides long-distance transportation, microtubules are involved in docking mitochondria to meet the local needs in different cellular regions. For example, the anchoring protein syntaphilin docks mitochondria on microtubules to repair sites of elevated Ca^{2+} level (60, 61). Microtubules are important for proper

distribution and organization of peripheral mitochondrial networks through mitochondrial dynamic tubulation (33) and are thus essential for long distance transport and organization of mitochondrial networks.

Actin filaments and their motor proteins, myosins, are involved in anchorage and short-range transport of mitochondria. The actin filaments (F-actin) are a polymer of globular-actin (G-actin) assembled by actin nucleators and crosslinkers (62). Actin branching protein Arp2/3-mediated assembly of F-actin assembly is involved in mitochondrial transport to the newly emerging yeast bud (63, 64). In mammalian cells, actin-based motor myosin 19 (Myo19) regulates mitochondrial transport along F-actin cables through its interaction with Miro2 on OMM (65, 66). In addition, Myo19 docks mitochondria in the peripheral regions of the cell to meet the local energy demands (67). Actin filaments play an important role in the distribution of mitochondria within the cell. In neuronal cells, actin filaments regulate axonal mitochondrial transport and anchor mitochondria at presynaptic nerve terminals. Depletion of the actin motor proteins Myo V and Myo VI prevents the anchoring of mitochondria and enhances their movement along microtubules (68). Actin also plays an important role in mitochondrial fission. Regulatory factors in actin assembly such as cortactin, cofilin, Septin 2, and Arp2/3 (branching complex) are important for DRP1 mediated mitochondrial fission (69-71).

Mitochondrial organization is also influenced by intermediate filaments (IF), especially in muscle and neuronal cells (72-76). Thus, in general, cytoskeletal networks play an important role in the positioning, transport, and organization of mitochondrial based on the local needs of the cell.

1.3.3 Interorganelle contact regulates the mitochondrial network

Cellular organelles dynamically interact with each other to maintain cellular homeostasis. Pioneer studies first identified endoplasmic reticulum (ER)-mitochondria interactions by electron microscopy (77). Over the past few decades, studies have revealed that mitochondria also interact with other organelles (78, 79). This physical association

between the organelles is implicated in the regulation of different biological processes, including mitochondrial dynamics (79). Among the inter-organelle contacts studied so far, ER-mitochondria interactions and their functional importance are well explored. In particular, mitochondrial fission and fusion sites have been found to be associated with the ER (80). Though the functional role of the ER in fission has been well studied, its role in fusion is poorly understood. In addition to ER, lysosomes and the Golgi complex are linked to mitochondrial fission (81-83). A detailed description of the mechanism of interoganelle contact mediated mitochondrial dynamics has been explained later (section 1.5.2,1.7).

1.4 Roles of mitochondrial dynamics

Mitochondrial networks are dynamically modulated to adapt to cellular metabolic demands. In addition to regulating mitochondrial network morphology and controlling mitochondria distribution across the cell, mitochondrial dynamics are essential for regulating mitochondrial maintenance. Furthermore, it helps in the proper maintenance of mitochondria through facilitating the homogenous distribution of mitochondrial proteins and mtDNA within mitochondrial networks and eliminating damaged regions of mitochondria from the network. The benefits of mitochondrial dynamics in mitochondrial maintenance and distribution will be discussed in detail in the following sections.

1.4.1 Dynamics in mitochondrial distribution

Mitochondrial fission and fusion are essential for the distribution of mitochondria across the cell. In polarized cells such as neuronal cells, mitochondria are transported across the soma to the nerve terminals to facilitate the formation of synapses. However, this mitochondrial transport process along the cytoskeleton is regulated by mitochondrial dynamics. Loss of mitochondrial fission results in elongated mitochondria in the soma of the neuronal cells. This prevents the transport of mitochondria to the nerve terminals (38). On the other hand, a fragmented mitochondrial network due to loss of fusion proteins impairs mitochondrial transport. Studies have shown that the mitochondrial fusion

proteins, MFNs interacts with the mitochondrial microtubule adaptor complex Miro2. Hence, depletion of MFNs affects axonal mitochondrial transport in neuronal cells (84).

1.4.2 Mitochondrial dynamics in mitochondrial content exchange

Modulation of mitochondrial networks by mitochondrial fission and fusion also results in the elimination of damaged mitochondrial segments. For instance, mitochondrial membrane potential (MMP) is essential for maintaining a healthy mitochondrial population. However, defective mitochondria will have less MMP. If the damage level is minimal, mitochondria undergo transient fusion with healthy mitochondria to regain their function (85). On the other hand, an irreversibly damaged mitochondrion is excluded from mitochondrial networks by fission and is instead sent to lysosomes for degradation.

Most mitochondrial proteins are nuclear encoded and hence need to be transported into the mitochondria and distributed uniformly. Mitochondrial fusion facilitates the equal distribution of proteins along mitochondrial networks. However, in certain cases, cells have an excess accumulation of proteins within certain regions of mitochondrial networks even though they are hyperfused, as with fission defects (52, 86). Altogether, this suggests that a balanced level of fission and fusion is essential to maintain a healthy mitochondrial population within the cell.

1.4.3 Mitochondrial dynamics in mtDNA maintenance

Mitochondrial function depends on proper mtDNA maintenance. This includes maintenance of mtDNA copy number and integrity and also proper distribution of nucleoids along mitochondrial networks. mtDNA maintenance genes are nuclear encoded. Especially, mitochondrial dynamics and cristae organization influence mtDNA maintenance.

Conditional knockout of mitochondrial outer membrane fusion proteins MFN1 and MFN2 interrupts mtDNA replication, causing severe loss of mtDNA content (87) and

affecting mtDNA integrity in skeletal muscles (88, 89). Loss of MFNs also causes nucleoid clustering in the enlarged fragmented mitochondria (89). On the other hand, mutation, or knockdown of the inner mitochondrial membrane fusion protein OPA1 affects both mtDNA integrity and content. However, unlike MFNs, nucleoids are not clustered in OPA1 conditional knockout mice (89).

Fission regulates mitochondrial division and hence, defect or loss of the mitochondrial fission proteins DRP1 and MFF results in a hyperfused network. In addition, fission is essential during mitochondrial biogenesis to segregate daughter mitochondria (Figure 1.4). Defects in the mitochondrial fission proteins DRP1 and MFF cause enlargement of nucleoids without necessarily affecting mtDNA content (90, 91). These enlarged nucleoids are entrapped in a bulb-like mitochondrial structure called the mitobulb (86, 91). This results in a decrease in nucleoid numbers and the enrichment of mitochondrial proteins in the mitobulb region (86, 90). This evidence suggests that mitochondrial fission could be involved in nucleoid segregation and distribution, which otherwise causes mosaic functioning of the organelle, although the mechanism behind this is unclear. Overall, mitochondrial dynamics play an important role in mtDNA maintenance.

1.4.4 Dynamics in mitochondrial quality control

Mitochondrial dynamics play an important role in some mitochondrial quality control processes. Irreversibly impaired mitochondria need to be eliminated to protect the rest of the network from damage. These impaired mitochondria are eliminated by a process called mitophagy where fission helps in eliminating damaged mitochondria with the help of mitophagy proteins, PINK and parkin. However, to avoid re-fusion of defective mitochondria with the rest of the network, parkin ubiquitinates OMM proteins, including MFNs and Miro resulting in their degradation (92-95). Further, at the IMM level, OPA1 is inactivated due to depolarization of damaged mitochondria, thereby preventing IMM fusion (96, 97).

1.5 Mechanisms of mitochondrial dynamics

1.5.1 Mitochondrial Fusion

Mitochondrial fusion involves merging of two opposing mitochondria at the OMM and IMM. This results in increased mitochondrial tubules length. Two mitochondria can fuse together at their ends and cause mitochondrial elongation. Alternatively, the mitochondrial end can fuse laterally with another mitochondrial tubules, resulting in the formation of mitochondrial branches. An increase in mitochondrial fusion significantly alters mitochondrial network shape. However, certain fusion events are transient events that involve the transfer of ions (H^+) to regain mitochondrial membrane potential (85). Since these kiss-and-run events are transient, they are less likely to affect mitochondrial network structure (85). Complete mitochondrial fusion requires the fusion of both the OMM and the IMM, which are thought to occur independently.

1.5.2 Mitochondrial outer membrane fusion

OMM fusion is regulated by the transmembrane GTPase proteins MFN1 and MFN2. During fusion, MFNs on the opposed mitochondrial membranes tether together to form homo- or heterodimers (98). Different models of MFN mediated OMM fusion have been proposed based on structural studies. MFN has been proposed to have two transmembrane (TM) domains inserted into the OMM with the heptad repeat (HR1 and HR2) domains facing the cytosol along with the GTPase domain. In this model, dimerization of HR2 domains on opposing mitochondria brings them close to each other (99). Finally, GTP hydrolysis causes conformational changes in MFNs, thereby resulting in the merging of the OMM (99, 100) (Figure 1.3). In vitro studies suggest that mitochondrial membrane tethering, and lipid mixing are regulated by the GTPase dependent activity of HR1(101). However, the process of trans-dimerization of HR2 was challenged by a recent model proposing reactive oxygen species-based dimerization.

This model proposes that the human MFNs have instead a single transmembrane domain with the HR2 domain facing the IMS side whereas the GTPase and HR1 domains

face the cytoplasm. Contrary to the trans-dimerization model, an oxidative environment in the IMS would promote dimerization of HR2 through disulfide bond formation. In that context, mitochondria would be tethered by the GTPase dependent HR1 domain, resulting in membrane fusion (102). However, further research is essential to understand the mechanism of MFNs mediated OMM fusion.

1.5.3 Mitochondrial inner membrane fusion

Mitochondrial inner membrane fusion is regulated by the GTPase protein OPA1. In humans, there are eight different isoforms of OPA1 generated by alternate splicing of exons (103). Long isoforms of OPA1 (L-OPA1) are attached to the IMM through their transmembrane domain (104). The short OPA1 isoforms (S-OPA1) are processed by two different proteases, namely Oma1 and Yme1L, and lack a transmembrane domain (43, 105-107) (Figure 1.3). Long and short isoforms form complexes on the IMM and that regulate fusion. Although long or short isoforms have been shown to have some inherent level of fusion activity, specific combinations of both isoforms are essential for proper mitochondrial membrane fusion under physiological conditions (43, 108).

Unlike MFNs, the presence of OPA1 on one of the opposing mitochondrial membranes is sufficient to induce IMM fusion (109). However, this process is dependent on the presence of cardiolipin in the IMM of opposing mitochondria (110). Cardiolipin is a negatively charged phospholipid enriched on IMM that is essential for the assembly and stability of the cristae-regulating protein complex MICOS and electron transport chain (ETC) protein complexes (111, 112). In vitro reconstruction experiments demonstrated that heterotypic interaction of L-OPA1 with cardiolipin promotes fusion, which is further augmented in the presence of S-OPA1(110) (Figure 1.3). Till date, the mechanism coordinating IMM and OMM fusion is poorly understood. Cardiolipin could be a potential linking factor because of its enrichment at OMM-IMM contact sites (113). Further studies are essential to understand this process.

In addition to its role in fusion, OPA1 is essential for regulating cristae structure. As mentioned earlier, proper cristae structure is essential for mitochondrial energy production and cell survival. Cristae width is controlled by OPA1 depending on the energetic state of the cell. For instance, during nutrient stress, OPA1 oligomerizes at the cristae junction and narrows the cristae width. This facilitates the assembly of ETC proteins together as a supercomplex assembly. Loss of OPA1 completely disrupts cristae structure and affects mitochondrial OXPHOS activity (114). Unlike its fusion activity, homotypic interaction of OPA1 is predicted to be involved in cristae regulation (110).

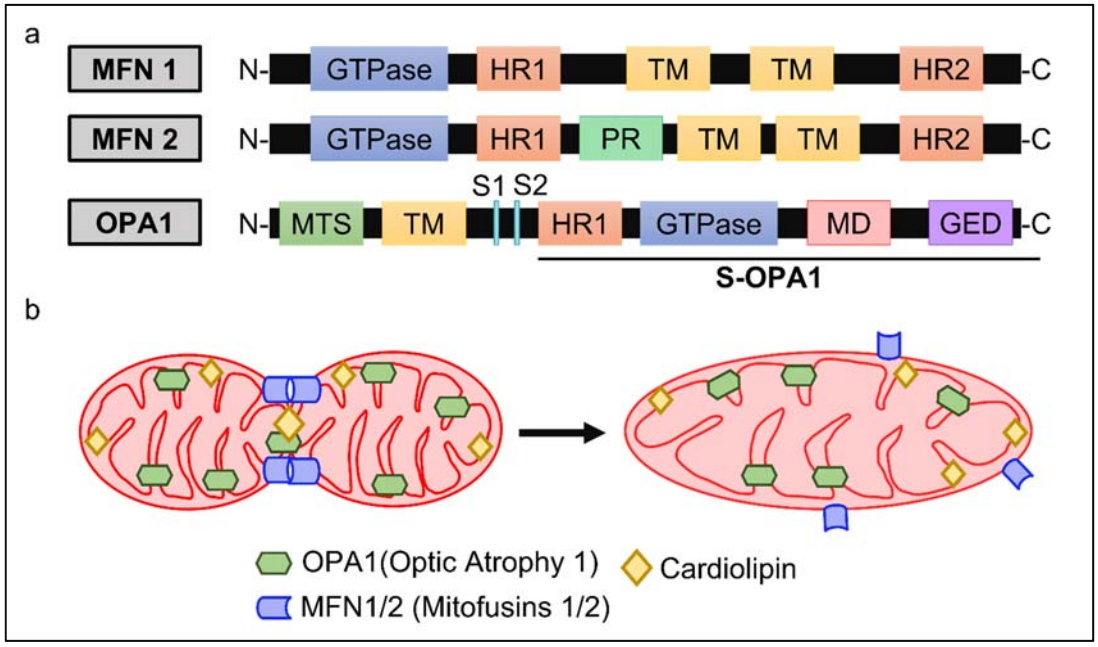

Figure 1.3 Mitochondrial Fusion.
Mitochondrial fusion process results in the merging of the mitochondrial membrane. (a) Structural domain of mitochondrial fusion protein (MFN 1/2, OPA1). (b) MFN 1/2 and OPA1 regulate mitochondrial outer and inner membrane fusion respectively. PR, proline-rich domain; GED, GTPase effector domain; MTS, mitochondrial targeting sequence; MD, middle domain; S1 and 2, protease cleavage sites.

1.5.4 Mitochondrial Fission

Mitochondrial fission is a multi-step complex process dependent on the interaction between mitochondria and regulated by the GTPase protein DRP1. Also, during fission

process, other cellular organelles (endoplasmic reticulum (ER), lysosomes and Golgi apparatus) help to regulate different stages of mitochondrial membrane scission. Mitochondrial fission is essential during the process of mitochondrial biogenesis and to eliminate damaged mitochondria by mitophagy. Recent studies suggest that different fission machineries are involved depending on the site of fission within the mitochondrial network. For instance, during mitochondrial biogenesis, newly divided daughter mitochondria are separated by fission. This occurs in the middle of a mitochondrial tubule and is hence referred to as mid-zone fission. On the other hand, damaged mitochondria are eliminated from the periphery/tip of the mitochondrial tubule by peripheral zone fission (82).

1.5.4.1 DRP1 and its receptors in mitochondrial fission

Mitochondrial fission is regulated by the GTPase protein DRP1, a cytosolic protein that is recruited on the OMM to facilitate mitochondrial membrane constriction. DRP1consists of different domains, namely, a GTPase domain in the N-terminus, a middle domain, a variable domain, and a GED domain in the C-terminus. DRP1 middle domain is essential for DRP1 oligomerization on the mitochondrial surface (115) (Figure 1.4). However, unlike other dynamins (Dnm), DRP1 lacks a pleckstrin homology domain necessary for phospholipid binding. Thus, DRP1 is recruited on the mitochondrial membranes by receptor proteins.

In mammalian cells, there are several different DRP1 receptors on the OMM, including MFF, MiD49/51, and FIS1(116-119) (Figure 1.4). Loss of MFF phenocopies DRP1 deletion/mutation, resulting in hyperconnected mitochondrial networks, suggesting a prime role of MFF as a DRP1 receptor (116, 120). On the other hand, the role of MiD49/51 in mitochondrial fission is not straightforward. Double knockout of MiD49 and MiD51 results in hyperfused mitochondria phenocopying MFF deletion (121). However, overexpression of these proteins also causes mitochondrial elongation (122). In vitro studies suggest that MiD proteins recruit GTP bound DRP1 and stimulate DRP1 oligomerization as linear filaments that are incompetent to induce scission.

GTP hydrolysis facilitates the dissociation of DRP1 from MiD protein and a conformational change in the oligomers that stimulates the formation of the ring structure necessary for membrane scission (123). These studies suggest that MFF and MiD proteins might recruit different forms of DRP1.

In yeast, FIS1 plays a key role in the recruitment of DRP1 to mitochondria. However, the role of mammalian FIS1 in mitochondrial fission is controversial. Some studies suggest that loss of FIS1 has no significant effect on mitochondrial networks, suggesting that FIS1 may not be the main driver of mitochondrial fission in mammalian cells (120, 124). However, there is increasing evidence suggesting that FIS1 recruits DRP1 and specifically regulates peripheral zone fission to eliminate damaged mitochondria (82, 125). This suggests that FIS1 could be mainly involved in mitochondrial quality control, unlike other DRP1 receptors. Thus, DRP1 mediated mitochondrial fission is likely controlled by different receptors depending on the site of fission or its functional role (biogenesis, quality control).

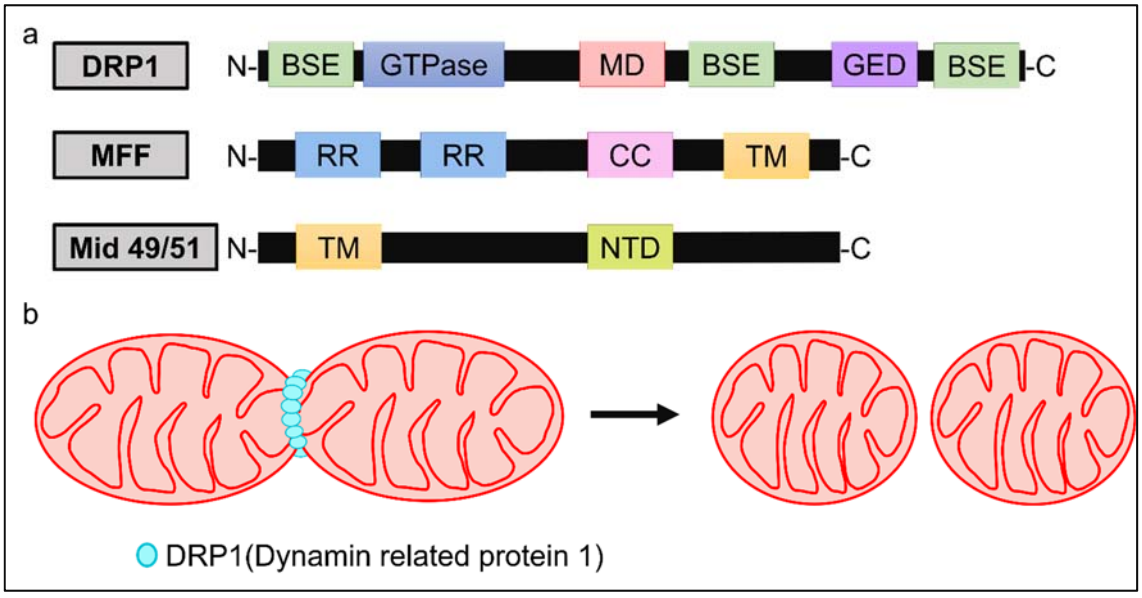

Figure 1.4 Mitochondrial Fission.
Mitochondrial fission process results in mitochondrial membrane scission. (a) Structural domain of mitochondrial fission protein (DRP1) and its mitochondrial membrane receptor (MFF, MiD 49/51). (b) DRP1 mediated mitochondrial division. BSE, bundle signaling element; RR, repeat region; CC, coiled coil; NTD, nucleotidyl transferase domain.

1.5.4.2 Post-translational regulation of DRP1

DRP1 recruitment on mitochondria is further regulated through post-translational modifications. This includes phosphorylation, nitrosylation, SUMOylation and ubiquitinylation. DRP1 is either activated or inactivated depending on the phosphorylation site. For example, phosphorylation of the serine residue (S616) in the GED domain activates DRP1 activity. Different kinases have been reported to phosphorylate S616 and induce mitochondrial fragmentation, including protein kinase C (PKC), calcium/calmodulin-dependent proteinase kinase-1 (CAMK1), ERK 1/2 (extracellular-signal-regulated kinase 1/2) and CDK1 (cyclin-dependent kinase 1)/cyclin B (126-129). On the other hand, DRP1 (S637) phosphorylation by protein kinase A (PKA) inactivates the protein and prevents mitochondrial fission (130). Calcineurin mediates the dephosphorylation of S637 to reactivate DRP1. In addition to these phosphorylation sites, S693 phosphorylation by glycogen synthase kinase 3β (GSK 3β) blocks fission and protects against apoptosis (131). Besides phosphorylation, DRP1 ubiquitination results in its degradation. For example, the OMM protein membrane associated ring finger 5 (MARCH5/MITOL) ubiquitinylates DRP1 and activates its degradation (132). However, the role of MARCH5 ubiquitination on DRP1 activity is controversial (133, 134). DRP1 stability on the OMM is influenced by SUMOylation especially during apoptosis (135). SUMOylation proteins such as Ubc9 (SUMO-conjugating enzyme) and MAPL (OMM SUMO E3 ligase) stabilize DRP1 on the OMM (136, 137). On the other hand, Sentrin/ SUMO specific protease 5 (SENP5) can counteract this process by removing the SUMO group from DRP1(138). In addition to these modifications, DRP1 is activated by S-nitrosylation and O-gluNAcylation under disease conditions (139, 140).

1.5.4.3 Initiation of mitochondrial fission

Mitochondrial fission is initiated with the identification of a fission site. ER tubules are speculated to scan along mitochondrial tubules and identify a site of fission. However, the mechanism of ER mediated identification of fission sites is unknown so far. ER tubule-mitochondria interaction plays an important role in the initial constriction of the mitochondrial membrane. Studies have shown that an ER tubule initially wraps around

the mitochondrion and marks the site of DRP1 mediated fission (141) (Figure 1.5). This ER mediated pre-constriction of the mitochondrial tubule is important for the subsequent recruitment of DRP1 at later stages of the fission process. During fission, DRP1 is recruited on the OMM, undergoes oligomerization, and spirals around the mitochondrial membrane to further constrict the mitochondrial tubule. However, DRP1 oligomerization occurs exclusively on pre-constricted mitochondrial membranes (141). In summary, the ER initially identifies and preconditions the fission site for the recruitment of the mitochondrial fission machinery in the later stages.

1.5.4.4 Actin and myosin in mitochondrial membrane constriction

In addition to ER tubules, the actin cytoskeleton creates an additional physical force necessary for the pre-constriction of the mitochondrial membrane (Figure 1.5). Actin filaments assemble around ER-marked fission sites. During mitochondrial fission, actin nucleators such as INF2 (Inverted Formin-2) and Spire 1C on the ER and the OMM, respectively, promote the formation of linear actin filaments at ER-mitochondria contact sites (142, 143). In addition, other regulatory factors involved in actin assembly such as cortactin, cofilin, Septin 2 and Arp2/3 (branching complex) are implicated in mitochondrial fission (69-71). Thus, actin filaments assembled at the fission site cooperate with ER tubules to create an inward force to constrict the mitochondrial membrane.

Actin filaments at the fission site require a contractile force necessary to pull them inward and constrict the mitochondrial membrane. Non-muscle Myosin II (NMII) drives this process by attaching to actin filaments and creating tension on the mitochondrial membrane (144). NMII is a dimeric protein containing a pair of heavy chains (HC), each associated with an essential light chain (ELC) and a regulatory light chain (RLC). The head group of NMII binds to actin and has an Mg^{2+}-ATPase activity that generates the propelling force. Based on the heavy chain, there are three different isoforms of NMII, namely NMIIA, NMIIB, NMIIC encoded by MYH9, MYH10 and MYH14, respectively (145). Knockdown of NMIIA/B impairs DRP1 recruitment to mitochondria and results in mitochondrial elongation (146). We have recently shown that a dominant negative mutation (R941L) in NMIIC (MYH14) impairs mitochondrial fission in patient fibroblast

cells (147). Altogether, the actomyosin complex, along with ER tubules, constricts the mitochondrial membrane to facilitate DRP1 oligomerization (Figure 1.5). Further, these machineries are exclusively involved in mid-zone fission or during mitochondrial biogenesis (82).

1.5.4.5 Lysosomes in mitochondrial fission

In addition to the previously discussed factors, a recent study demonstrated that lysosomes are recruited at mitochondrial fission sites (148). Specifically, this lysosome-mitochondrial contact is prevalent during peripheral zone fission to eliminate damaged mitochondria by mitophagy (82). Lysosomes/late endosomes are tethered to mitochondria by the GTPase protein Rab7. Following fission, Rab7 GTP hydrolysis by TBC1D15 (Rab7 GAP) which is recruited on the OMM by FIS1, untethers lysosomes and mitochondria (148) (Figure 1.5). Nevertheless, the functional role of lysosomal-mitochondrial contacts during fission is still poorly understood. There is evidence suggesting that the lysosome is recruited before IMM fission (148). It is speculated that this contact site would modulate IMM fission through calcium (Ca^{2+}) signaling.

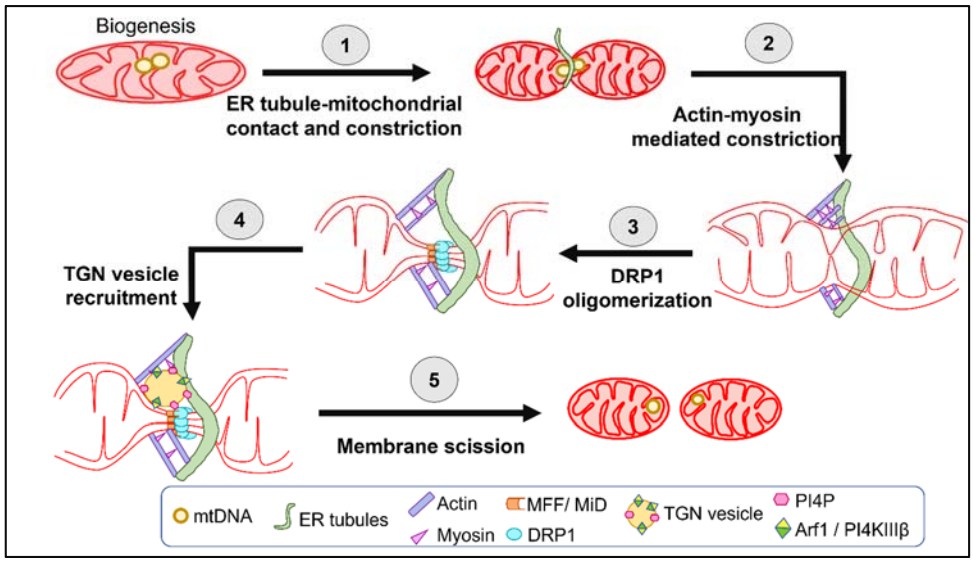

Figure 1.5 Process of fission.
DRP1 mediated mitochondrial fission process is a multi-step process involving different cellular organelles, resulting in mitochondrial membrane scission.

1.5.4.6 IMM fission

Contrary to OMM fission, our understanding of the mechanism and protein machineries regulating IMM fission is limited. There is evidence suggesting that IMM fission occurs prior to OMM fission (149). IMM fission is regulated by OPA1 and Ca^{2+} signaling plays an important role in this process. Fission initiates with an ER-mitochondria contact, which in turn activates Ca^{2+} influx, resulting in an acute drop in mitochondrial membrane potential (82, 150). Actomyosin filaments play an important role in this process by increasing ER-mitochondrial contact (150). Ca^{2+} influx at the contact site activates OMA1 mediated cleavage of L-OPA1 to s-OPA1. Accumulation of s-OPA1 untethers IMM-OMM by destabilizing the MICOS complex. Thus, IMM constriction occurs before OMM, and it is independent of DRP1(149). However, IMM constriction occurs independent of OMA1-mediated OPA1 processing in U2OS (human osteosarcoma) cells (150). This suggests that different protein players could be involved in regulating IMM fission dependent on the cell origin. Further studies could shed light on those key IMM fission proteins.

1.5.4.7 Termination of mitochondrial fission

The final stage of fission is marked by mitochondrial membrane scission. In vitro studies suggest that DRP1 can severe membranes (151). However, the severing abilities of DRP1 have not been demonstrated in mammalian cells. It has been proposed that another dynamin (Dnm2) could be involved in this process. Dnm2 is known to cleave endocytic vesicles budding off from cell membranes (152). However, the role of Dnm2 in mitochondrial fission is controversial. A study reported that Dnm2 is selectively recruited on DRP1 mediated mitochondrial constriction sites and regulates membrane scission in a GTP dependent manner. (153). In contrast to this observation, knockout studies demonstrated that dynamins (Dnm1,2,3) are dispensable for mitochondrial fission (151, 154).

A recent study reported the involvement of trans-Golgi network (TGN) vesicles in mitochondrial membrane scission. TGN vesicles are recruited on the fission site following DRP1 mediated constriction. These vesicles carry cargo on their membrane such as Arf1 (ADP-ribosylation factor-1) and PI4KIIIβ (phosphatidylinositol 4-kinase IIIβ) which are essential for fission (Figure 1.5). Loss of Arf1 or PI4KIIIβ impairs fission and results in hyperconnected mitochondrial networks (83). However, the mechanism of Arf1-PI4KIIIβ containing TGN vesicles in mitochondrial membrane scission is unknown. Arf1 recruits PI4KIIIβ in TGN vesicles (155). PI4KIIIβ is known to phosphorylate phospholipids in the membrane, which has been reported to regulate vesicle scission (155). Similarly, it is speculated that these vesicles could be regulating mitochondrial membrane scission by modulating lipid composition of the constricted membrane (156, 157). Further research is essential to understand the mechanism involved in mitochondrial membrane scission. Overall, mitochondrial fission is a complex process involving multiple organelles' contact and signaling to regulate different stages of mitochondrial division.

1.6 Mitochondrial diseases

Mitochondria are essential to maintain cellular homeostasis and, hence, defects in their maintenance and function result in mitochondrial diseases. Mitochondrial diseases can arise due to an inherited genetic mutation, a de novo genetic mutation, or a secondary effect due to stress stimuli (e.g., oxidative stress, environmental factors, drug toxicity). Genetic mutations in mtDNA or nDNA encoded mitochondrial genes lead to mitochondrial diseases. Usually, the severity of these diseases varies based on the nature of the mutation and the human organ that is affected. Generally, mitochondrial dysfunction can affect different organs, but certain energy demanding organs such as the heart, muscles, and brain are much more drastically affected. In addition to these inherited mutations, mitochondrial dysfunction could result from somatic mutations (mtDNA and nDNA) acquired during a person's life or due to external stress factors. This kind of mitochondrial dysfunction is common in different diseases such as diabetes, cancers, Alzheimer, Parkinson, autism, cardiovascular diseases and hepatopathy.

The inheritance of genetically linked mitochondrial diseases varies depending on the DNA that is affected. Mutations in mtDNA are exclusively inherited from the mother (maternal inheritance). Patients with mtDNA mutations develop clinical symptoms depending on the mutation load. Generally, patients have both wild-type and mutant mtDNA in their mitochondria, a condition called heteroplasmy. Patients develop symptoms only when the mutant population exceeds that of wild type mtDNA. Different disease-linked mtDNA mutations have been reported in humans. These variations commonly occur either in tRNA encoding genes or ETC protein subunit genes. Some mtDNA variations that are quite commonly found include defects in $tRNA^{Leu(UUR)}$ and $tRNA^{Lys}$,which result in mitochondrial encephalomyopathy, lactic acidosis, stroke-like episodes (MELAS), and myoclonus epilepsy, and ragged red fibers (MERRF) in patients, respectively. Mutations in mtDNA-encoded ETC genes (ND1, ND4, ND6, ATP6, CYTB, COX1, COX2 and COX3) similarly affect muscles and neurons. For example, ETC complex I gene mutations cause Leber's hereditary optic neuropathy (LHON), whereas defect in the complex V gene result in muscle weakness and ataxia.

Along with mtDNA, mitochondrial function and maintenance are regulated by different nDNA-encoded mitochondrial genes. Defect in those genes result in the onset of disease at early stages of life. Mutations in those genes are either autosomal or X-chromosome linked. Different nDNA-encoded mitochondrial gene mutations have been reported to affect mtDNA maintenance, transcription and translation, mitochondrial dynamics, protein quality control, apoptosis, protein import, lipid metabolism, ion transport and ETC complex proteins. nDNA mutations result in similar clinical symptoms to mtDNA and severely affect muscles and neurons. For example, defects in mtDNA replication enzymes such as POLγ and twinkle cause Alpers-Huttenlocher syndrome and ataxia neuropathy syndrome, respectively. Some of the mutations in nDNA-encoded mitochondrial genes either directly or indirectly affect mtDNA integrity and copy number. This in turn influences mitochondrial energy production, creates an imbalance in ROS levels, alters Ca^{2+} signaling and thereby activates cellular apoptosis. However, there are some nDNA mutations that indirectly affect mtDNA maintenance by

altering ETC and increasing ROS levels. Overall, clinical data suggests that mtDNA maintenance and OXPHOS function are highly linked to each other.

1.6.1 Mitochondrial dynamics and disease

As discussed earlier, mitochondrial dynamics plays an important role in mtDNA maintenance and OXPHOS activity. Hence, defects in mitochondrial dynamics proteins result in mitochondrial disease. Mutation in mitochondrial dynamic related genes alter mitochondrial morphology and distribution, affecting mtDNA integrity and/or copy number and OXPHOS function.

1.6.1.1 Mitochondrial fusion related diseases

Mitochondrial fusion proteins are essential for mitochondrial dynamics and mtDNA maintenance. Mutation in nuclear encoded fusion proteins severely affects energy demanding organs such as the brain and muscles. Optic atrophy is an OPA1 autosomal dominant disorder that selectively affects ganglion cells in the optic nerve. This heterozygous mutation results in progressive loss of vision in patients (158, 159). Nevertheless, mutations in the GTPase domain of OPA1 are reported to cause additional symptoms, including hearing loss, myopathy, and peripheral neuropathy. Further, these patients have multiple mtDNA deletions in their skeletal muscles, thus demonstrating the importance of OPA1 in mtDNA maintenance (160, 161).

Mutations in the MFN2 gene cause Charcot-Marie Tooth disease type 2A, which affects peripheral motor and sensory neurons. Patient loses sensation at the distal end with muscular atrophy and weakness (162, 163). Like OPA1, mtDNA maintenance is impaired in MFN2 mutants (164, 165). Based on in vitro and in vivo studies, it is hypothesized that MFN2 mutations impairs mitochondrial movement in neuronal cells, thereby resulting in neuronal degeneration (166).

1.6.1.2 Mitochondrial fission related diseases

Mitochondrial fission is essential for regulating mitochondrial dynamics and quality control. Additionally, mitochondrial fission is important for mitochondrial biogenesis with a potential role in mtDNA maintenance and distribution. Mitochondrial fission genes are nucleus-encoded and defects in these genes are implicated in mitochondrial diseases. Imbalance in fission protein levels and activities are associated with clinical conditions such as cardiomyopathies, neurodegenerative disease, diabetes, cancer, and other metabolic disorders (167).

Genetic mutations in the mitochondrial fission protein DRP1 are reported to cause rare mitochondrial diseases. Generally, patients have poor brain development (microencephaly) and experience untreatable seizures (epilepsy). The disease phenotype varies depending on the nature and position of the mutation in DRP1. Pathological variations have been reported primarily in its GTPase domain (10 genetical variants), middle domain (11 genetical variants) and GED domain (1 genetical variant).

The GTPase domain is important for the formation of higher-order DRP1 structures through GTP hydrolysis. Clinically different pathogenic variants are reported in the DRP1 GTPase domain: dominant-negative (E2A, A192E, G32A, D146N, G223V) and recessive (S36G and E116K, W88M and E129, T102M) (168-175). Patients with DNM1L autosomal dominant variants develop a dominant optic atrophy condition, resulting in progressive loss of vision. The other DNM1L variants result in encephalopathy, hypotonia (loss of muscle tension) and developmental defects, with some patients displaying higher degrees of symptoms including seizures, optic atrophy, and limb ataxia. Clear exceptions to these clinical symptoms include de novo variants S39G and D146N, where patients develop sensory neuropathy (loss of sensory nerves). All these mutations affect mitochondrial dynamics and patient cells have highly elongated mitochondria.

The middle domain is important for DRP1 oligomerization and thus necessary for mitochondrial membrane constriction. Clinical variants reported so far in the middle

domain are heterozygous, dominant negative mutations (G350R, G362D, G362S, F370C, A395D, R403C, L406S, E410K, L416P, C431Y, C446F) (169, 171, 176-181). Like GTPase domain mutations, these patients develop similar pathological phenotypes, though their clinical manifestations are comparatively more severe (182). These patients have a poor prognosis compared to those with GTPase mutations. Unlike other domains, only one clinical case has been reported so far in the GED domain. The GED is involved in the exchange of GDP for GTP and is necessary for the proper GTPase activity. This patient was found to have encephalopathy with seizures due to a heterozygous, dominant negative mutation (Y691C) in DNM1L (183).

Like DRP1 patients, defects in DRP1 receptors that regulate DRP1 activity develop similar clinical phenotypes. Patients with MFF mutations have encephalopathy and other neurological defects. Patient fibroblast cells have tubular mitochondria due to defective fission (184-187). Recently, two novel heterozygous mutations (Y240N and R146W) have been reported in MID51. These mutations result in mitochondrial fragmentation and manifest optic neuropathy (188). Besides DRP1 receptors, we have recently shown that mutations in the non-muscle myosin MYH14 (encoding NMIIC) result in peripheral neuropathy (147). A dominant-negative mutation (R941L) in MYH14 blocks mitochondrial fission, notably in the cell periphery (147). The other reported cases with autosomal dominant MYH14 mutations have hearing impairment (189, 190).

Clinical data suggests that mitochondrial fission defects severely impact neurological development. However, we have limited knowledge about the cellular mechanism being altered during the development of fission related diseases. Conditional knockout (KO) studies in mice suggest the importance of DRP1 in neuronal development. Mice with Drp1-/- in neurons have poor cerebral development and die shortly after birth (191). Also, mouse Drp1-/-neural cells have impaired synapse formation due to the improper mitochondrial distribution (192). DRP1 is essential for the survival of post-mitotic neurons. Drp1-/- purkinje cells have elongated mitochondria and they eventually die after a certain period in culture due to the accumulation of oxidative damage (193). These animals have defects in motor coordination (193). In vivo KO experiments suggest

the potential role of DRP1 in neuronal development and survival. Further in vitro and in vivo experiments are essential to understand the link between the clinical phenotype and the cellular mechanism that is altered in these patients.

1.7 Interorganelle contact sites

Interorganelle contact sites are a platform for the transfer of signaling molecules, and biomolecules (lipids, proteins). As discussed earlier, ER-mitochondria interactions regulate mitochondrial dynamics. In addition, these contact sites are involved in regulating different biological processes such as lipid trafficking (phospholipids, sterol), Ca^{2+} signaling, apoptosis and autophagy. Depending on the growth factors and metabolic conditions, different combinations of tethering proteins regulate interorganelle contact site length and spacing. How different ER subdomains interact with mitochondria is discussed in detail below.

1.7.1 ER structural dynamics

The ER is the largest organelle in the cell and a biogenesis factory. The ER is involved in protein synthesis, assembly, and transport, as well as lipid and sterol synthesis. It is the largest reservoir of Ca^{2+} molecules in the cell. The ER has a complex structural organization to perform these multiple functions. The ER is a dynamic membrane bound organelle that spreads across the cytoplasm and is organized into three luminally interconnected structural compartments: the nuclear envelope, rough ER (ER sheets/ cisternae) and smooth ER (ER tubules). These compartments constitute structurally and functionally distinct domains. The Nuclear envelope is a double membrane structure that consists of an inner nuclear membrane and an outer nuclear membrane. The nuclear envelope protects the genetic material and controls the transport of RNA and proteins in / out of the nucleus (194). The nuclear envelope is luminally linked to ER sheets.

ER sheets are primarily engaged in protein synthesis. ER sheets are highly enriched with ribosomes. Hence, membrane and secretory proteins are synthesized on the ER

sheets' surface and assembled on the ER membrane and lumen, respectively. ER sheets are flattened sac- like structures stacked together by helicoidal membranes. ER sheet structure is regulated by the integral membrane protein cytoskeleton-linking membrane protein of 63kDa (CLIMP63) (195). CLIMP63 homo-oligomerizes at the luminal side to keep ER membranes apart from each other, thereby regulating ER sheet width. Overexpression of CLIMP63 expands ER sheets, suggesting that it plays an important role in ER sheet formation (195). However, knockdown of CLIMP63 affects ER sheet luminal width but does not prevent ER sheet formation, suggesting the involvement of other regulatory factors along with CLIMP63 in ER sheet formation (195). Among these factors, polyribosomes involved in protein synthesis are suggested to regulate ER sheet structure, as the dissociation of ER-bound ribosomes affects the stability of ER sheets (196). Similarly, ribosome-translocon complex protein p180/RRBP1 (Ribosome Binding Protein 1) has been reported to modulate ER sheet proliferation (197). In addition to these proteins, loss of the ER membrane proteins Reticulons (RTNs) and DP1 (deleted in polyposis 1) also results in ER sheet expansion (195, 198). RTN and DP1 are present on the outer leaflet of the membrane bilayer and regulate the membrane curvature of ER sheet edges (195, 198-200). In addition to these membrane proteins, it is speculated that ER sheet and microtubule interactions can regulate ER sheet structure. Reports suggest that CLIMP63 and p180 interact with microtubules. However, the effect of this interaction on ER sheet structure is poorly understood.

ER tubules are high curvature membranes that extend from ER sheets and spread towards the cell periphery. Tubular ER is involved in lipid synthesis, calcium signaling, and interorganelle contacts. ER tubule structure is regulated and stabilized by RTNs and DP1. In yeast, depletion of RTN1 and Yop1 (mammalian ortholog of DP1) results in loss of ER tubules (195, 198). ER tubules constantly undergo homotypic fusion that results in the formation of three-way junctions. Atlastin (ATL) is enriched in ER tubular junctions and defects in this protein result in loss of ER branching (201). Further, in vitro liposome fusion studies suggest that ATL is an ER fusion protein. ATL tethers ER membranes in a GTPase dependent manner (202, 203). The ER tubular network is maintained by a balance between RTN and ATL function (204). In addition to ATL, Lunapark (Lnp) is reported to

regulate ER tubules and preferentially localize to ER junctions (205). Lnp regulates three-way junction formation based on its expression level. Low levels of Lnp result in a highly reticulated ER network, suggesting that Lnp acts antagonistically with ATL/Sey1(204). Recently, DRP1 was reported to modulate ER tubulation independent of its role in mitochondrial dynamics. Interestingly, DRP1 regulates this process independent of ER tubule dynamics proteins (206).

The growth of the ER tubular network by ER fusion proteins requires additional force to bring ER tubules into contact with each other. Microtubules have been proposed to regulate ER dynamics by two different pathways. First, ER tips bind to microtubule tips by the tip attachment complex (TAC), and ER tubules grow and shrink based on microtubule dynamics (207, 208). The second pathway is based on ER sliding along the microtubules where molecular motors such as kinesin-1 and dynein pull the ER along the existing microtubule network (209, 210). Rab10 facilitates ER tubule extension along microtubules by stabilizing ER tubule-microtubule interaction. Rab10 is localized at the growing end of ER tubules and is speculated to modulate ER tubule-microtubule interactions. Defect in Rab10 causes loss of ER tubules and results in ER sheet expansion (211).

Cells need both ER tubules and ER sheets to maintain cellular homeostasis. The balance between sheets and tubules varies depending on the presence of ER dynamics proteins and is cell- type specific. For example, secretory cells such as pancreatic cells have more ER sheets to facilitate secretory protein synthesis and release. On the other hand, endocrine cells involved in steroid hormone production have predominantly ER tubules. ER network alterations are speculated to modulate the interaction between the ER and other organelles. Since these interaction sites regulate different signaling pathways, they are essential for maintaining cellular homeostasis.

1.7.2 ER tubules - mitochondria contact

As discussed earlier, ER tubules-mitochondria contact sites (ERMCS) are linked to mitochondrial dynamics. In addition, ERMCS are involved in lipid metabolism, Ca^{2+} signaling, and mitochondrial quality control.

1.7.2.1 ERMCS in Lipid metabolism

Phospholipids and cholesterol are essential to maintain fluidity in cell membranes and organelles, including the ER and mitochondria (212). Though ER is a major site of lipid metabolism, mitochondria have some enzymes necessary for the synthesis of certain lipids such as cardiolipin and some phospholipids. ERMCS forms a hotspot for the transfer and synthesis of phospholipids. These sites are tethered between the OMM and the ER membrane by PTPIP51 and ORP5/8, which facilitates trafficking of phospholipid intermediates between the organelles (213). The OMM solute carrier protein SLC25A46 is another potential candidate reported to regulate phospholipid trafficking, although its interacting partners and other key players involved in this process are yet to be explored (214). At ERMCS, ER synthesized phosphatidylserine (PS) is transferred to mitochondria where it is further converted to phosphotidylethanolamine (PE) by PS decarboxylase. PE is transferred back to the ER where it is further processed to phosphotidylcholine (PC) by PE-N-methyltransferase. PC is then shuttled back to mitochondria (215, 216). In addition, a few studies suggest that ERMCS could be involved in cholesterol metabolism, although this needs further investigation (217, 218) (Figure 1.6).

1.7.2.2 ERMCS in Ca2+ signaling

Ca^{2+} signaling is important for proper cellular function. Regulation of Ca^{2+} level is crucial as this in turn regulates the activities of different metabolic enzymes. Mitochondria and the ER are important reservoirs of calcium in the cell. Ca^{2+} is important for proper maintenance of mitochondrial health and for energy production as Krebs cycle (isocitrate dehydrogenase, oxoglutarate dehydrogenase) and glycolytic (pyruvate dehydrogenase) enzymes are dependent on Ca^{2+}(219). Ca^{2+} is transferred from the ER to mitochondria

through the Inositol trisphosphate receptor (IP_3R in the ER)-voltage dependent anion-selective channel (VDAC in the OMM) (220, 221). The mitochondrial Ca^{2+} uniporter (MCU) then transfers Ca^{2+} into the mitochondrial matrix (222, 223). (Figure 1.6). However, excess Ca^{2+} transfer from ER to mitochondria can activate apoptosis (224, 225).

1.7.2.3 ERMCS in mitochondrial dynamics and biogenesis

As it has been discussed in detail earlier, ERMCS plays an important role in mitochondrial dynamics and mtDNA replication (80, 226). Mitochondrial fission is regulated by ERMCS-mediated Ca^{2+} signaling. Further, ERMCS create the physical force necessary to constrict mitochondrial tubules for DRP1 mediated fission. Modulation of these contact sites by regulating ERMCS tether proteins are known to alter mitochondrial morphology. For instance, MFN2 independently regulates ERMCS in addition to their role in mitochondrial dynamics. Loss of MFN2 affects ERMCS formation, thereby dysregulating Ca^{2+} signaling (227-229) (Figure 1.6). Furthermore, ER is associated with mitochondrial fusion sites (80). However, the functional role of ERMCS at fusion sites is unclear. In addition to regulating mitochondrial dynamics, ERMCS is essential for proper mtDNA replication (226) (Figure 1.5) and loss of ER tubules significantly affects this process (226). Altogether, ERMCS plays an important role in regulating mitochondrial functions and maintenance.

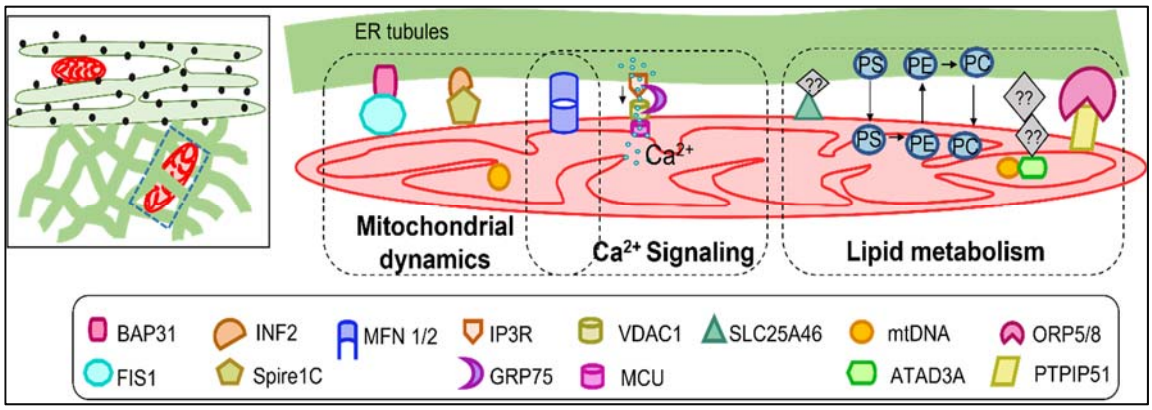

Figure 1.6 ER tubules-mitochondrial contact sites.
ER tubules tether to the mitochondrial membrane by protein linkers. These contact sites are essential for Ca^{2+} signaling, lipid metabolism, and

mitochondrial dynamics. Studies have revealed distinct roles for protein linkers in modulating different processes at contact sites.

1.7.3 ER sheets-mitochondria contacts

Contrary to ER tubules, our knowledge of ER sheets-mitochondria interactions is limited. In addition, proteins involved in regulating these contact sites and their functional significance are poorly understood. Electron microscopic studies revealed the existence of ER sheets-mitochondria contact sites (230-232). Due to the presence of ribosomes on the surface of ER sheets, ER sheets-mitochondria contact sites are proposed to have a complex protein tethering system.

ER sheets-mitochondria contact sites are modulated by growth factors. For example, insulin-activated mammalian target of rapamycin complex 2 (mTORC2) kinase is enriched at ER sheets-mitochondria contact sites. mTORC2 interacts with ribosomes, which is essential in activating mTORC2 dependent downstream signaling (233). In addition, mTORC2 modulates mitochondrial activity through its interaction with IP_3R at ER sheets- mitochondria contact sites and activates Ca^{2+} signaling in an Akt dependent manner (234) (Figure 1.7).

A recent study in human cells reported an interaction between SYNJ2BP (Synaptojanin-2-binding protein) and RRBP1 at the ER sheets-mitochondria interface (Figure 1.7). SYNJ2BP is an OMM tail-anchored protein with an unknown mitochondrial function (235). On the other hand, RRBP1/p180 is a transmembrane single-pass ER sheet protein (195) that is associated with ribosomes. It has recently been shown to interact with microtubules, which could regulate ER sheet structure. SYNJ2BP-RRBP1 tethering regulates ER sheets-mitochondria interactions though its functional importance is still unknown (235). Recently, it has been shown that RRBP1 regulates lipid metabolism at ER sheets-mitochondria contact sites. Loss of RRBP1 impairs ER-sheets-mitochondria interaction and thereby affects the secretion of very-low-density lipoproteins (VLDL) (236). Thus, a SYNJ2BP-RRBP1 tether could be involved in lipid metabolism and trafficking between organelles.

ER sheets-mitochondria interactions are also involved in Ca^{2+} signaling. The E3 ubiquitin ligase protein Gp78, otherwise known as the autocrine motility factor receptor (AMFR), regulates Ca^{2+} signaling through modulating ER sheets-mitochondria interactions (237). Gp78 regulates this process through MFN2 degradation (238, 239). As mentioned earlier, MFN2 regulates ER-mitochondria interaction, though its impact is still controversial, with some studies reporting that a loss of MFN2 increases ER-mitochondria interaction (227, 240, 241). The presence of AMF prevents this Gp78 mediated Ca^{2+} signaling at ER sheet-mitochondrial interaction (232, 238, 239).

Besides the availability of tethering proteins, post-translational modifications of proteins also regulate contact sites. Calnexin (CNX) is an ER chaperone protein necessary for the folding of glycosylated proteins and is present throughout the ER. However, s-palmitoylation of CNX results in its enrichment at ER sheets (242) (Figure 1.7). It is known that palmitoylated calnexin is recruited at ER-mitochondria contact sites, although its role in ER sheets-mitochondria interaction is unclear. Similarly, the ER sheet protein TMX4 shifts to ER-mitochondria contact sites upon palmitoylation (243). Thus, palmitoylation could be one of the potential mechanisms involved in modulating ER sheets-mitochondria interactions, although it needs further investigation.

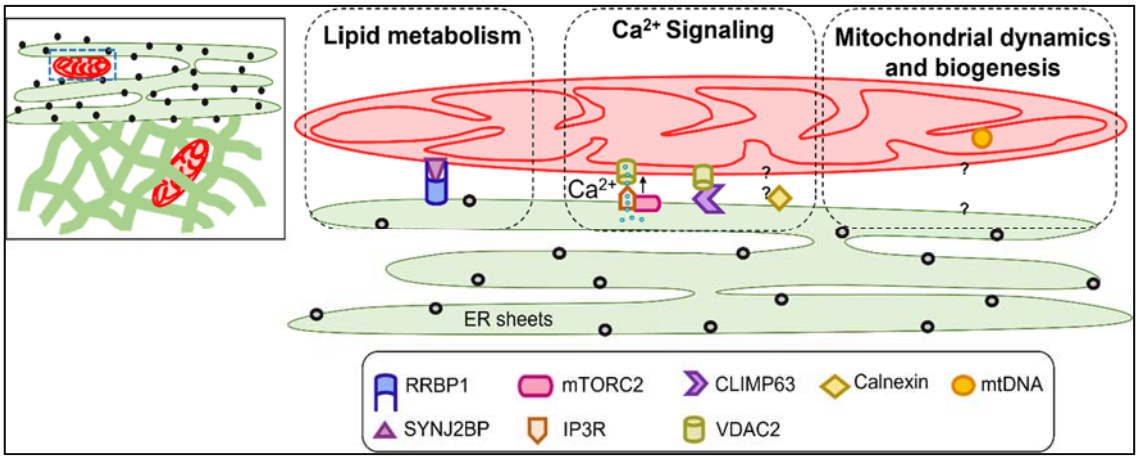

Figure 1.7 ER sheets-mitochondrial contact sites.
Like ER tubules, ER sheets tether to the mitochondrial membrane by specific protein tethers. These contact sites are implicated in Ca^{2+} signaling and lipid metabolism.

Contrary to ER tubules, the functional roles of ER sheets-mitochondria contact in mitochondrial dynamics are poorly defined. ER tubules are well known to regulate mtDNA replication and mitochondrial fission (141, 226). On the other hand, the role of ER sheets in these processes has yet to be properly addressed. Loss of ER tubules due to overexpression of the ER sheet protein CLIMP63 affects mtDNA replication (226). However, the direct effects of ER sheet-mitochondria interaction on mtDNA replication remain unknown.

1.8 Problem Statement

Mitochondria are dynamic, multifaceted organelles that regularly modify their network shape to adapt to cellular demands. Mitochondrial genes are encoded by nuclear and mtDNA. Though the majority of mitochondrial proteins are nDNA encoded, mtDNA encodes essential components of the ETC necessary for proper energy production. Hence, proper maintenance and distribution of nucleoids is crucial for mitochondrial function. A defect in their distribution results in heterogenous functioning of the organelle. However, the active mechanisms involved in regulating the homogenous distribution of nucleoids are poorly understood.

Mitochondrial dynamics proteins are essential for mtDNA maintenance. Defects or absence of mitochondrial fusion proteins, in particular, have a significant impact on mtDNA copy number and integrity. On the other hand, loss of fission proteins does not necessarily affect mtDNA copy number but results in enlarged nucleoids entrapped in bulb-like mitochondrial structures called mitobulbs. Although this evidence suggests a potential role of mitochondrial fission in nucleoid maintenance and distribution, the mechanism behind it is unclear.

My thesis aims to address the following two important questions:

(1) How are nucleoids distributed along the mitochondrial network?

(2) How does mitochondrial fission regulate nucleoid distribution?

(1) Global distribution pattern of nucleoids

Nucleoids are primarily attached to the mitochondrial inner membrane. However, studies suggest that this association does not necessarily restrict the movement of nucleoids along mitochondrial networks. Furthermore, mitochondrial dynamics-mediated changes in network structure could alter the global distribution pattern of nucleoids. Limited studies have reported nucleoid distribution and these few studies were limited to the measurement of inter-nucleoid distance between the neighboring nucleoids, independently of mitochondrial network organization. Given that nucleoids are distributed within mitochondrial networks, we need a computational tool that can characterize nucleoid distribution while considering the complex organization of mitochondrial networks. An automated computational tool will speed-up the process of characterization and help investigate protein machineries involved in nucleoid distribution. In our first paper, we will develop an automated tool to measure nucleoid distributions along mitochondrial networks. The primary objectives of this research work are:

(i) To understand the global distribution pattern of nucleoids within mitochondrial networks

(ii) To decipher the role of mitochondrial fission in nucleoid distributions

(iii) To understand nucleoid and mitochondrial network features that could affect nucleoid distributions

To address these questions, we will use immortalized mouse embryonic fibroblasts (MEFs) and primary human fibroblasts (HFs). Further, to demonstrate the role of mitochondrial fission, we will study nucleoid distribution in patient fibroblasts with defective mitochondrial fission proteins (DRP1, MYH14). This study will address the first aim of my thesis, to understand the global distribution pattern of nucleoids and the role played by fission.

(2) Mechanism of mitochondrial fission-mediated nucleoid distribution

In addition to their role in mitochondrial dynamics, DRP1 independently associates with ER and regulate ER tubules formation. On the other hand, ERMCS play an important in DRP1 mediated mitochondrial fission. Especially, ER tubules and fission proteins are known to be essential for mtDNA replication and mitochondrial division, respectively. Loss of ER tubules affects mtDNA replication. Similarly, a defect in fission results in nucleoid enlargement. Altogether, this suggests a potential link between ER and fission proteins in nucleoid segregation and distribution, though the mechanism behind it is unclear. Based on this evidence, we hypothesize that DRP1 regulates nucleoid distribution through modulating ER structure. To address this hypothesis, we put forward the following objectives:

(i) To understand the role of DRP1 on ER structures (tubules and sheets)

(ii) To investigate the effect of DRP1 on ER-mitochondria interactions

(iii) To establish the link between ER-mitochondria interactions and nucleoid distribution

To understand the role of DRP1 in these processes, we will use MEFs that lack DRP1, or HFs with defective DRP1. Thus, this work will address the second aim of my thesis, which is to understand the process of mitochondrial fission-mediated nucleoid distribution.

In summary, my PhD thesis work will define nucleoid distribution patterns within mitochondrial networks and their regulation by mitochondrial fission. Proper mtDNA distribution is essential for mitochondrial function and defects in this process result in mitochondrial diseases. Especially, defective DRP1 in humans severely affects energy demanding organs such as the brain and results in developmental defects, microencephaly, peripheral neuropathy, and epilepsy. Unfortunately, there are no cures for mitochondrial diseases due to our limited understanding of disease development. This work will bridge this knowledge gap and demonstrate the fundamental cellular process that is altered in these patients.

CHAPTER II

A NEW AUTOMATED TOOL TO QUANTIFY NUCLEOID DISTRIBUTION WITHIN MITOCHONDRIAL NETWORKS

The content of this article was published in English. Hema Saranya Ilamathi and Mathieu Ouellet are shared first author of the paper and contributed equally.

Scientific Reports 11, 22755 (2021). DOI: 10.1038/s41598-021-01987-9

Hema Saranya Ilamathi[1,2,3], Mathieu Ouellet[1,2,8], Rasha Sabouny[4,5], Justine Desrochers-Goyette[1,2,3], Matthew A. Lines[4], Gerald Pfefer[5], Timothy E. Shutt[4,5,6,7] & MarcGermain[1,2,3*]

[1] Groupe de Recherche en Signalisation Cellulaire, Département de Biologie Médicale, Université du Québec à Trois-Rivières, Trois-Rivières, QC, Canada.

[2] Centre d'Excellence en Recherche sur les Maladies Orphelines-Fondation Courtois, Université du Québec à Montréal, Montréal, QC, Canada.

[3] Réseau Intersectoriel de Recherche en Santé de l'Université du Québec (RISUQ), Montréal, Canada.

[4] Department of Medical Genetics, Cumming School of Medicine, University of Calgary, Calgary, AB, Canada.

[5] Department of Clinical Neurosciences, Cumming School of Medicine, University of Calgary, Calgary, Canada.

[6] Department of Medical Genetics, Alberta Children's Hospital Research Institute, Cumming School of Medicine, University of Calgary, Calgary, AB, Canada.

[7] Department of Biochemistry and Molecular Biology, Cumming School of Medicine, University of Calgary, Calgary, AB, Canada.

[8] Present address: Department of Engineering, University of Pennsylvania, Philadelphia, USA.

*email: marc.germain1@uqtr.ca

Author Contributions

H.S.I. performed all the experiments in DRP1 mutants. R.S. performed the imaging of MYH14 mutants. M.O. designed and tested the analysis tools and did the experimental analysis using them. H.S.I., M.O. and M.G. designed the experiments. H.S.I., M.O, J.D.G. and M.G. analyzed the nucleoid distribution data of MYH14 and DRP1 mutants. R.S. and T.E.S. provided the MYH14 raw data. M.A.L. and G.P. provided the clinical samples. H.S.I. and M.G. wrote the paper. All authors reviewed and discussed the manuscript.

Abstract

Mitochondrial DNA (mtDNA) maintenance is essential to sustain a functionally healthy population of mitochondria within cells. Proper mtDNA replication and distribution within mitochondrial networks are essential to maintain mitochondrial homeostasis. However, the fundamental basis of mtDNA segregation and distribution within mitochondrial networks is still unclear. To address these questions, we developed an algorithm, Mitomate tracker to unravel the global distribution of nucleoids within mitochondria. Using this tool, we decipher the semi-regular spacing of nucleoids across mitochondrial networks. Furthermore, we show that mitochondrial fission actively regulates mtDNA distribution by controlling the distribution of nucleoids within mitochondrial networks. Specifically, we found that primary cells bearing disease-associated mutations in the fission proteins DRP1 and MYH14 show altered nucleoid distribution, and acute enrichment of enlarged nucleoids near the nucleus.

Further analysis suggests that the altered nucleoid distribution observed in the fission mutants is the result of both changes in network structure and nucleoid density. Thus, our study provides novel insights into the role of mitochondria fission in nucleoid distribution and the understanding of diseases caused by fission defects.

Introduction

Mitochondria require proteins encoded by both nuclear and mitochondrial DNA (mtDNA) to perform their key roles in cellular metabolism. Maintenance of mtDNA copy number and integrity, as well as mtDNA distribution across mitochondrial networks, is crucial for proper mitochondrial function. mtDNA is packed into nucleoprotein complexes called nucleoids. Nucleoids are dynamic structures that actively move within mitochondrial networks and interact with neighboring nucleoids[1]. However, the mechanisms regulating nucleoid maintenance and distribution within mitochondrial networks are still not fully understood.

mtDNA replication is associated with mitochondrial dynamics, the process of mitochondrial fission and fusion[2]. Mitochondrial fusion is regulated by the GTPases Mitofusins (MFN1 and MFN2; outer membrane) and Optic Atropy-1 (OPA1; inner membrane) and is required for the maintenance of mtDNA copy number and integrity[3–5]. Mitochondrial fission is mediated by dynamin related protein 1 (DRP1). DRP1-dependent fission occurs at endoplasmic reticulum (ER)-mitochondrial contact sites (ERMCS) following the initial constriction of the mitochondrial tubule by actin and myosin[6,7]. mtDNA replication occurs at ERMCS[8]. Mutation of the fission proteins non-muscle myosin II (MYH14) or silencing/genetic ablation of DRP1 causes a decrease in nucleoid number, generally without a change in total mtDNA content[9–12]. In the case of DRP1 deletion, these nucleoids are enlarged and confined to an abnormal modified mitochondrial structure called mito-bulbs[9,10,12,13]. While these results suggest that mitochondrial fission is required for nucleoid segregation, it remains unclear how fission contributes to nucleoid maintenance and the spatial distribution of nucleoids within mitochondrial networks.

A small number of studies have previously measured nucleoid distribution using custom scripts on manually annotated images[14–18]. These studies reported either the overall nucleoid density or the average distance between the two closest nucleoids (nearest neighbor distance; nndist), sometimes calculated without considering the positional constraints imposed by the mitochondrial network[14,15]. While these studies give an overview of inter-nucleoid distances, other descriptors describing the global distribution of nucleoids within networks could provide a more informative description of nucleoid distribution. As such, the pair correlation function (pcf) calculates the probability of finding a nucleoid at any distance from a first one within the mitochondrial network, allowing for a finer mapping of nucleoid distribution compared with nndist (which only provides an average distance between adjacent nucleoids). In addition, automation of this quantification would allow more efficient analysis of nucleoid distribution patterns across a large number of mutants affecting nucleoids, leading to a better understanding of nucleoid biology.

Here, we have developed Mitomate Tracker, an automated tool that evaluates the distribution of nucleoids within mitochondrial networks using both nndist and pcf. Using this tool, we demonstrate that nucleoids are distributed in a semi regular fashion within mitochondrial networks, maintaining a minimal spacing between each other. These features were affected by mutations in MYH14 or DRP1, indicating that mitochondrial fission plays an important role in nucleoid distribution and maintenance.

Results

Mitomate tracker, a new tool to analyze the distribution of nucleoid across mitochondrial networks

Using the DNA binding dye picogreen, nucleoids can be visualised as punctate structures along TMRM-labeled mitochondria in live cells (Fig. 1). To study nucleoid distribution in an automated manner, we developed an algorithm (Mitomate tracker) that takes advantage of our previously published mitochondrial network quantification tool (Momito[19]), to which we combined two other tools: the ImageJ plugin, Trackmate which

allows nucleoid identification[20], and the R package, spatstat which calculates point pattern distributions[21]. This results in two distinct outputs: (1) a quantification of network and nucleoid parameters (nucleoid number and density, network length and connectivity), and (2) a point pattern distribution calculated by two distance-based metrics. The first metric, nndist, measures the average distance between a nucleoid and its closest neighbour within the mitochondrial network. The second metric, pcf, estimates the probability of finding a nucleoid at any distance from a first nucleoid within the mitochondrial network (Fig. 1).

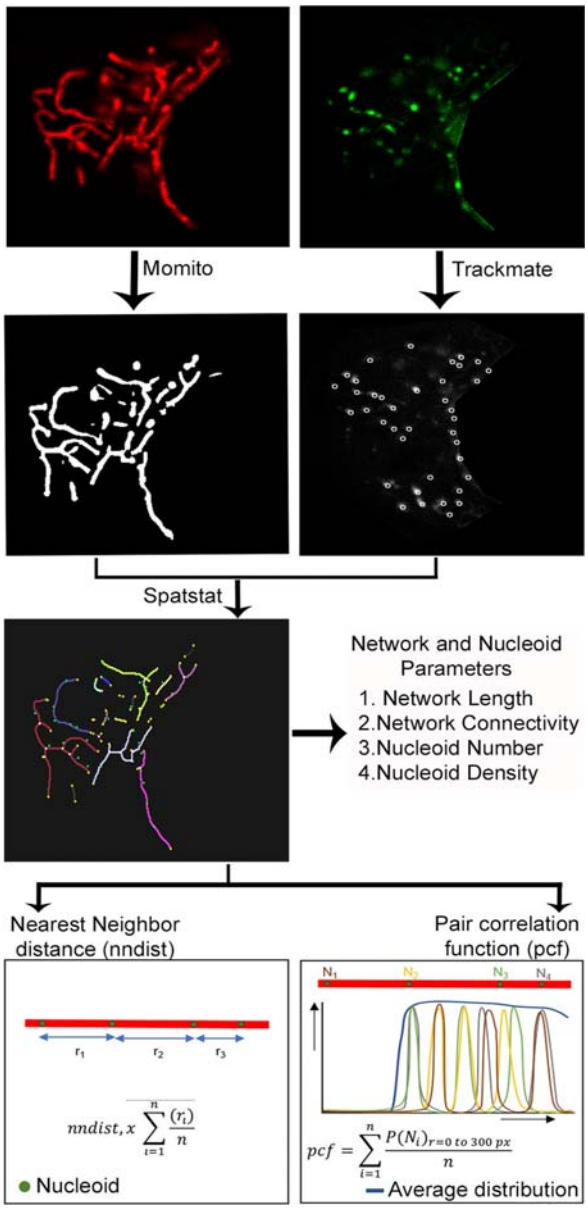

Figure 1. Schematic representation of nucleoid distribution analysis by Mitomate tracker. Confocal live cell Images of mitochondria (TMRM, red) and

nucleoids (Picogreen, green- nucleus manually removed) are analyzed using Mitomate tracker. Mitochondria are segmented and their components are identified using Momito while nucleoids are identified using the Image J Plugin Trackmate. The information extracted from Momito and Trackmate is then analyzed by the R package spatstat. Mitomate Tracker provides detailed descriptors of network and nucleoid features and measures nucleoid distribution pattern by two metrics, the nearest neighbor distance (nndist) and the pair correlation function (pcf).

Validating the robustness of nucleoid distribution metrics

As previous studies of nucleoid distribution used the average distance between adjacent nucleoids (nndist) as their primary metric[14,16,17], we first examined the nndist output of Mitomate tracker. Not surprisingly, the absolute distance between nucleoid was dependent on nucleoid density (Fig. 2a; $r^2 = 0.55$, $p < 0.001$). To take this into account, we normalised the actual nndist to an independent random process (IRP), where the same number of points are distributed within the same network independently of each other and network structure. The resulting nndist Ratio should be equal to 1 for a random distribution (actual and random values being equal). However, the normalised nndist was still somewhat dependent on nucleoid density (Fig. 2b; $r^2 = 0.30$, $p < 0.001$). This suggests that nndist is not a robust approach to measure nucleoid distribution owing to its persistent dependence on point density.

We then evaluated the robustness of the pcf. Contrary to the nndist which gives a single average distance per cell, the pcf computes the probability to find a point at any distance of a first point, making it impossible to achieve a simple correlation analysis as used for nndist. We thus used a small number of highly connected mitochondrial networks to which we randomly added points representing the highest and the lowest nucleoid densities found in mouse embryonic fibroblasts (MEFs) and primary human fibroblasts (HFs) (Fig. 2c, d). To avoid measuring effects due to specific random distributions, six different distributions were averaged for each image/condition (see “Methods” for details on the normalisation process). Using these, we then evaluated the influence of point density on the pcf. In this analysis, a random distribution (IRP) has a pcf value of 1 at all distances from the first point (Fig. 2e, black dashed line), values above 1 indicate correlation and values below 1, avoidance (Fig. S1). Consistent with this, points randomly

distributed across our test mitochondrial networks resulted in pcf values close to 1 for all densities tested (Fig. 2e; lines, distribution; colored area, SD). Pcf values also remained close to 1 when connectivity was reduced in our test images by manually unbranching the networks within the images using ImageJ (Fig. 2d, e), while keeping point density constant. Overall, our data indicate that the pcf provides a robust approach to study nucleoid distribution within mitochondrial networks.

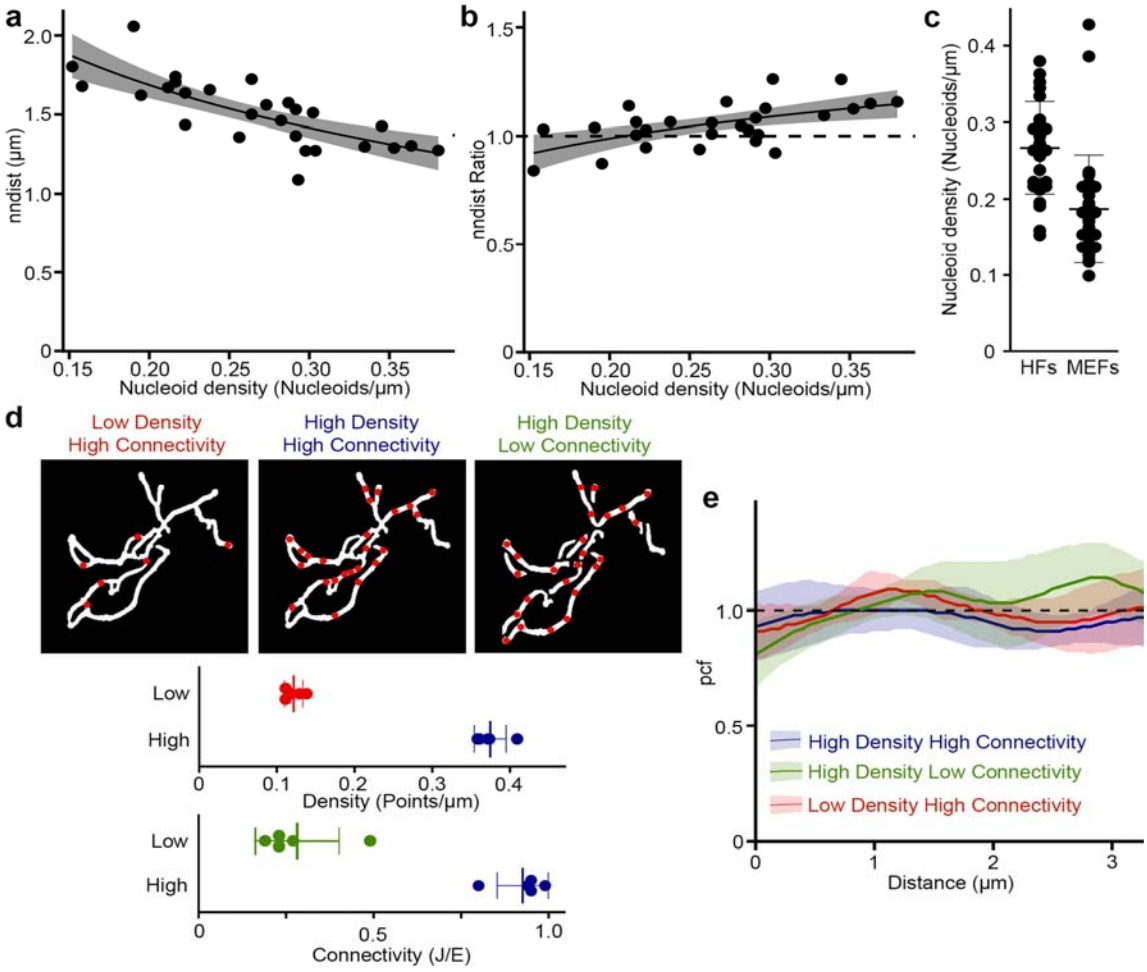

Figure 2. Measurement of nucleoid distribution by Mitomate tracker. (a,b) nndist is dependent on point density even after normalization. Scatter plot of Actual (a) and normalized (relative to an IRP; b) nndist values relative to nucleoid density in primary human fibroblasts. Each data point represents an individual cell (n = 27). The dashed line represents a random distribution. Linear regression formula y ~ log(x). (c) Nucleoid density in primary human fibroblast (HF) and mouse embryonic fibroblast (MEF) cells. Each point represents an individual cell. (d,e) Network connectivity and point density do not affect the pcf of random point distribution. (d) The networks were either left connected or manually unbranched and overlayed with a low or a high point density.

Top, Representative test network used for the analysis. Bottom, measures of point density and network connectivity for the 5 test networks. Each point represents a distinct network. (e) pcf curves. Solid lines represent the average point distribution for the indicated conditions and the shaded areas, the SD (n = 5 images). The dashed line represents the expected random distribution.

Nucleoids have a well-defined organization within mitochondrial networks

To study nucleoid distribution, MEFs and primary human fibroblasts were stained for mitochondria (TMRM) and nucleoids (picogreen) and imaged by confocal microscopy. The images were then processed and analyzed by Mitomate tracker, which identifies individual picogreen foci as a distinct nucleoid (97 ± 1% accuracy of identification, n = 10 cells), irrespective of its mtDNA content (larger nucleoids probably containing more mtDNA copies). This allows us to analyse nucleoid distribution independently of nucleoid segregation following mtDNA replication.

The pcf showed a strong nucleoid avoidance at short distances (pcf value < 1) but not at distances greater than 1 μm (pcf value > 1) for both MEFs (Fig. 3a) and primary human fibroblasts (Fig. 3b). The maximal likelihood to find a neighboring nucleoid as estimated from the pcf curve peak for each cell, occurred at 1–3 μm (average 2 μm; Fig. 3c). Similar results were obtained in fixed cells stained for TOM20 (mitochondria) and TFAM (nucleoids) (Fig. 3d). In addition, we tested the effect of cell thickness on the pcf output by comparing a single z-plane with the projection of the entire z stack from the same cell. Consistent with the fact that fibroblasts are flat cells, there were no significant differences between the two sets of images (Fig. 3e, f).

To quantify the differences between the observed nucleoid distribution pattern and an IRP-based distribution, we then measured the entropy (Shannon entropy) of individual pcf curves. In information theory, entropy represents the amount of information present in a variable[22,23]. In the context of a pcf, this means that any horizontal line, including an IRP (pcf = 1) has an entropy of zero, and entropy increases as it deviates from this horizontal line (Fig. S1). The entropy thus provides a measure of the variability of the pcf curve. Accordingly, the entropy values of actual MEFs pcf was significantly higher than

for their corresponding IRPs (Fig. 3g). Overall, our results indicate that nucleoid distribution is regulated to maintain a minimal distance between nucleoids, consistent with previous quantifications of inter-nucleoid distances using nndist in yeast cells[16,17].

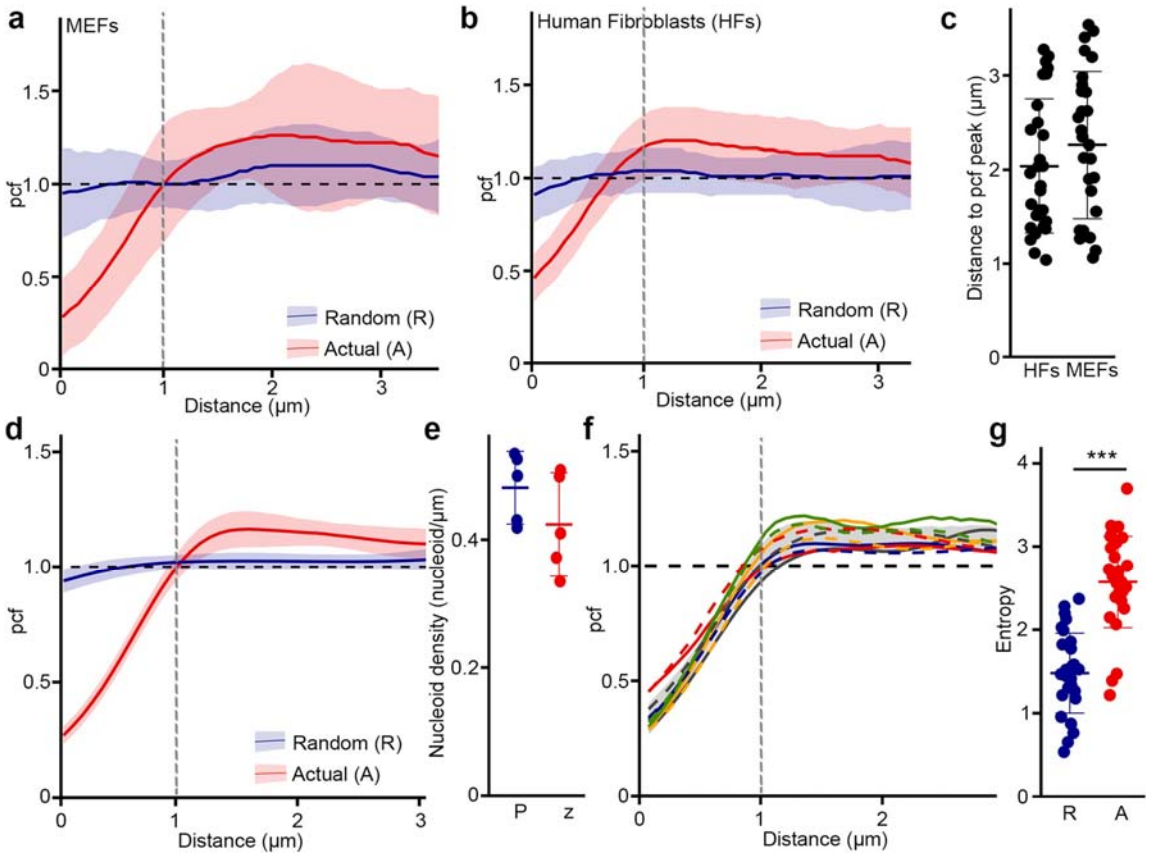

Figure 3. Nucleoid distribution is highly regulated. Pcf curves of nucleoid distribution in MEFs (a) and HFs (b), Solid lines represent the average of nucleoid distribution and the shaded areas the SD (n = 30 cells). Actual (A, Red) and Random (R, Blue) distributions for the same point densities are shown. (c) Distance between nucleoids as determined by the distance of the maximal pcf value. (d) Pcf curves of nucleoid distribution in HFs stained with TFAM and TOM20, Solid lines represent the average of nucleoid distribution and the shaded areas the SD (n = 20 cells). The dashed line represents the expected random distribution. Actual (A, Red) and Random (R, Blue) distributions for the same point densities are shown. (e,f) z-Stacking does not affect pcf results. Control cells were stained for TFAM and TOM20 and the projection of the full z-stack (P) compared to the single focal plane capturing most of the mitochondrial network (z). (e) Nucleoid density. Each point represents an individual cell. (f) pcf analysis. Each colour represents a distinct cell, the solid line being the single z image and the dashed line the projection. The shaded area represents the average ± SD for the single z images and the black dashed line the expected random distribution. (g) Entropy values calculated from MEFs pcf curves in (a). Actual nucleoid distribution (A), random distribution (R). Each data point represents one cell. Bars represent the average of 30 cells ± SD. *** $p = 2 \times 10^{-11}$. Two-tailed t-test.

Loss of mitochondrial fission impairs the distribution of nucleoids within mitochondrial networks

Mitochondrial networks are shaped by mitochondrial dynamics, including mitochondrial fusion and fission. Importantly, sites of mitochondrial fission have been associated with sites of mtDNA replication[8]. However, whether this actively contributes to nucleoid distribution within mitochondrial networks and in relation to the nucleus remains unclear. To determine the role of fission in nucleoid distribution, we investigated nucleoid content and distribution in patient fibroblasts with a dominant-negative mutation in MYH14 (R941L), a protein required for the initial constriction of mitochondrial tubules prior to DRP1-dependent scission[10]. MYH14 mutation causes an increase in mitochondrial length[10] while somewhat decreasing overall mitochondrial content but did not strongly impact mitochondrial connectivity (Fig. 4a). On the other hand, as we previously reported[10], MYH14 mutant fibroblasts had fewer nucleoids, resulting in a lower overall nucleoid density (Fig. 4a, b).

We then analyzed nucleoid distribution in MYH14 mutants. Consistent with MYH14 mutation affecting nucleoid distribution, all mutant cells showed an altered pcf relative to control cells (Fig. 4c, each curve represents a distinct cell). However, we could not observe any conserved pattern across cells, and there were no specific changes in correlation at either short (pcf_{R1}, 0–0.5 μm) or longer distances (pcf_{R2}, 1.2–1.7 μm) (Fig. 4c, d). In fact, while some cells showed nucleoid clustering at short distances, other cells had a strong avoidance at short distances and a distinct correlation at longer distances (Fig. 4c, d). The increased pcf variability found in MYH14 mutants was also reflected in their increased entropy (Fig. 4e). Overall, the increased variance we observed in the pcf suggests that nucleoids are disorganized in MYH14 mutants in comparison to the control.

We previously reported that MYH14 mutant cells had fewer, but larger nucleoids than control cells[10]. These were evident in mutant cells stained for nucleoids (picogreen) and mitochondria (mitotracker) (Fig. 4b). Importantly, these enlarged nucleoids (possibly cluster of mtDNAs) were restricted to the perinuclear region, which was confirmed by the quantification of nucleoid size close to the nucleus and in the periphery (average size and

size ratio; Fig. 4b, f). In contrast, control nucleoids were of similar size irrespective of their localization (Fig. 4b, f). Thus, our results indicate that MYH14 significantly influences nucleoid maintenance and distribution, supporting the idea that mitochondrial fission is essential for the distribution of nucleoids.

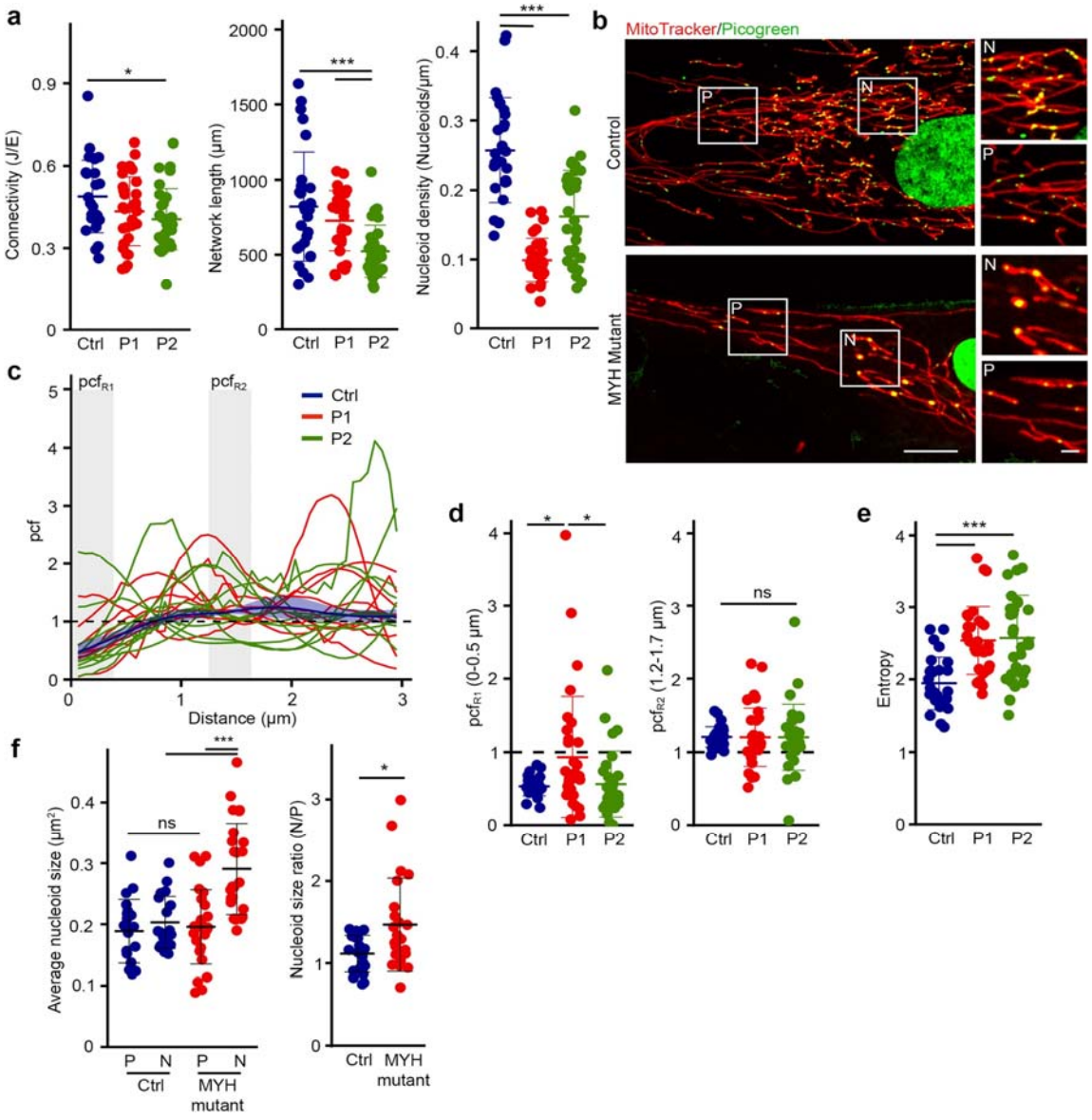

Figure 4. MYH14 is required for proper nucleoid distribution. (a) Mitochondrial parameters in Control and MYH14 mutant primary human fibroblasts (P1: Patient 1, P2: Patient 2). Each data point represents one cell. Bars represent the average of 30 cells ± SD. *p = 0.032 (Connectivity, Ctrl vs P2), ***p = 0.0000869 (Network length, Ctrl vs P1), p = 0.0073460 (Network length P1 vs P2), p = 1×10^{-6} (Nucleoid density, Ctrl vs P1/P2). One-way ANOVA. (b) Representative live cell confocal images of control and MYH14 mutant primary fibroblasts stained with mitotracker red (mitochondria) and

picogreen (DNA) Scale bar, 10 μm; 2 μm for zoomed images. P, periphery; N, perinuclear. (c–e) Nucleoid distribution in control and MYH14 primary human fibroblasts. (c) pcf curves. The solid line for the control (Blue) represents the average distribution and the shaded area, the SD (n = 8 cells). For the MYH14 mutants, each solid line represents one individual cell (n = 9 cells per patient line), highlighting the variability of the pcf. The dashed line represents the expected random distribution and the grey areas, the distances for which the average pcf was quantified in (d; pcf_{R1}: 0–0.5 μm, pcf_{R2}: 1.2–1.7 μm). (d) Average pcf values at short and longer distances. Each data point represents one cell. Bars represent the average of 30 cells ± SD. *p = 0.0182065 (Ctrl vs P1), p = 0.0280752 (P1 vs P2), ns not significant. One-way ANOVA (e) Entropy values calculated from the pcf curves in (c). Each data point represents one cell. Bars represent the average of 30 cells ± SD. ***p = 0.0000502 (Ctrl vs P1), 0.0000891 (Ctrl vs P2). One-way ANOVA. (f) Average nucleoid size in peripheral (P) and perinuclear (N) regions (Left) and nucleoid size ratio (Perinuclear/periphery) of control and MYH14 mutant primary fibroblasts (right). Each data point represents one cell. Bars represent the average of 20 cells ± SD. ***p = 0.0000015 (MYH mutant P vs N), p = 0.0000287 (N Ctrl vs N Mutant), ns not significant, One-way ANOVA (Left). *p = 0.01949, Two-tailed t-test (Right).

Dominant-negative mutation in DRP1 causes perinuclear nucleoid clustering and altered nucleoid distribution

While these results support an important role for mitochondrial fission in the regulation of nucleoid distribution, it remained possible that the nucleoid phenotype we observed in MYH14 mutant cells was restricted to myosin defects. Thus, to confirm the role of fission in nucleoid distribution, we used primary fibroblasts from patients with a mutation in DRP1 (G362D), an essential component of the fission machinery[24]. Mutations in DRP1 or its genetic deletion results in elongated and hyperconnected mitochondria and causes the formation of enlarged nucleoids termed mitobulbs[9,24]. While these previous studies did not determine the subcellular localization of these mitobulbs, our MYH14 mutant results predict that they accumulate preferentially in the perinuclear region of mutant cells. To verify this, primary human fibroblast cells were stained for mitochondria (TMRM) and nucleoids (picogreen) and imaged by confocal microscopy (Fig. 5a). Similar to MYH14 mutant, the mitobulbs present in DRP1 mutants were mainly restricted to the perinuclear region of the cells (Fig. 5a). In fact, nucleoid size was significantly larger in the perinuclear region of the DRP1 mutants (Fig. 5b). Also, as with MYH14 mutants, the changes in nucleoid size and distribution were accompanied by a reduction in overall nucleoid density (Fig. 5c).

We then measured nucleoid distribution in DRP1 mutants. Similar to MYH14 mutant, the pcf of DRP1 mutant cells was variable, with some mutant cells showing greater correlation at short distances while others avoided each other at short distance (pcf_{R1}- 0–0.5 µm) (Fig. 5d, e). Pcf analysis of fixed cells labelled for TOM20 (mitochondria) and TFAM (nucleoids) showed similar pattern (Fig. 5f). As with the MYH mutants, the change in pcf caused by DRP1 mutation also resulted in an increase in entropy (Fig. 5g). Overall, our data indicates that defects in mitochondrial fission impairs proper nucleoid distribution, resulting in their perinuclear clustering and enlargement.

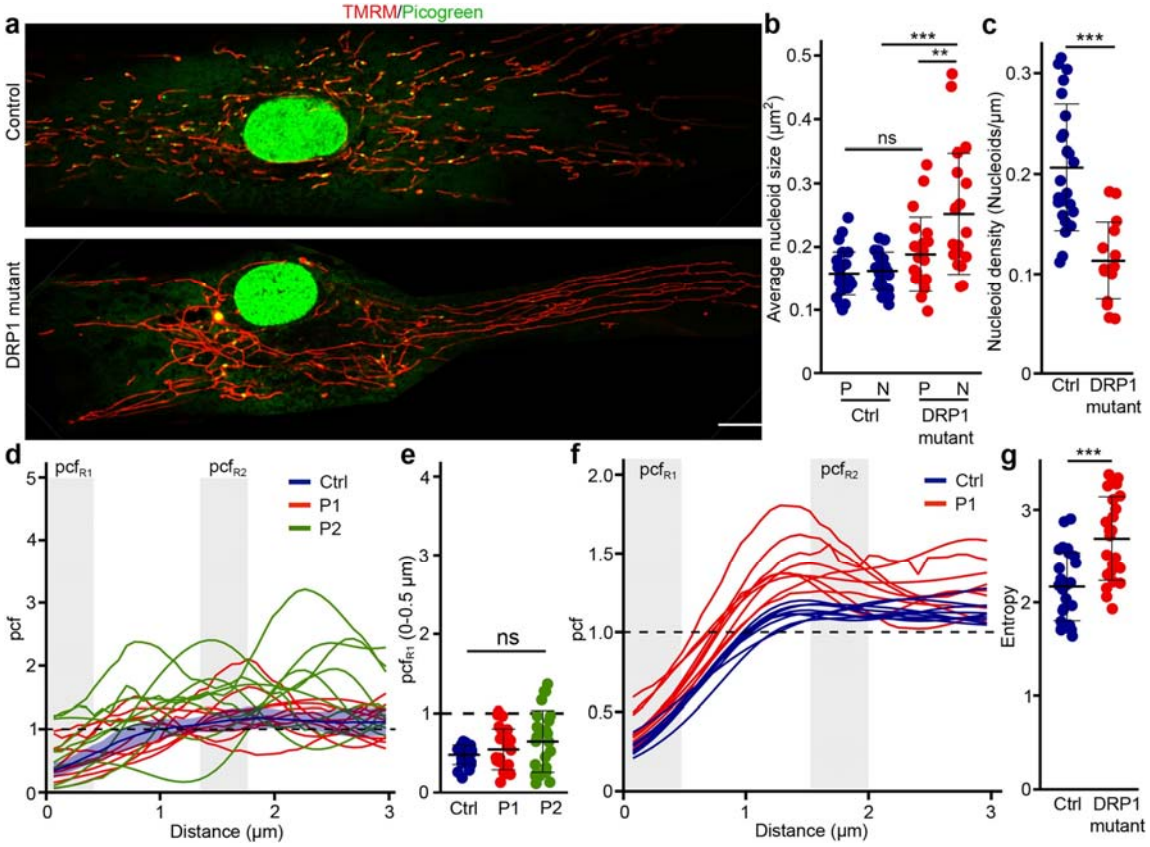

Figure 5. DRP1 is required for proper nucleoid distribution. (a) Representative live cell confocal images of control and DRP1 mutant primary fibroblasts stained with TMRM (mitochondria) and picogreen (DNA) Scale bar, 10 µm. (b) Average nucleoid size in peripheral (P) and perinuclear (N) regions of control and DRP1 mutant primary fibroblasts. Each data point represents one cell. Bars represent the average of 20 cells ± SD. **, p = 0.0047718 (DRP1 mutant P vs N), ***p = 0.0000130 (N Ctrl vs N Mutant), ns not significant. One-way ANOVA. (c) Nucleoid density in control and DRP1 mutant primary fibroblasts. Each data point represents one cell. Bars represent the average of 20 cells ± SD. ***p = 2.164e-06. Two-tailed t-test. (d–f) Nucleoid distribution in control and DRP1 primary human fibroblasts. (d) pcf curves. The solid line for the

control (Blue) represents the average distribution and the shaded area, the SD (n = 9 cells). For the DRP1 mutants, each solid line represents one individual cell (n = 9 cells per patient line), highlighting the variability of the pcf. The dashed line represents the expected random distribution and the grey areas, the distance for which the average pcf was quantified (e; pcf_{R1}: 0–0.5 µm). (e) Average pcf values at short distances. Each data point represents one cell. Bars represent the average of 30 cells ± SD. ns not significant. One-way ANOVA. (f) Nucleoid distribution in control and DRP1 primary human fibroblasts stained with TFAM (nucleoids) and TOM20 (mitochondria). Each line represents a distinct cell (n = 9 for control (Blue) and DRP mutants (Red)). The dashed line represents the expected random distribution and the grey areas, pcf_{R1} (0–0.5 µm) and pcf_{R2} (1–1.5 µm)). (g) Entropy values calculated from the pcf curves in (d). Each data point represents one cell. Bars represent the average of 30 cells ± SD. ***p = 3.377e05. Two-tailed t-test.

Synergistic effect of mitochondrial features influences nucleoid distribution in fission mutants

To understand how impaired mitochondrial fission leads to such alterations in nucleoid distribution, we first determined whether network features (mitochondrial length, connectivity) and nucleoid parameters (total nucleoids, size ratio) correlated with the pcf changes observed in the two fission mutants. To do this, we calculated Pearson coefficient between each parameter independently for each cell type. Control lines for MYH14 and DRP1 mutants behaved similarly, with the same parameters showing a correlation (Pearson coefficient $\geq \pm 0.5$, Boxed in Fig. 6a). Among these was a predictable correlation between network size and total nucleoid numbers, but also a correlation between these two parameters and entropy. Importantly, the correlation pattern clearly varied between genotypes (Fig. 6a), suggesting that each genotype behaves differently.

The distinct behavior of each genotype was evident when comparing network features (network size vs connectivity shown in Fig. 6b; Pooled controls $r^2 = 0.07$, $p = 0.10$; MYH14 $r^2 = 0.32$, $p = 0.006533$; DRP1 $r^2 = 0.38$, $p = 0.04492$) but also when nucleoid parameters were correlated with the pcf. For example, the pcf at close distance (Pcf_{R1}) correlated with nucleoid number specifically in the DRP1 mutants (Fig. 6a,c; DRP1: $r^2 = 0.77$, $p = 0.001182$; pooled controls: $r^2 = 0.16$, $p = 0.02054$; MYH14: $r^2 = 0.00$, $p = 0.58$), while pcf_{R1} correlated with nucleoid size ratio only in MYH14 mutants (Fig. 6a,d; pooled controls: $r^2 = 0.02$, $p = 0.53$; MYH14: $r^2 = 0.45$, $p = 0.0001829$; DRP1:

$r^2 = 0.07$, $p = 0.67$). These results suggest that the differences observed across genotypes are the consequence of distinct changes in mitochondrial features. This is supported by the fact that mitochondrial networks were distinctly affected in MYH14 and DRP1 mutants: MYH14 mutation mainly caused mitochondrial elongation while DRP1 mutants showed a large increase in connectivity (Fig. 6e).

On the other hand, a principal component analysis (PCA) of the same genotypes indicated that both mutants segregated away from control cells (Fig. 7a, suggesting that the fission mutants nonetheless share common features relative to mitochondrial network features. In fact, examination of the correlation data indicated that the entropy was correlated with nucleoid content for all genotypes (Fig. 6a; Fig. 7b, overall: $r^2 = 0.49$, $p = 4.102e{-}13$; pooled controls: $r^2 = 0.49$, $p = 2.05e{-}07$; DRP1: $r^2 = 0.67$, $p = 0.0001879$; MYH14: $r^2 = 0.26$, $p = 0.005405$), suggesting that pcf variability is a consequence of the smaller number of nucleoids present in the mutant cells (Figs. 4a, 5c). In order to verify whether nucleoid density affects nucleoid distribution, we analyzed nucleoid distribution in control cells where nucleoid density was decreased to match that of MYH14 mutants. To do this, we modified Mitomate tracker to be able to randomly remove points from each input image and analyze it as if it was the actual image (which is distinct from Fig. 2e where several random distributions were averaged—see “Methods”). This resulted in alterations in pcf curves and entropy (Fig. 7c–e) that were similar to those observed in MYH14 mutants (Fig. 4c–e), indicating that nucleoid density influences the nucleoid distribution pattern. Nevertheless, the relationship was different between control cells and MYH14 mutant cells (Fig. 7b, $p = 2.2e{-}16$), suggesting that factors other than nucleoid number affect the entropy. This is also supported by the observation that the relationship between the entropy and p cfR1 varied across genotypes (Fig. 7f; Pooled controls: $r^2 = 0.17$, $p = 0.004394$; MYH14: $r^2 = 0.02$, $p = 0.46$; DRP1: $r^2 = 0.74$, $p = 4.482e{-}05$).

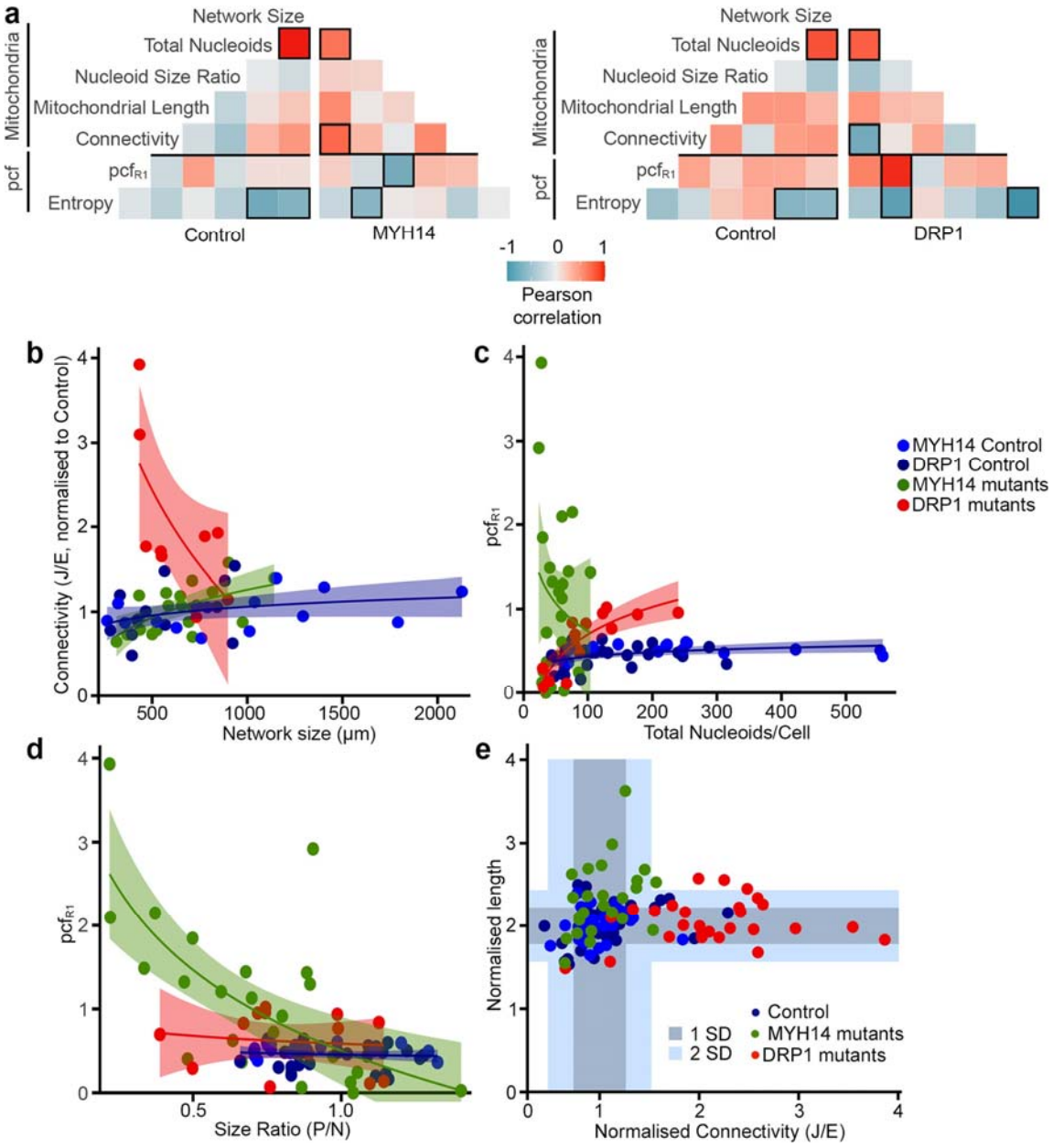

Figure 6. Fission mutants show a distinct relationship between mitochondrial parameters and the pcf. (a) Pearson correlation of pcf and mitochondrial parameters for the indicated genotypes. Number of cells used for the analysis: Control MYH14 (24), MYH14 mutants (25), Control DRP1 (17), DRP1 mutants (14) (b–d) Scatter plots showing the correlation between the indicated parameters for each genotype. The shaded areas represent the 95% confidence interval. Each data point represents one cell (n as in (a)). Linear regression formula y ~ log(x). (e) Distribution of mitochondrial connectivity and length across genotypes in individual cells. Connectivity was calculated as the number of junctions (J)/number of ends (E) (e). For length, we used the number of mitochondria < 2 µm but, to have an increasing value with increasing length, we used 1/this number. All values were normalized to the control for the same experiment. The shaded areas represent 1 SD and 2 SD from the control values. Each data point represents one cell.

Altogether, these results suggest that while both fission mutants globally affect nucleoid features and their distribution in a similar way (Fig. 7a), the manner in which they modulate this process likely differs as a consequence of distinct changes in mitochondrial network features.

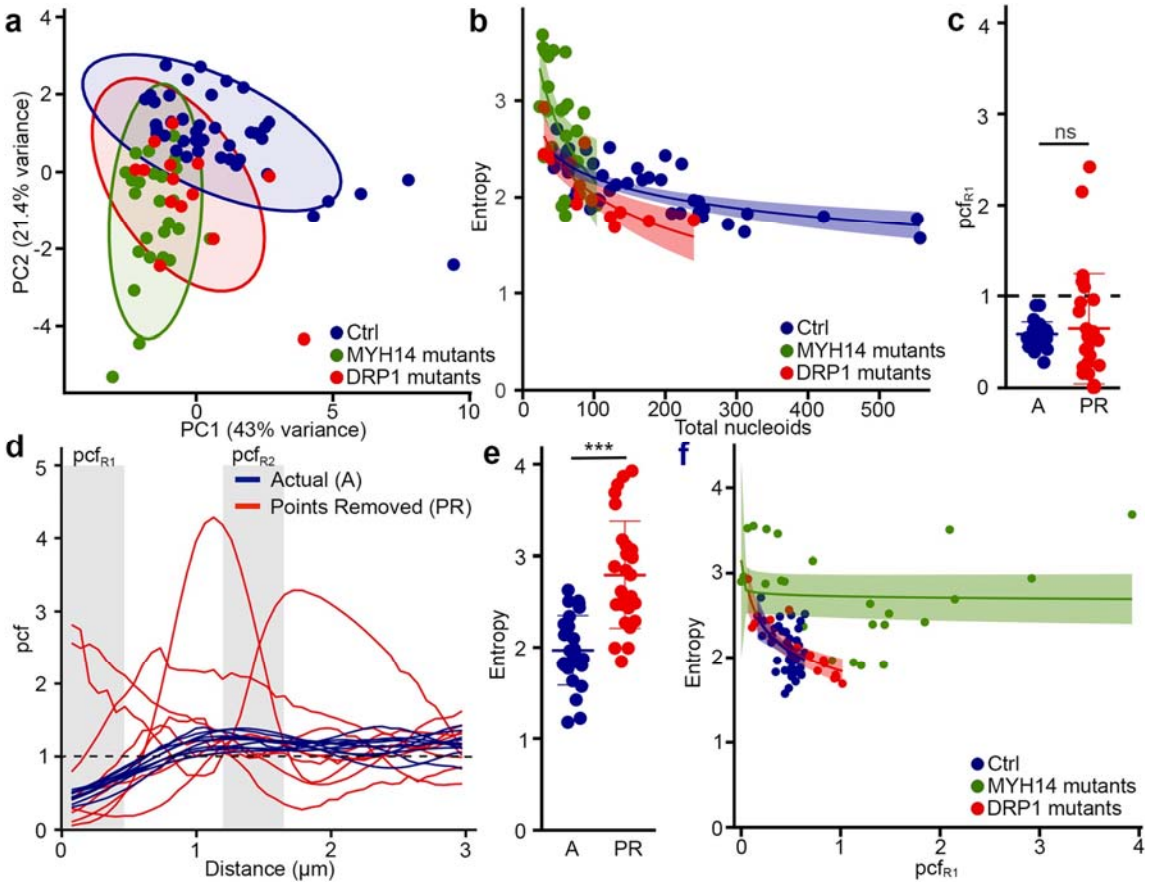

Figure 7. Nucleoid density influences the variability of the pcf curves (Entropy) across genotypes. (a) PCA analysis showing the segregation of mutant and control lines. Each data point represents one cell. Circles represent the 95% confidence interval (b) Dot plots showing the correlation between Entropy and total number of nucleoids for each genotype. The shaded areas represent the 95% confidence interval. Each data point represents one cell. (c–e) Decreasing nucleoid density in control cells recapitulates the pcf variability found in fission mutants. Individual cells are shown for pcf_{R1} values (c), pcf curves (d) and Entropy (e). ns. not significant, p = 1.122e−07, two-sided t-test. (f) Relationship between pcf_{R1} and Entropy in different genotypes. The shaded areas represent the 95% confidence interval. Each data point represents one cell.

Discussion

Mitochondrial function depends on the proper maintenance of mtDNA and its distribution across the mitochondrial networks. While mitochondrial fusion plays an important role in mtDNA maintenance[25], the role of mitochondrial fission in this process remains poorly understood. In fact, impaired fission is associated with the presence of enlarged nucleoids but not necessarily a loss of mtDNA content[9,10,12]. In addition, while mitochondrial dynamics have been suggested to control nucleoid distribution across mitochondrial networks, the underlying mechanisms remain poorly understood. To address these questions, we developed an automated tool, Mitomate tracker to quantify nucleoid distribution within mitochondrial networks. Mitomate tracker allows to use minimally pre-processed images to provide detailed quantitative data on mitochondrial network and nucleoids features and distribution. We initially measured both nndist and pcf to quantify nucleoid distribution. However, we found that the pcf is a more robust metric than the nndist. This is likely because the pcf globally measures the distribution probability relative to an IRP instead of the single average distance provided by the nndist. In addition, unlike the nndist, the calculation of the pcf probability takes into account the fact that points are closer when density is higher, providing a normalization relative to density. While we used it here to demonstrate the importance of mitochondrial fission in the regulation of nucleoid distribution, it could be utilized to characterize the distribution of any mitochondrial proteins dispersed as individual foci along mitochondrial networks.

Our results indicate that in healthy cells, nucleoids are distributed in a semi-regular manner, with nucleoids strongly avoiding each other at closer distances (Fig. 3a, b). This is consistent with previous manual nndist measurements in yeast and human cells[15,16] and strongly support the notion that nucleoid distribution is actively regulated in the cells.

Recently, we have shown that mutation of the mitochondrial fission protein MYH14 reduced total nucleoid population without altering mtDNA content[10]. Similarly, knock down or genetic ablation of DRP1 altered nucleoid content by causing the formation of mitobulbs[9,12,13]. As these results suggest a potential role for fission in nucleoid maintenance, we have used both mutants to directly address the role of

mitochondrial fission in the regulation of nucleoid distribution. Our results show that inhibiting mitochondrial fission disrupted nucleoid distribution as reflected by the high variability of the pcf curves and the perinuclear accumulation of enlarged nucleoids in both MYH14 and DRP1 mutants. Specifically, some mutant cells showed strong short distance correlation while in others, nucleoids avoided each other. The reduced nucleoid density observed in MYH14 and DRP1 mutants significantly contributed to this variability (entropy). Nevertheless, the specific contribution of distinct nucleoid or network parameters to the pcf varied across genotypes, suggesting a complex interplay between nucleoid and mitochondria network topologies in regulating nucleoid distribution. Consistent with this, mitochondrial networks were distinctly affected in MYH14 and DRP1 mutants, likely reflecting the distinct role of these proteins in mitochondrial fission. While DRP1 is an essential fission protein required for the physical severing of mitochondrial tubules, MYH14 encodes one of three non-muscle myosin II proteins that are involved in the initial ER-mediated constriction of the mitochondrial tubule[10,26–28]. In addition, we previously found that the mitochondrial phenotype of MYH14 mutants was most evident in the peripheral area of the cells[10], which could further affect the nucleoid distribution pattern.

The fact that our findings differed between the MYH14 and DRP1 mutant cells is not surprising, given the disparate clinical phenotypes in the patients from whom they were isolated. The MYH14 patients developed axonal sensorimotor neuropathy and sensorineural hearing loss[10], whereas the DRP1 patient had severe central nervous system involvement[24]. A question of interest for future study with this tool may be to determine whether it can resolve differences in nucleoid distribution correlated to phenotypic variation from mutations in the same gene, implicating differing biological mechanisms for alternate clinical presentations. For example, MFN2 is a major human disease gene associated with numerous mitochondrial functions (including mitochondrial fusion) and highly variable clinical phenotypes, which are not consistently correlated to cellular phenotypes[29]. In the specific case of MYH14, other mutations result in isolated and severe hearing loss or later-onset sensorineural hearing loss[30–32]. In the case of DRP1, phenotypes can vary, and recently severe cardiac involvement has been described from a novel

mutation[33]. The automated and quantitative approach described in this work presents an additional tool to assess these differences at the cellular level.

It is nevertheless important to note that in our setup, mtDNA clusters less than about 300 nm apart are not resolved and thus do not contribute to the pcf curves. While this probably does not affect wild-type cells, this could alter the analysis of the fission mutants as they contain enlarged nucleoids that likely represent a cluster of mtDNAs that failed to separate following mtDNA replication. It is thus possible that, under conditions where individual mtDNA molecules could be resolved, the pcf would detect a strong correlation at very short distances (< 300 nm) in these cells. In addition, the thickness of the cells used for imaging could affect the outcome of the pcf. Here, we used flat cells (fibroblasts), which allowed us to consider single plane images without affecting the overall results. However, while Momito has been designed to address the 3D structure of mitochondrial networks[19], the proper identification of mitochondria and nucleoids could be affected in thicker cells, altering the pcf analysis. Nevertheless, our data supports the idea that mitochondrial fission regulates nucleoid distribution and prevents nucleoid clustering to facilitate homogenous distribution of nucleoids within mitochondrial networks.

In conclusion, our results indicate that, while mitochondrial fission might not directly control mtDNA replication, it plays an essential role by regulating nucleoid distribution across mitochondrial networks. This process is likely required to facilitate homogenous distribution of mtDNA and OXPHOS protein subunits and its alteration in fission mutants likely contribute to the development of associated pathological conditions.

Methods

Reagents

Cell culture reagents were obtained from Wisent. Other chemicals were purchased from Sigma-Aldrich, except where indicated.

Cell culture and live cell imaging

Primary human fibroblasts (controls, MYH14 mutants and DRP1 mutants) were generated from skin biopsies, collected as part of an approved research protocol (University of Calgary Research Ethics Board (MYH14 mutants), Research Ethics Board of the Children's Hospital of Eastern Ontario (DRP1 mutants)), and written informed consent from participants was obtained. This study was performed in accordance with the Declaration of Helsinki. Biopsy samples were processed as described and cultured in Dulbecco's modified Eagle's medium (DMEM) containing 10% fetal bovine serum (FBS), supplemented with Penicillin/Streptomycin (100 IU/ml/100µL/mL)[24,34]. Immortalized Mouse Embryonic Fibroblasts (MEFs) were cultured in DMEM supplemented with 10% fetal bovine serum. For live cell imaging, cells were seeded onto glass bottom dishes and stained for 30 min with 250 nM TMRM (Thermo fisher Scientific, T668) (MEFs and DRP1 mutant and control human fibroblasts) or 50 nM Mitotracker Red (Thermo fisher scientific, M7512) (MYH14 mutant and control fibroblasts) and the DNA dye PicoGreen (Thermo Fisher Scientific, P11495) (3 µL/ mL). After staining, cells were washed 3 times with pre-warmed 1 × phosphate buffered saline (PBS), and normal growth media was added prior to imaging.

Microscopy

Images for MEFs, DRP1 mutant fibroblasts and their wild-type control were acquired with a Leica TSC SP8 confocal microscope fitted with a 63×/1.40 oil objective using the optimal resolution for the wavelength (determined using the Leica software). Images from MYH14 cells and their control were taken with an Olympus spinning disc confocal system (Olympus SD-OSR) (UAPON 100XOTIRF/1·49 oil objective) operated by Metamorph software. The SD-OSR was equipped with a cellVivo incubation module to maintain cells at 37ºC and 5% C O2 during live cell imaging.

Image analysis using Mitomate tracker

Red and green channels were separated, nuclei were manually removed from the Picogreen channel, and the images converted to 8-bit using ImageJ. The mitochondrial channel was then segmented using the ImageJ filter tubeness and global thresholding. To measure the correlation between nucleoids on the mitochondrial network, the images were analyzed using the R package spatstat (flowchart in Fig. S2). This analysis requires two inputs: a linear network (mitochondria) and a point pattern (nucleoids). Mitochondrial components (tubules, ends (E), junctions (J)) were extracted from the segmented mitochondrial image and the most probably network configuration determined using Momito[19].While Momito takes into account the presence of overlapping tubules for its analysis of the most probable mitochondrial network, care was taken to use cells that have a flat and clearly identifiable mitochondrial network to avoid issues related to cell thickness. This was used as the input for the linear network. Nucleoids were identified using the ImageJ plugin TrackMate[20] and the coordinates of the nucleoids associated with the mitochondrial network (within 6 pixels center to center) used to generate the point pattern. Overall, 97 ± 1% of the nucleoids were properly identified in control cells, although 38%of the larger nucleoids (> 0.6 μm) present in mutant cells were identified as 2 or more nucleoids. Each nucleoid was assigned to a single mitochondrial cluster (connected mitochondrial tubules) and only nucleoids within the same cluster were analyzed together.

The pcf analysis was then carried using the spatstat linear pcf function for distances from 0 to 300 pixels (although distances < 5 pixels (< 0.3 μm) are within the resolution limit of the images) with a bias correction at each end of the interval (*correction = "Ang"*) and a bandwidth of 5 pixels (corresponding to the size of control nucleoids), while the nndist was calculated using the spatstat nndist function. As Spatstat computes the pcf for individual mitochondrial clusters, we had to sum the contribution of each cluster to generate the total pcf by taking into consideration the size of each mitochondrial cluster and the number of nucleoids that it contains. This was achieved as follows:

In Spatstat, the estimator for the pcf $\hat{g}_k(r)$ for a given subgraph G_k(a mitochondrial cluster) is given by

$$\hat{g}_k(r) = \frac{l(G_k)}{n_k(n_k-1)} \sum_{i=1}^{n_k} \sum_{j \neq i} \frac{\kappa\left(d_{G_k}(x_i, x_j) - r_k\right)}{m\left(x_i, d_{G_k}(x_i, x_j)\right)}$$

Where κ is the gaussian kernel of 5 pixels used for smoothing and m is analogous to the perimeter for a network of radius $d_{G_k}(x_i, x_j)$ around the point x_i. The length of the subgraph is $l(G_k)$ and it contain $n_k$points. We have normalized the pcf $\hat{g}_k(r)$ for the whole network (graph, G) by

$$\hat{g}_G(r) = \frac{\sum_{G_k \in G} l(G_k)}{\sum_{G_k \in G} n_k(n_k-1)} \sum_{G_k \in G} \frac{n_k(n_k-1)\, \hat{g}_k(r)}{l(G_k)}.$$

In addition, to avoid spurious effects caused by variation in nucleoid density and network features (length and connectivity), we normalized both nndist and pcf by dividing the observed value (actual nndist or pcf) by the value obtained using an IRP with the same point density distributed across the same network. For the pcf, this was done for each distance (r) measured. The randomized point pattern used to correct for network effects was generated using the spatstat *runiflpp* function with the same number of points as the actual point pattern. The coordinates of the IRP points were directly fed to the *linearpcf* and *nndist* functions. Each image was run six times and averaged. To simplify the process, the analysis was automated using a Java script run on Eclipse. Network features and the total number of nucleoids were directly extracted from the Mitomate tracker analysis, except for the connectivity that was defined as the total number of junctions (J)/total number of mitochondrial ends (E) for each individual cell[19].

To compare the effect of nucleoid and mitochondrial features on the pcf with random distributions, we generated random point patterns with a similar density as that of the actual point patterns (distinct from the IRP used above to correct for network effects

but still fed directly to spatstat) using the same Java script. However, as each of these IRPs represent a specific distribution that can somewhat vary from the expected random distribution (especially when point density is low), 6 distributions were averaged for each experiment to avoid measuring effects due to specific random distributions. In the case of experiments where nucleoids were randomly removed, an individual distribution with points removed was considered as the actual data that was normalized over the average of 6 random distributions.

Analysis of spatial distribution

8-bit nucleoid images and segmented mitochondria networks were manually separated into perinuclear and peripheral mitochondrial clusters using ImageJ. The perinuclear region was defined based on the relative distribution of nucleoid from the nucleus. The perinuclear area corresponds to 1/3rd of the total cellular area (long axis distance from nuclear membrane ~ 23 μm). However, care was taken to keep individual mitochondrial clusters intact when separating the mitochondrial network (each independent cluster were labeled as either perinuclear or peripheral). These images were then used to measure nucleoid size (ImageJ—*Analyze Particle* function).

Data analysis and statistics

All data analysis was done in R. To quantify the entropy, pcf values for each distance first needed to be converted into a character string. This was achieved by first converting the decimal numbers into a whole number between 1 and 26 and attributing a letter to each number. The entropy of the resulting character string was then calculated using the entropy function of the R package a css[35]. The PCA was done using the R function *prcomp* while Pearson correlations were determined using the *ggcorr* function (GGally package).

Statistical analysis was done using Student's t test (between 2 groups) or one-way ANOVA with a Tukey post hoc test (multiple comparisons). Differences between nucleoid distributions were calculated using a KS test (*ks.test* function from the stats

package). Linear regressions for correlation analysis were calculated using a lm method with y ~ log(x) as the general formula.

Code availability

The code for Mitomate tracker is available on GitHub (https://github.com/ GermainLab/mitomate).

Acknowledgements

We thank Andrea Bertolo for his help with the entropy calculations and A Micheil Innes who, with GP, provided the MYH14 mutants. This work was supported by grants from the Natural Sciences and Engineering Research Council of Canada and the Fondation de l'UQTR to MG, as well as the Alberta Children's Hospital Research Institute to TS. HSI was supported by a Queen Elizabeth II Diamond Jubilee Scholarship and a FRQ-NT scholarship, while RS was supported by a QEII Graduate Scholarship. MO received a CIHR undergraduate scholarship for this work.

References

1. Sasaki, T., Sato, Y., Higashiyama, T. & Sasaki, N. Live imaging reveals the dynamics and regulation of mitochondrial nucleoids during the cell cycle in Fucci2-HeLa cells. Sci. Rep. 7, 11257. https:// doi. org/ 10. 1038/ s41598- 017- 10843-8 (2017).

2. Giacomello, M., Pyakurel, A., Glytsou, C. & Scorrano, L. The cell biology of mitochondrial membrane dynamics. Nat. Rev. Mol. Cell Biol. 21, 204–224. https:// doi. org/ 10. 1038/ s41580- 020- 0210-7 (2020).

3. Barsh, G. S. et al. Mitochondrial fusion is required for regulation of mitochondrial DNA replication. PLOS Genet. https://d oi.org/ 10. 1371/ journ al. pgen. 10080 85 (2019).

4. El-Hattab, A. W., Craigen, W. J., Wong, L. J. C. & Scaglia, F. in GeneReviews((R)) (eds. Adam, M. P. et al.) (1993).

5. Viscomi, C. & Zeviani, M. MtDNA-maintenance defects: Syndromes and genes. J. Inherit. Metab. Dis. 40, 587–599. https:// doi. org/ 10. 1007/ s10545- 017- 0027-5 (2017).

6. Friedman, J. R. et al. ER tubules mark sites of mitochondrial division. Science 334, 358–362. https://d oi.org/1 0 .1126 /s cience.1 207 3 85 (2011).

7. Pagliuso, A., Cossart, P. & Stavru, F. The ever-growing complexity of the mitochondrial fission machinery. Cell. Mol. Life Sci. (CMLS) 75, 355–374. https:// doi. org/ 10. 1007/ s00018- 017- 2603-0 (2018).

8. Lewis, S. C., Uchiyama, L. F. & Nunnari, J. ER-mitochondria contacts couple mtDNA synthesis with mitochondrial division in human cells. Science 353, aaf5549. https:// doi. org/ 10. 1126/ scien ce. aaf55 49 (2016).

9. Ban-Ishihara, R., Ishihara, T., Sasaki, N., Mihara, K. & Ishihara, N. Dynamics of nucleoid structure regulated by mitochondrial fission contributes to cristae reformation and release of cytochrome c. Proc. Natl. Acad. Sci. U.S.A. 110, 11863–11868. https://doi.org/ 10. 1073/ pnas. 13019 51110 (2013).

10. Almutawa, W. et al. The R941L mutation in MYH14 disrupts mitochondrial fission and associates with peripheral neuropathy. EBioMedicine 45, 379–392. https:// doi. org/ 10. 1016/j. ebiom. 2019. 06. 018 (2019).

11. Parone, P. A. et al. Preventing mitochondrial fission impairs mitochondrial function and leads to loss of mitochondrial DNA. PLoS ONE https:// doi. org/ 10. 1371/ journ al. pone. 00032 57 (2008).

12. Ota, A., Ishihara, T. & Ishihara, N. Mitochondrial nucleoid morphology and respiratory function are altered in Drp1-deficient HeLa cells. J. Biochem. 167, 287–294. https:// doi. org/ 10. 1093/ jb/ mvz112 (2020).

13. Ishihara, T. et al. Dynamics of mitochondrial DNA nucleoids regulated by mitochondrial fission is essential for maintenance of homogeneously active mitochondria during neonatal heart development. Mol. Cell. Biol. 35, 211–223. https:// doi. org/ 10. 1128/ MCB. 01054- 14 (2015).

14. Kukat, C. et al. Super-resolution microscopy reveals that mammalian mitochondrial nucleoids have a uniform size and frequently contain a single copy of mtDNA. Proc. Natl. Acad. Sci. U.S.A. 108, 13534–13539. https://d oi.org/1 0 .1073 /p nas.110926 310 8 (2011).

15. Tauber, J. et al. Distribution of mitochondrial nucleoids upon mitochondrial network fragmentation and network reintegration in HEPG2 cells. Int. J. Biochem. Cell Biol. 45, 593–603. https:// doi. org/ 10. 1016/j. biocel. 2012. 11. 019 (2013).

16. Osman, C., Noriega, T. R., Okreglak, V., Fung, J. C. & Walter, P. Integrity of the yeast mitochondrial genome, but not its distribution and inheritance, relies on mitochondrial fission and fusion. Proc. Natl. Acad. Sci. U.S.A. 112, E947-956. https:// doi. org/ 10. 1073/ pnas. 15017 37112 (2015).

17. Jajoo, R. et al. Accurate concentration control of mitochondria and nucleoids. Science 351, 169–172. https://doi.org/10.1126 /s cien ce. aaa87 14 (2016).

18. Iborra, F. J., Kimura, H. & Cook, P. R. The functional organization of mitochondrial genomes in human cells. BMC Biol. 2, 9. https:// doi. org/ 10. 1186/ 1741-7007-2-9 (2004).

19. Ouellet, M., Guillebaud, G., Gervais, V., Lupien St-Pierre, D. & Germain, M. A novel algorithm identifies stress-induced alterations in mitochondrial connectivity and inner membrane structure from confocal images. PLOS Comput. Biol. https://doi.org/10.1371 / journ al. pcbi. 10056 12 (2017).

20. Tinevez, J. Y. et al. TrackMate: An open and extensible platform for single-particle tracking. Methods 115, 80–90. https:// doi. org/10. 1016/j. ymeth. 2016. 09. 016 (2017).

21. Baddeley, A., Rubek, E. & Turner, R. Spatial Point Patterns: Methodology and Applications with R (Chapman and Hall/CRC Press, 2015).

22. Shannon, C. E. A mathematical theory of communication. Bell Syst. Tech. J. 27, 623–656. https://d oi.org/1 0 .1002 /j.1 538-7305.1 948. tb009 17.x (1948).

23. Shannon, C. E. A mathematical theory of communication. Bell Syst. Tech. J. 27, 379–423. https://d oi.org/1 0 .1002 /j.1 538-7305.1 948. tb013 38.x (1948).

24. Vanstone, J. R. et al. DNM1L-related mitochondrial fission defect presenting as refractory epilepsy. Eur. J. Hum. Genet. (EJHG) 24, 1084–1088. https://doi. org/ 10. 1038/ ejhg. 2015. 243 (2016).

25. Silva Ramos, E. et al. Mitochondrial fusion is required for regulation of mitochondrial DNA replication. PLoS Genet 15, e1008085. https:// doi. org/ 10. 1371/ journ al. pgen. 10080 85 (2019).

26. Kamerkar, S. C., Kraus, F., Sharpe, A. J., Pucadyil, T. J. & Ryan, M. T. Dynamin-related protein 1 has membrane constricting and severing abilities sufficient for mitochondrial and peroxisomal fission. Nat. Commun. https://doi.org/10 .1038 /s 41467-018-0 7543- w (2018).

27. Smirnova, E., Shurland, D.-L., Ryazantsev, S. N. & van der Bliek, A. M. A human dynamin-related protein controls the distribution of mitochondria. J. Cell Biol. 143, 351–358. https:// doi. org/ 10. 1083/ jcb. 143.2. 351 (1998).

28. Korobova, F., Gauvin, T. J. & Higgs, H. N. A role for myosin II in mammalian mitochondrial fission. Curr. Biol. 24, 409–414. https:// doi. org/ 10. 1016/j. cub. 2013. 12. 032 (2014).

29. Sharma, G. et al. Characterization of a novel variant in the HR1 domain of MFN2 in a patient with ataxia, optic atrophy and sensorineural hearing loss. bioRxiv. https:// doi. org/ 10. 1101/ 2021. 01. 11. 426268 (2021).

30. Kim, B. J. et al. Discovery of MYH14 as an important and unique deafness gene causing prelingually severe autosomal dominant nonsyndromic hearing loss. J. Gene Med. https:// doi. org/ 10. 1002/ jgm. 2950 (2017).

31. Wang, M. et al. A novel MYH14 mutation in a Chinese family with autosomal dominant nonsyndromic hearing loss. BMC Med. Genet. 21, 154. https:// doi. org/ 10. 1186/ s12881- 020- 01086-y (2020).

32. Donaudy, F. et al. Nonmuscle myosin heavy-chain gene MYH14 is expressed in cochlea and mutated in patients affected by autosomal dominant hearing impairment (DFNA4). Am. J. Hum. Genet. 74, 770–776. https:// doi. org/ 10. 1086/ 383285 (2004).

33. Vandeleur, D. et al. Novel and lethal case of cardiac involvement in DNM1L mitochondrial encephalopathy. Am. J. Med. Genet. Part A 179, 2486–2489. https:// doi. org/ 10. 1002/ ajmg.a. 61371 (2019).

34. Martens, K. et al. Case Report: Calpainopathy presenting after bone marrow transplantation, with studies of donor genetic content in various tissue types. Front. Neurol. 11, 604547. https:// doi. org/ 10. 3389/ fneur. 2020. 604547 (2020).

35. Gauvrit, H. S., Soler-Toscano, F. & Zenil, H. Algorithmic complexity for psychology. A user-friendly implementation of the coding theorem method. arXiv 1409.4080 (2014).

Supplementary Figures

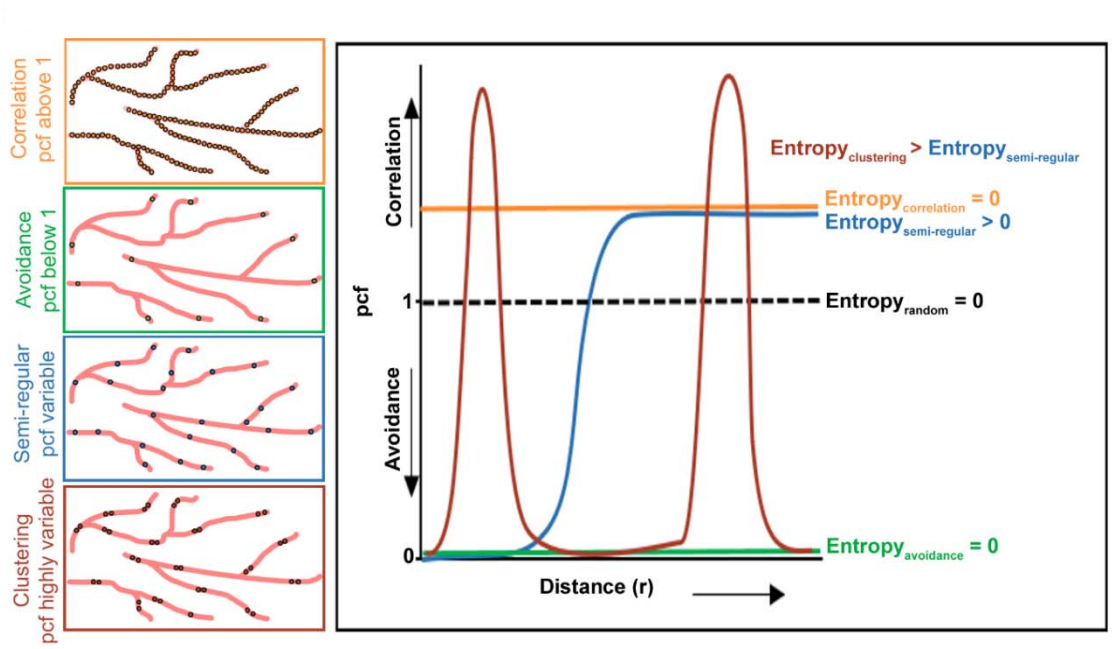

Sup. Figure S1. Entropy, a measure of variability in nucleoid distribution. The left panel represent different possible nucleoid distributions within mitochondrial networks. The right panel shows the expected pcf curves for the same distributions. Pcf value above 1 suggest correlation and anything below 1 suggest avoidance between nucleoids. The entropy, calculated from the pcf curves, increases with increasing variability of the pcf curve (an horizontal line has an entropy value of zero).

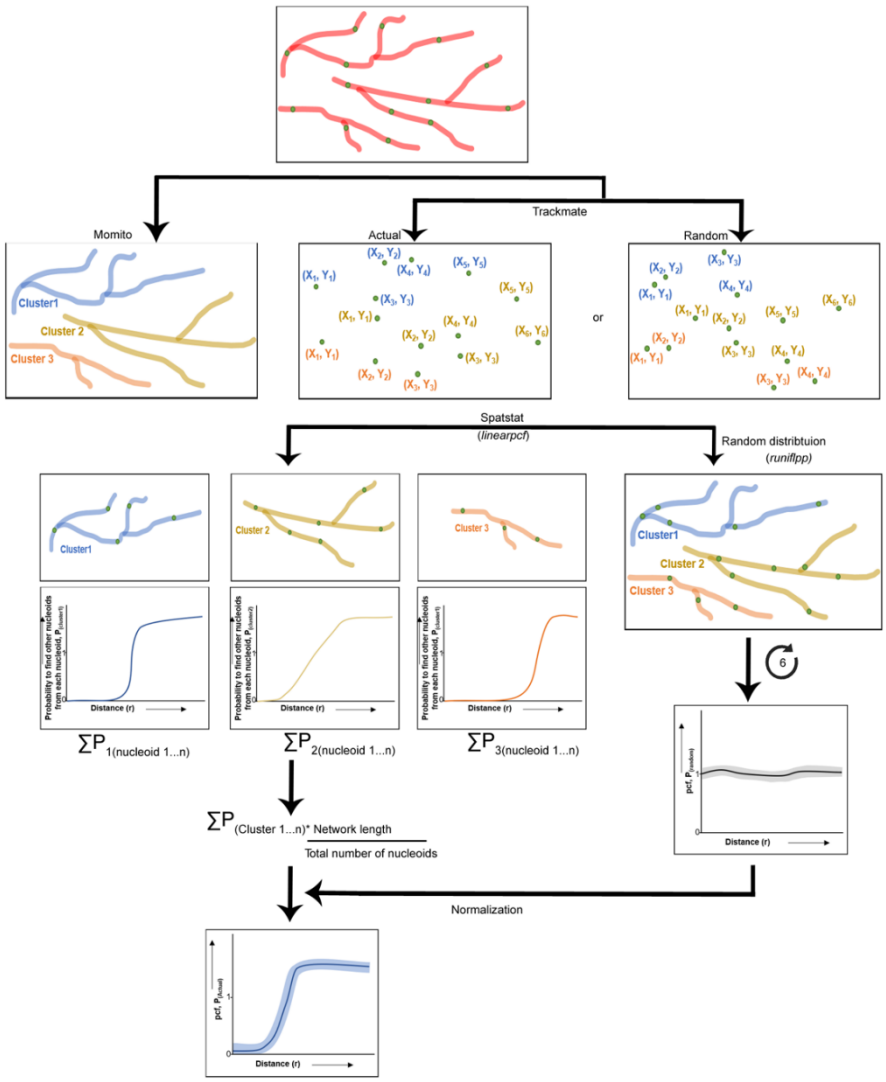

Sup. Figure S2. Workflow of Mitomate tracker. The preprocessed mitochondrial images are analyzed by Momito to extract mitochondrial network features. The coordinates of nucleoid in actual or random distributions are extracted by the Image J plugin Trackmate. Based on this information, Spatstat measures the probability of nucleoid distribution in each individual mitochondrial cluster (independent mitochondrial network). Overall nucleoid distribution is calculated by summing up the probability in all mitochondrial clusters. To take into account the effect of network features and nucleoid density, 6 random distributions (using *runiflpp* function) are averaged and used to normalize the actual distribution.

CHAPTER III

DRP1 REGULATES ENDOPLASMIC RETICULUM SHEETS TO CONTROL MITOCHONDRIAL DNA REPLICATION AND SEGREGATION

Under review; Pre-print available in bioRxiv (2021).
DOI : https://doi/:10.1101/2021.12.09.472002

Hema Saranya Ilamathi[1,2,3], Sara Benhammouda[1,2,3], Justine Desrochers-Goyette[1,2,3], Matthew A., Lines[4], Marc Germain[1,2,3#]

[1] Groupe de Recherche en Signalisation Cellulaire and Département de Biologie Médicale, Université du Québec à Trois-Rivières, Trois-Rivières, Québec, Canada

[2] Centre d'Excellence en Recherche sur les Maladies Orphelines - Fondation Courtois, Université du Québec à Montréal, Montréal, Québec, Canada

[3] Réseau Intersectoriel de Recherche en Santé de l'Université du Québec (RISUQ)

[4] Department of Medical Genetics, Cumming School of Medicine, University of Calgary, Calgary, Alberta, Canada

Correspondence: Marc Germain (marc.germain1@uqtr.ca)

Author contributions

HSI performed all the experiments. HSI and MG designed the experiments. HSI, JDG, and MG analyzed all the data either manually or using pre-exiting image J tools. SB manually quantified data related to mitochondrial network organization in CLIMP63 expressing cells. MAL provided the clinical samples. HSI and MG wrote the paper. All authors reviewed and discussed the manuscript.

Abstract

Mitochondria are multi-faceted organelles crucial for cellular homeostasis that contain their own genome. Mitochondrial DNA (mtDNA) codes for several essential components of the electron transport chain, and mtDNA maintenance defects lead to mitochondrial diseases. mtDNA replication occurs at endoplasmic reticulum (ER)-mitochondria contact sites and is regulated by mitochondrial dynamics. Specifically, mitochondrial fusion is essential for mtDNA maintenance. In contrast, while loss of mitochondrial fission causes the aggregation of nucleoids (mtDNA-protein complexes), its role in nucleoid distribution remains unclear. Here, we show that the mitochondrial fission protein DRP1 regulates nucleoid segregation by altering ER sheets, the ER structure associated with protein synthesis. Specifically, DRP1 loss or mutation leads to altered ER sheets that enhance physical interaction with mitobulbs, mitochondrial structures containing aggregated nucleoids. Importantly, nucleoid distribution and mtDNA replication were rescued by expressing the ER sheet protein CLIMP63. Thus, our work identifies a novel fission-independent mechanism by which DRP1 regulates mtDNA replication and distribution.

Keywords: mtDNA, DRP1, fission, ER sheets, CLIMP63, mitochondria

Introduction

Mitochondria are dynamic organelles regulating an array of cellular processes including energy production, cellular metabolism, apoptosis, calcium signaling, ROS signaling, cellular differentiation and immune response against pathogens (1-6). These mitochondrial functions are regulated by mitochondrial dynamics, the processes of mitochondrial fusion and fission. Mitochondrial fission requires DRP1 (Dynamin-Related Protein 1) (7, 8), while fusion is regulated by Mitofusins 1 and 2 (MFN1 & 2) and Optic Atrophy Protein 1 (OPA1) present on mitochondrial outer and inner membrane respectively (9, 10). Mitochondrial dynamics are also essential for mitochondrial DNA (mtDNA) maintenance, with defects in mitochondrial fusion affecting mtDNA integrity

and copy number (11, 12). On the other hand, while defective mitochondrial fission does not generally affect overall mtDNA content, it alters the distribution of nucleoids (mtDNA-protein complexes), leading to the formation of bulb-like mitochondrial structures termed mitobulbs (13-16). Importantly, both mitochondrial fission and mtDNA replication are initiated at sites of contact between mitochondria and the endoplasmic reticulum (ERMCS) (17-19), indicating a crucial role for the ER in the regulation of mitochondrial structure and function.

The ER is a complex web-like organelle that includes flattened cisternae/sheets around the perinuclear region and tubulated structures towards the cellular periphery (20). ER sheets/ rough ER (rER) are enriched with ribosomes and regulate the production and assembly of proteins for secretion (21). On the other hand, ER tubules / smooth ER (sER) play important roles in lipid synthesis and calcium signaling, but also in mitochondrial dynamics and mtDNA replication (17-19, 21). At the molecular level, the ER resident protein CLIMP63 (CKAP4) is essential for the maintenance of ER sheets, while reticulons (RTN) and DP1/Yop1p are essential for both ER tubule formation and the maintenance of ER sheet curvature (22, 23). The ratio of sheet to tubule proteins regulates the balance between the two ER structures (22). In addition, recent studies showed that the mitochondrial fission protein DRP1 associates with the ER independently of mitochondria where it helps regulate ER tubulation (24, 25). While this suggests a complex interplay between mitochondria-shaping proteins and ER tubules, the role of ER sheets in these processes remains poorly understood. This is an important question because some reports suggest that ER sheets also contact mitochondria (26).

Here, we show that DRP1 controls the interaction between ER sheets and mitochondria by regulating ER sheet structure. Specifically, primary human fibroblasts from patients with a mutation in DRP1 showed altered ER sheet structure and increased interaction with mitochondria that were associated with a reduction in mtDNA replication and distribution. Importantly, modulating ER sheets through the expression of CLIMP63 normalized ER sheets-mitochondrial interaction, thereby rescuing mtDNA replication and distribution in DRP1 mutants. Altogether, our results demonstrate that DRP1-dependent

control of ER sheet structure regulates replication and distribution of mtDNA independently of mitochondrial dynamics.

Results

DRP1 associates with ER sheets

DRP1 is a key mitochondrial dynamics protein required for mitochondrial fission. (27). Recent evidence suggest that DRP1 also alters ER tubules in a manner that is independent of its GTPase activity (25) and ER shaping proteins (CLIMP63, RTN4). To perform these roles, DRP1 directly associates with the ER (24, 25), especially ER tubules. However, a large portion of perinuclear ER adopts a specific sheet structure that is morphologically and functionally distinct from ER tubules. To determine whether DRP1 associates with ER sheets, we marked primary human fibroblasts for mitochondria (mitotracker orange), ER sheets (endogenous CLIMP63), and endogenous DRP1 and imaged them by confocal microscopy. We found that the majority of DRP1 foci present in the perinuclear region were associated with mitochondrial tubules (Fig. 1A, arrows in left panel, line scan in right panel, quantification in B). Of these, 30% were also colocalized with ER sheets (Fig. 1B). In addition, we observed a sub-population of DRP1 (10%) associated with ER sheets independently of mitochondria (Fig. 1A, arrowheads in left panel, line scan in right panel, quantification in B). To further define the interaction between DRP1 and ER sheets relative to mitochondria, we transfected control human fibroblasts with mCherry-CLIMP63 and GFP-DRP1 and performed live cell imaging. Consistent with our results in fixed cells, some DRP1 foci remained associated with CLIMP63 over time in the absence of mitochondrial signal (Fig. 1C, arrows). In addition, several DRP1 foci were associated with both ER sheets and mitotracker labelled mitochondria (Fig. 1C, open arrowheads). Altogether, these results indicate that DRP1 interacts with ER sheets.

As a significant fraction of DRP1 was associated with both ER sheets and mitochondria, we then determined whether this was linked to mitochondrial fission.

In fact, while the majority of DRP1 foci associated with both ER sheets and mitochondria did not lead to fission, all observed DRP1-dependent fission events were marked by an ER sheet (Fig. 1C, arrowhead; quantification in 1D). The ER sheet was then usually released from one of the mitochondrial ends following the segregation of the two daughter mitochondria (Fig. 1D, average time to release 50±23 sec), while the DRP1 foci present at the fission site remained associated with the ER (Fig. 1C, arrowhead; quantification in 1E). Altogether, these results indicate that DRP1 associates with ER sheets where it regulates mitochondrial fission. In addition, the observation that DRP1 stays associated with ER sheets following fission suggests that this process could regulate ER sheet-mitochondria contact sites.

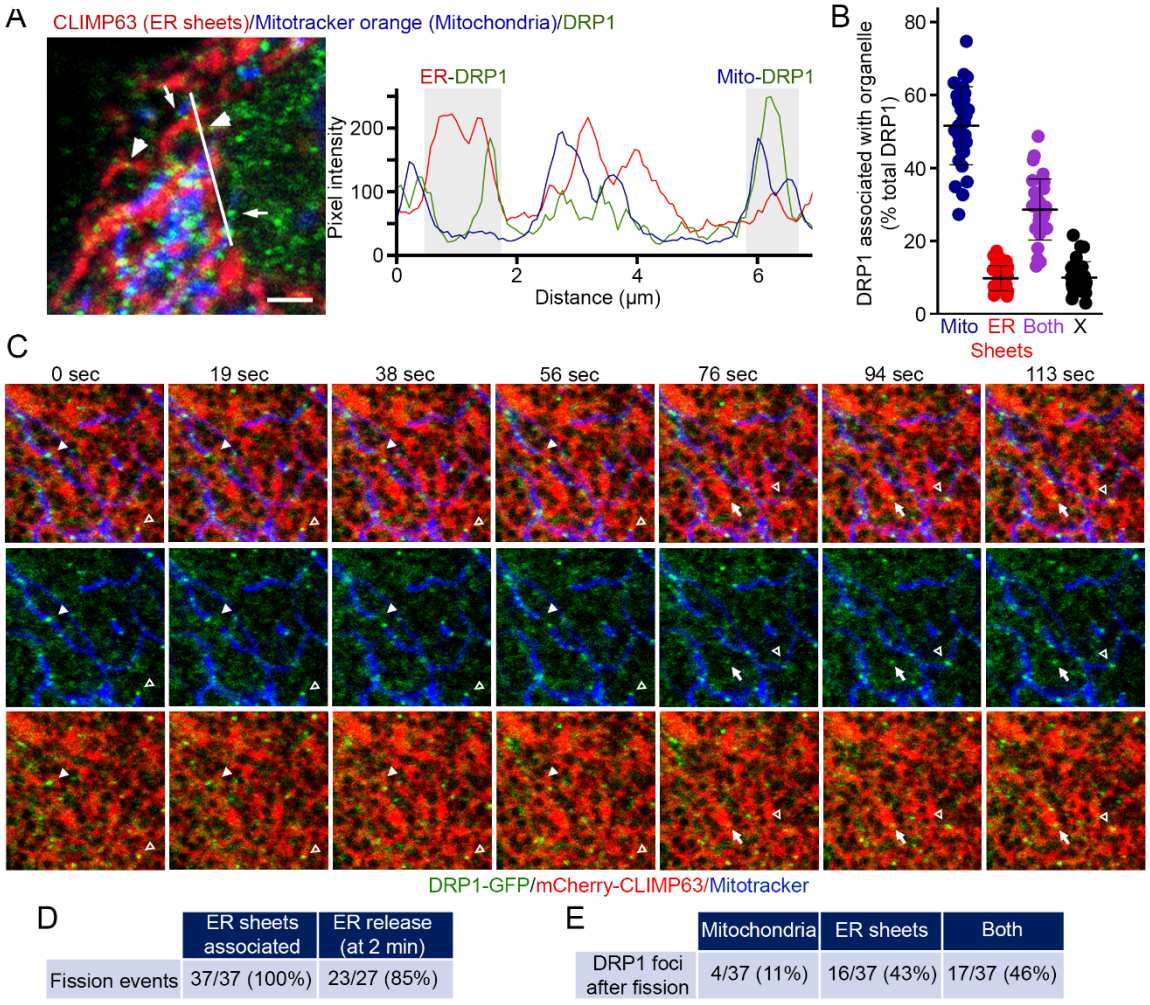

D

	ER sheets associated	ER release (at 2 min)
Fission events	37/37 (100%)	23/27 (85%)

E

	Mitochondria	ER sheets	Both
DRP1 foci after fission	4/37 (11%)	16/37 (43%)	17/37 (46%)

Figure 1. DRP1 associates with ER sheets. (A) DRP1 associates with ER sheets. Representative image of control human fibroblasts showing DRP1 (Green), mitochondria (Mitotracker orange, Blue) and ER sheets (CLIMP63, Red). Colocalization of DRP1 with mitochondria (arrows) and ER sheets (arrowheads). Line scan analysis confirmed the colocalization (right panel). (B) Quantification of the association of DRP1 with mitochondria (mitotracker orange) and ER sheets (RRBP1). Each data point represents one cell. Bars represent the average of 41 cells in 3 independent experiments ± SD (C) Live cell imaging of control human fibroblasts transfected with DRP1-GFP (Green) and mCherry-CLIMP63 (Red). Mitochondria were labelled with Mitotracker Deep Red (Blue). DRP1 foci associated with ER sheets (arrow), ER sheets and mitochondria (open arrowheads) and ER sheets at the site of mitochondrial fission (filled arrowheads) are indicated. (D-E) Quantification of mitochondrial fission from time lapse videos as in (C). A total of 37 fission events were observed in 15 cells (5 minutes total/video). Fission events occurring in the last two frames of the videos were excluded from the calculation of the number of fission events where ER sheets dissociated from mitochondria within 2 minutes of the fission event (D).

Mutation in DRP1 affects ER sheets-mitochondria interaction

To determine whether DRP1 mutation alters mitochondria-ER sheet contact sites, we measured the interaction between the two organelles in primary fibroblasts from patients with a dominant-negative mutation in the middle domain of DRP1 which is required for DRP1 oligomerization (25, 28). Mitochondria-ER sheet contact sites were identified using a proximity ligation assay (PLA) for CLIMP63 (ER sheets) and TOM20 (mitochondria). To assess the specificity of the interaction, we also co-labelled the cells for CLIMP63 and TOM20. Clear PLA foci were present at sites where CLIMP63 and TOM20 signals overlapped (Fig. 2A, IgG control in Sup. Fig. S1A), suggesting that ER sheets interact with mitochondria (Fig. 2A, Zoom image). We specifically measured this interaction by manually counting PLA foci at the sites where CLIMP63 and TOM20 signals overlapped (Fig. 2A-B). We then measured mitochondria-ER sheet interactions in DRP1 mutants. As shown in Fig. 2A-B, DRP1 mutation significantly increased the interaction between mitochondria and ER sheets. A similar increase in PLA was also observed for the more general ER marker Calnexin (Fig. 2C, S1B), which marks both ER tubules and sheets, further suggesting that DRP1 regulates the interaction between the two organelles.

To further confirm our results, we imaged control and patient fibroblasts by TEM (Fig. 2D) and manually quantified the interaction between ER sheets and mitochondria ($\leq$ 30 nm) near the perinuclear region. We observed that mitochondria closely interacted with ER sheets in control fibroblasts. Consistent with the PLA data, this interaction was further enhanced in DRP1 mutant fibroblasts, as shown by the increase in both the number of ERMCS per mitochondrial length and the length of these ERMCS (Fig. 2D-F). Altogether, our data indicates that ER sheets interact with mitochondria and mutations in DRP1 alters this interaction.

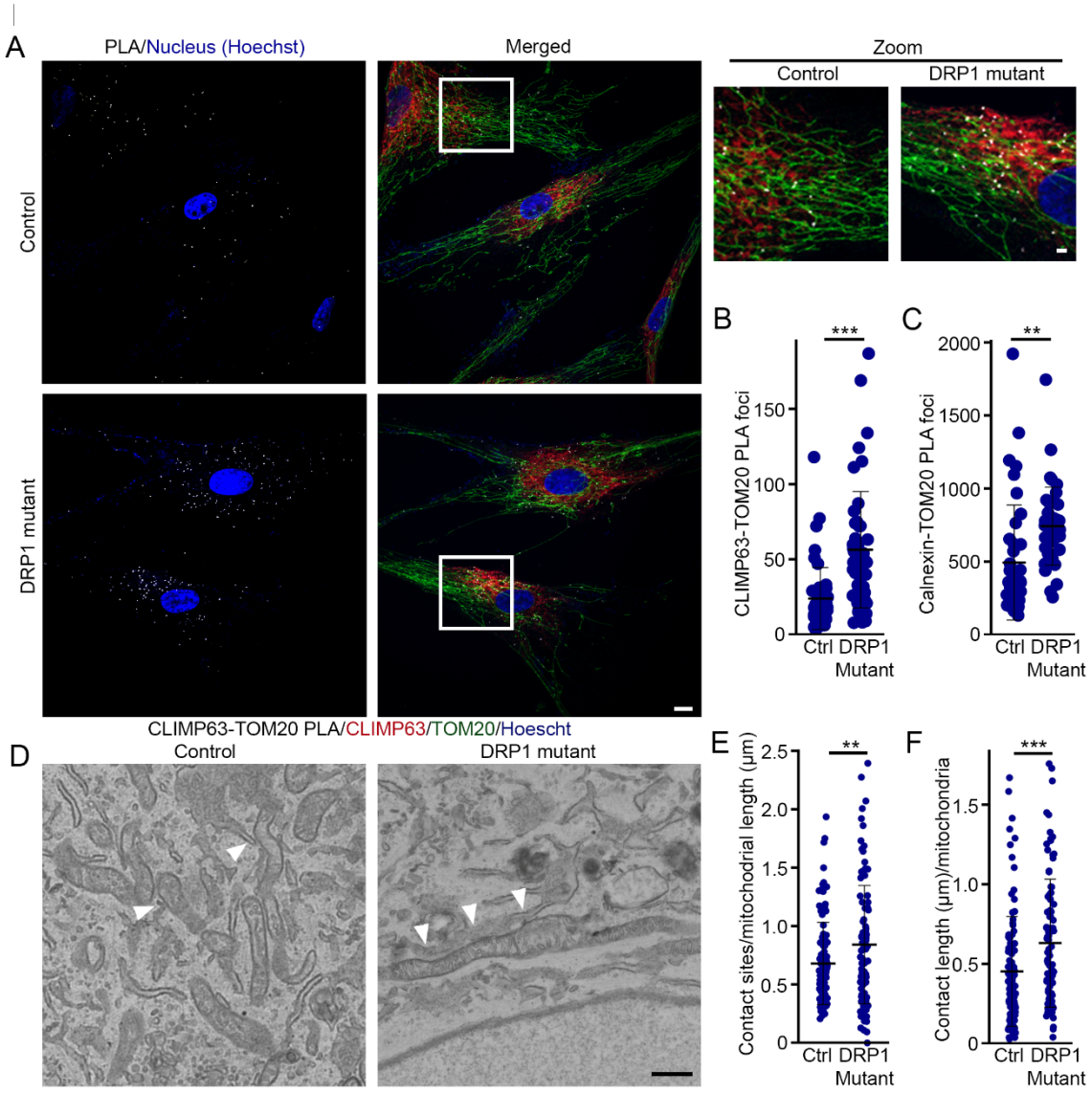

Figure 2. DRP1 regulates the interaction between ER sheets and mitochondria. (A) Representative images of control and DRP1 mutant fibroblasts showing the PLA for CLIMP63 and TOM20 (White), along with CLIMP63 (red), TOM20 (Green) and nuclei (Hoechst, Blue). Scale bar 10 µm, 2 µm for the zoomed images. (B) Quantification of CLIMP63-TOM20 PLA. Each data point represents one cell. Bars represent the average of 50 control and 48 mutant cells in 3 independent experiments ± SD *** $p < 0.001$ two-sided t-test (C) Quantification of Calnexin-TOM20 PLA. Each data point represents one cell. Bars represent the average of 40 cells per genotype in 3 independent experiments ± SD ** $p < 0.01$ two-sided t-test (D) Representative TEM images of control and DRP1 mutant fibroblasts. Scale bar 500 nm (E) Quantification of the number of ERMCS per mitochondrial length in the TEM images. Each data point represents one mitochondrion. Bars represent the average of 103 control and 97 mutant mitochondria ± SD ** $p < 0.01$ two-sided t-test (F) Quantification of ERMCs length (µm) per mitochondria in the TEM images. Each data point represents one mitochondrion. Bars represent the average of 103 control and 97 mutant mitochondria ± SD *** $p < 0.001$ two-sided t-test.

Mutation or knockdown of DRP1 alters ER sheet structure

Given that our results suggest an important functional role for ER sheets-mitochondria interaction, we then hypothesized that DRP1 mutation results in altered ER sheets. To address this question, we immunolabelled control and DRP1 mutant cells for the ER sheets marker CLIMP63 and found that DRP1 mutants had altered ER sheets compared to control cells. These alterations were characterized by a punctate appearance mostly apparent towards the periphery, and sometimes thick patches of sheets in the perinuclear region (Fig. 3A, enlarged image showing ER sheet structure; complete cell in Fig. S2). Similar alterations were observed in ER sheets marked with another ER sheet marker, RRBP1/p180 (Fig. 3B). Overall, 80% of mutant cells showed an altered ER sheet phenotype (Fig. 3C). Consistent with this, ER sheets were smaller in DRP1 mutant cells (Fig. 3D), but the overall area covered by ER sheets was expanded (Fig. 3E). Nevertheless, protein levels of ER proteins CLIMP63, RTN4, the general ER marker Calnexin and the mitochondrial proteins TOM20 and ATP5a were similar between control and DRP1 mutant cells, indicating that the changes induced by DRP1 mutation are not caused by changes in protein expression levels (Fig. 3F).

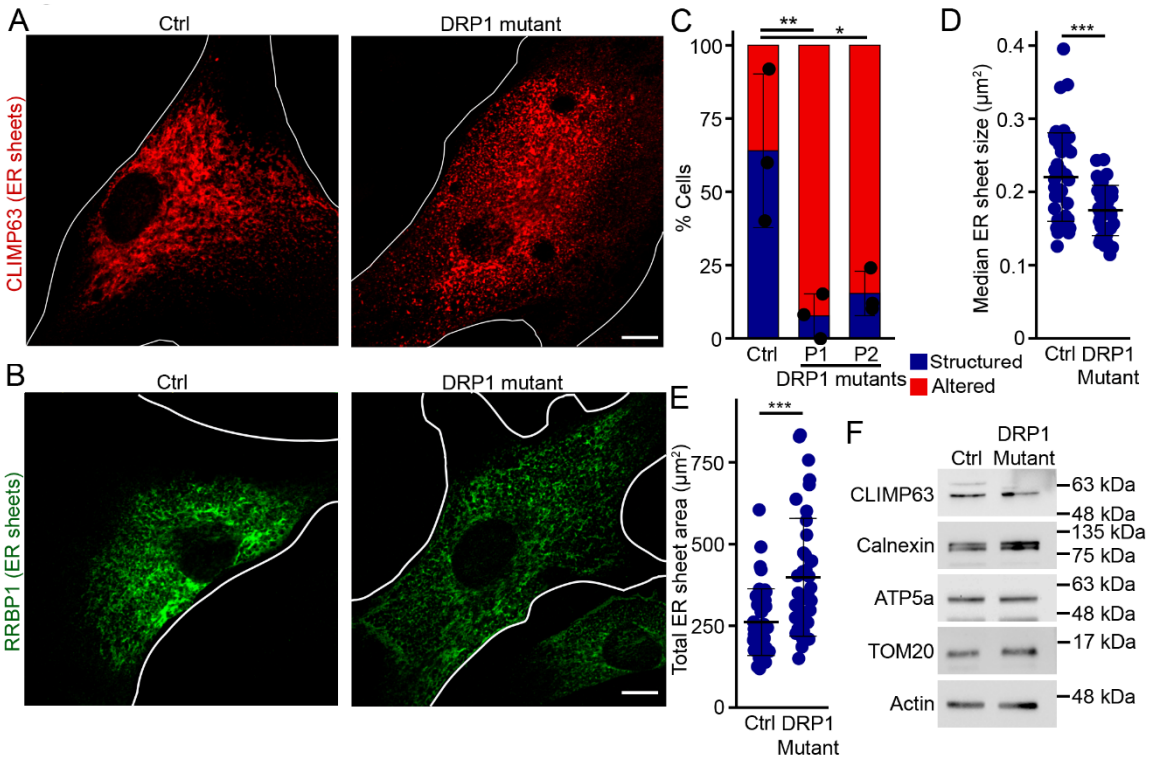

Figure 3. Loss of DRP1 function alters ER sheet structure. (A-B) Representative images of CLIMP63 (A) and RRBP1 (B) staining in control and DRP1 mutant fibroblasts. Scale bars 10 µm. (C) Quantification of ER sheet structure as Structured (Blue) or Altered (red; presence of punctate structures and thick ER sheet patches). Each point represents one independent experiment, with at least 20 cells quantified per experiment. Bars show the average ± SD. * $p < 0.05$, ** $p < 0.01$ One-way ANOVA using the data for Structured ER. (D-E) Quantification of the median size of individual ER sheets (D) and the total area covered by ER sheets (E). Each data point represents one cell. Bars represent the average of 41 cells in 3 independent experiments ± SD *** $p < 0.001$ two-sided t-test. (F) WB showing ER (CLIMP63, RTN4, calnexin) and mitochondrial proteins (TOM20, ATP5a) in control and DRP1 mutant human fibroblasts.

While our results indicates that loss of DRP1 function alters ER sheet structure, we wanted to eliminate the possibility of secondary effects in the human DRP1 mutants we used. We thus knocked down DRP1 (DRP1 KD) in mouse embryonic fibroblasts (MEFs) (Fig. S3A) and labelled them with CLIMP63 (ER sheets). Like patient fibroblasts, DRP1 KD MEFs had mostly punctate ER sheets (Fig. S3B-C) that covered an expanded area of the cell (Fig. S3D).

DRP1 has been shown to alter ER tubules in a manner that is independent of its GTPase activity (25). However, most disease associated DRP1 mutations (including the one used here (25, 28)) occur outside of the variable domain associated with ER tubulation. Consistent with this, there were no major differences between control and DRP1 mutant ER immunolabeled for endogenous RTN4 and imaged by confocal microscopy, with ER tubules clearly present in the periphery of cells from either genotype (Fig. S2). RTN4-labeled perinuclear ER was also similar in control and DRP1 mutant cells (Fig. S2). As with human fibroblasts, DRP1 KD MEFs did not show clear changes in ER tubules labelled with RTN4 (Fig. S3E).

To further confirm the structural alteration in ER sheets, we imaged control and DRP1 mutant fibroblasts by transmission electron microscope (TEM) (Fig. 4A), where ER sheets are identified as rER. ER sheets from DRP1 mutants were short with less surface area and narrower luminal width compared to control ER sheets (Fig. 4B-C), supporting our immunofluorescence data. On the other hand, ER tubule area and luminal width (identified as sER) were similar in control and DRP1 mutants (Fig. 4D-E). Altogether, our data suggest that DRP1 modulates ER sheet structure.

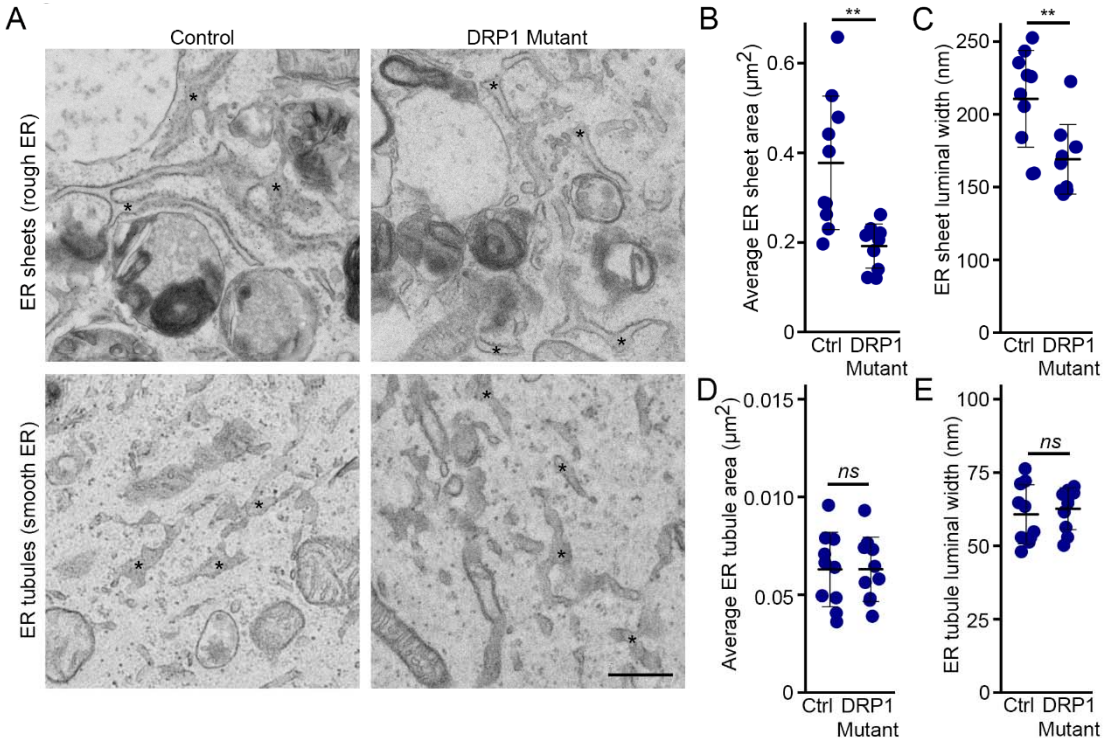

Figure 4. EM analysis of ER sheets and tubules in DRP1 mutant cells. (A) Representative EM images. Asterisks denote ER sheets (Top) or ER tubules (Bottom). Scale bar 500 nm. (B-C) Quantification of the average ER sheet area (B) and luminal width (C). Each data point represents one cell. Bars represent the average of 10 cells ± SD ** $p < 0.01$ two-sided t-test. (D-E) Quantification of the average ER tubule area (D) and luminal width (E). Each data point represents one cell. Bars represent the average of 10 cells ± SD. ns, not significant. two-sided t-test.

ER sheets are associated with mitobulbs in DRP1 mutants

Loss of DRP1 results in mitochondrial elongation with the formation of bulb-like mitochondrial structures containing enlarged nucleoids (mitobulbs) (13, 15, 16). We observed a similar phenotype in DRP1 mutant fibroblasts stained for mitochondria (TMRM) and nucleoids (picogreen) and imaged by confocal microscopy (Fig. 5A). Mitobulbs are present in the perinuclear region of DRP1 mutant cells (14) where ER sheets are present, but absent from the peripheral region characterized by RTN4-positive ER tubules (Fig. S2). These results thus suggest that the enhanced interaction between ER sheets and mitochondria leads to mitobulb formation. To test this, we analyzed the interaction between ER sheets and mitobulbs. We first immunolabelled primary

fibroblasts with CLIMP63 (ER sheets) and ATP5a (mitochondria) and imaged by confocal microscopy (Fig. 5B). Line scan analysis showed that mitobulbs are in close association with ER sheets in DRP1 mutants. (Fig. 5B-C). Further, we manually quantified the number of mitobulbs in close association with ER sheets. We found that the vast majority of mitobulbs are in close proximity to ER sheets (Fig. 5C), supporting the idea that ER sheets interact with mitobulbs. Stable association between ER and mitobulbs was also evident in live cell imaging of DRP1 mutants (ER, mCherry-Cyb5; mitochondria, mitotracker; Fig. 5D, arrows; arrowheads indicate sites of ER interacting with mitochondrial tubules).

To further confirm the presence of a physical interaction between mitobulbs and ER sheets, we performed PLA for CLIMP63 (ER sheets) and TOM20 (mitochondria). PLA foci were clearly visible at sites where ER sheets were in close proximity to mitobulbs (Fig. 5E, quantification in 5F), consistent with an interaction between the two structures. Similar results were observed when Calnexin was used instead of CLIMP63 for the PLA (Fig. 5F, S1C). Altogether, our results indicate that the altered ER sheets present in DRP1 mutants interact with mitobulbs.

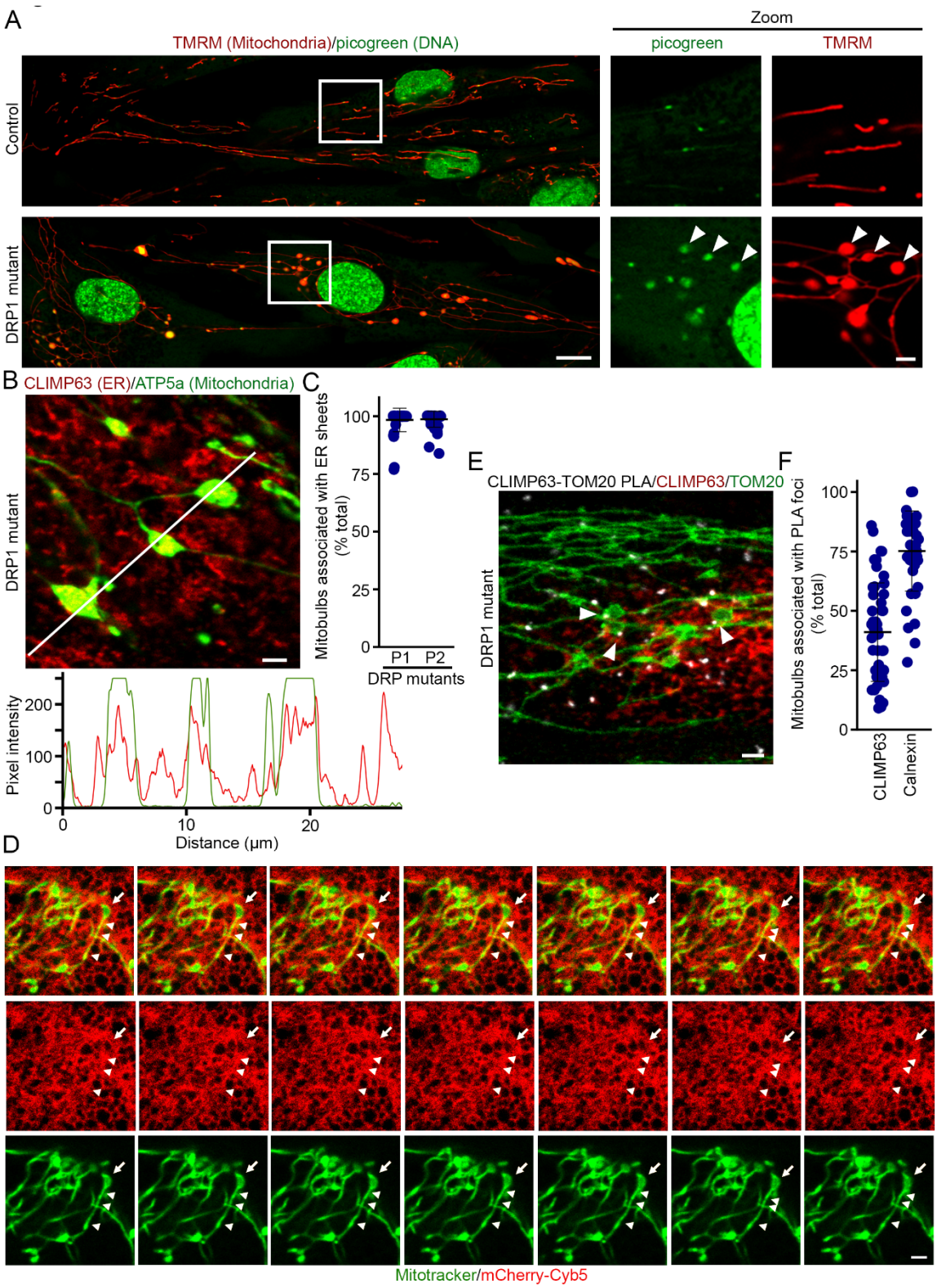

Figure 5. Modified ER sheets are associated with mitobulbs. (A) Representative live cell images showing the mitochondrial marker, TMRM and picogreen-stained DNA in

control and DRP1 mutant human fibroblasts. The zoomed images show the enlarged nucleoids present in mitobulbs (arrowheads). (B-D) Colocalisation between ER sheets and mitobulbs. Colocalisation was measured in cells immunolabelled for CLIMP63 (ER sheets) and ATP5a (mitochondria). (B) representative image (Top) and Line scan analysis (Bottom) along the line shown the image. (C) Quantification of the percent of mitobulbs that are associated with CLIMP63-positive ER sheets in two independent DRP1 mutant lines (P1 and P2). Each data point represents one cell. Bars represent the average of 45 control and 45 mutant mitochondria ± SD. (D) Live cell imaging of DRP1 mutant cells showing the interaction between ER sheets (mCherry-Cyb5, Red) and mitochondria (arrowheads) (Mitotracker, Green), including mitobulbs (arrow). (E-F) Interaction between ER sheets and mitobulbs as measured by PLA for TOM20 and CLIMP63 or Calnexin. (E) Representative image of TOM20-CLIMP63 PLA. Arrowheads denote PLA foci (White) on mitobulbs (TOM20, Green) at sites where they contact ER sheets (CLIMP63, Red). (F) Quantification of mitobulbs associated with PLA foci for TOM20-CLIMP63 and TOM20-Calnexin. Each data point represents one cell. Bars represent the average of 48 (CLIMP63 PLA) and 40 cells (Calnexin PLA) in 3 independent experiments ± SD. Scale bars 2 μm, 10 μm for (A), left panel.

Modulation of ER sheets recovers the nucleoid defects present in DRP1 mutants

To directly determine whether ER sheets affect nucleoid distribution, we modulated ER sheet structure by expressing mCherry-tagged CLIMP63 under conditions that did not overtly alter RTN4-positive ER tubules in control cells (Fig. S4A) to avoid nucleoid defects caused by the loss of ER tubules (19). Importantly, CLIMP63 expression did not rescue the fused mitochondrial phenotype of DRP1 mutant (Fig. S4B). Nevertheless, CLIMP63 expression altered ER sheet structure resulting in expanded web-like ER sheet network in both control and DRP1 mutant fibroblasts (Fig. S5). Importantly, this was accompanied by a loss of the punctate structures typically observed in mutant cells transfected with mCherry alone (Fig. S5), suggesting that CLIMP63 expression can at least partially rescue the ER sheet defects observed in DRP1 mutants. To determine if this was associated with a change in ER sheets-mitochondria interactions, we performed PLA for CLIMP63 (ER sheets) and TOM20 (mitochondria). CLIMP63 expression did not affect mitochondria-ER sheet interaction in control cells (Fig. 6A) but rescued the excessive contact sites found in DRP1 mutant cells (Fig. 6A). Similarly, the number of mitobulbs associated with PLA foci was reduced in DRP1 mutant cells expressing CLIMP63 (Fig. 6B), indicating that recovery of ER sheet structure in DRP1 mutants normalizes its interaction with mitochondria.

Loss of DRP1 results in enlarged nucleoids (Fig. 6C) that are likely caused by nucleoid aggregation (14-16). To confirm the presence of multiple mtDNA copies in the enlarged nucleoids present within mitobulbs, we labelled dividing nucleoids with the nucleotide analogue EdU and observed multiple EdU-positive foci within mitobulbs (Fig. 6D-E). To determine the effect of modulating ER sheets on this nucleoid aggregation, we transiently transfected control and DRP1 mutant fibroblasts with mCherry or mCherry-CLIMP63 and immunolabelled them for mitochondria (TOM20) and nucleoids (TFAM) (Fig. S6). We first determined the effect of mCherry-CLIMP63 expression on nucleoid aggregation by measuring nucleoid size. Nucleoid size was significantly reduced in DRP1 mutants expressing mCherry-CLIMP63 compared to cells expressing only mCherry (Fig. 6C, Fig. S6), consistent with CLIMP63 expression stimulating nucleoid distribution out of mitobulbs. We then reasoned that if CLIMP63 rescues nucleoid distribution, it should also rescue the decreased nucleoid numbers present in DRP1 mutant cells (Fig. 6F) (14). Indeed, while mCherry-CLIMP63 expression did not significantly affect nucleoid numbers in controls cells, it caused a significant increase in overall nucleoid content in DRP1 mutants (Fig. 6F, S6). Altogether, these results indicate that modulating ER sheet structure rescues nucleoid aggregation in DRP1 mutants. As the enlarged nucleoids present in DRP1 mutant cells are found within mitobulbs, we also determined the effect of mCherry-CLIMP63 expression on the presence of mitobulbs. While almost all mitobulbs present in mCherry-transfected DRP1 mutant fibroblasts contained TFAM-positive nucleoids, mCherry-CLIMP63 expression drastically reduced this number (Fig. 6G). On the other hand, the total number of enlarged, bulb-like mitochondrial structures was unchanged (Fig. 6H), suggesting that DRP1 is still required to maintain mitochondrial structure in these conditions. Altogether, our data indicates that nucleoid segregation is regulated by ER sheet-mitochondria interaction independently of DRP1-dependent fission.

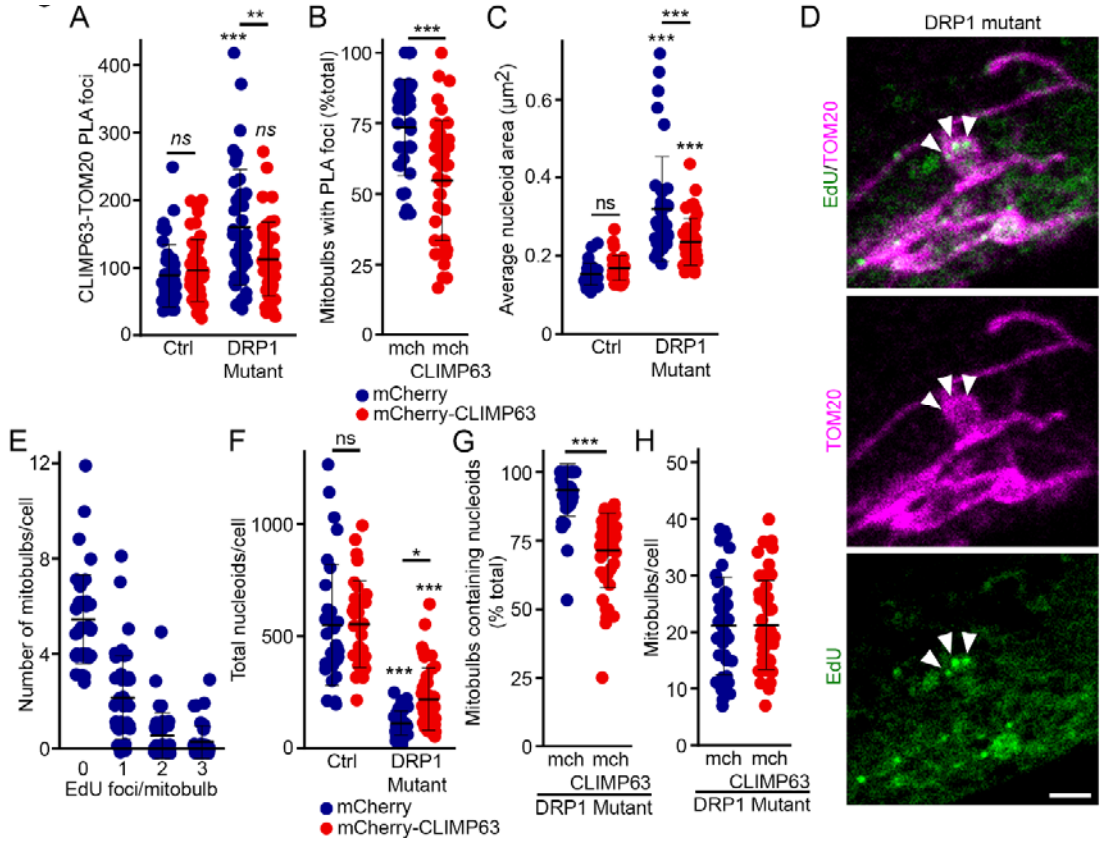

Figure 6. CLIMP63 expression rescues nucleoid distribution in DRP1 mutant fibroblasts. (A-B) Quantification of PLA foci (CLIMP63-TOM20) in mCherry and mCherrry-CLIMP63 expressing control and DRP1 mutant cells. Total PLA foci (A) and mitobulbs associated with PLA foci (B) were quantified. Each point represents one cell, with at least 43 cells quantified per condition in 3 independent experiments. Bars show the average ± SD. ** $p < 0.01$, *** $p < 0.001$, ns not significant. One-way ANOVA (C) Quantification of nucleoid area in mCherry and mCherry-CLIMP63 expressing control and DRP1 mutants from images in Figure S6. Each point represents one cell, with at least 32 cells quantified per condition in 3 independent experiments. Bars show the average ± SD. *** $p < 0.001$, ns not significant. One-way ANOVA. (D-E) Mitobulbs are mtDNA clusters. (D) Representative images of mCherry-expressing DRP1 mutants labeled for EdU (green) and TOM20 (mitochondria). Arrowheads indicate EdU-positive mtDNA in mitobulbs. Scale bar 10μm (E). Quantification of number of EdU foci/mitobulb. Each point represents an individual cell, with 45 cells quantified in 3 independent experiments. Bars show the average ± SD. (F-H) Rescue of nucleoid numbers in CLIMP63-expressing DRP1 mutant cells. Quantification of total nucleoids (TFAM-positive, F), mitobulbs containing nucleoids (TFAM-positive, G) and mitochondrial bulb-like structures (independently of the presence of nucleoids, H) in mCherry and mCherrry-CLIMP63 expressing control and DRP1 mutant cells. Each point represents one cell, with 40 mCherry (mch) and 47 mCherry-CLIMP63 cells quantified in 3 independent experiments. Bars show the average ± SD. One way ANOVA (F), two-sided t-test (G, H). * $p < 0.05$, *** $p < 0.001$, ns, not significant.

Altering ER sheets in DRP1 mutant promotes mtDNA replication and distribution

While our results are consistent with CLIMP63 expression promoting nucleoid distribution away from mitobulbs, it remained possible that it also altered mtDNA replication. Thus, we measured the effect of CLIMP63 expression on mtDNA replication. Replicating DNA was labelled with EdU, after which cells were directly fixed, immunolabelled for mitochondria (TOM20) and imaged by confocal microscopy. In cells expressing mCherry, DRP1 mutants had fewer EdU-positive nucleoids compared to control cells (Fig. 7A), suggesting that DRP1 is required for proper mtDNA replication. Importantly, expression of CLIMP63 rescued the number of EdU foci in DRP1 mutant cells (Fig. 7A), suggesting that the effect of DRP1 on nucleoid replication depends on its ability to modulate ER structure. On the other hand, CLIMP63 expression did not significantly alter the number of EdU foci in control cells (Fig. 7A), indicating that modulating ER sheets does not directly affect mtDNA replication.

As clusters of EdU-positive mtDNA are found within mitobulbs (Fig. 6D-E), we then specifically addressed the effect of CLIMP63 expression on mtDNA replication within mitobulbs. Consistent with the total EdU counts, expression of CLIMP63 in DRP1 mutant fibroblasts caused a large increase in EdU incorporation in mtDNA present within mitobulbs (Fig. 7B). We then took advantage of the accumulation of EdU foci within mitobulbs to determine whether the reduction in nucleoid size that we observed in CLIMP63-transfected DRP1 mutant cells (Fig. 6C) is due to the rescue of nucleoid segregation from mitobulbs towards the rest of the mitochondrial network. To do that, we chased EdU for 24 hours before fixing the cells. Consistent with our observation that the number of nucleoid-containing mitobulbs was decreased in CLIMP63-expressing cells (Fig. 6G), the number of EdU-positive mitobulbs was decreased in CLIMP63-expressing DRP1 mutant cells, but not the mCherry-expressing cells at 24 hours (Fig. 7B). Importantly, this was not due to the loss of overall EdU staining in mutant cells (Fig. 7C). Overall, our data indicates that modulating ER sheet structure through CLIMP63 expression reactivates both mtDNA replication and nucleoid distribution in DRP1 mutant cells even in the absence of mitochondrial fission. Thus, proper DRP1-mediated

regulation of ER sheet structure is essential to modulate mtDNA replication and nucleoid segregation.

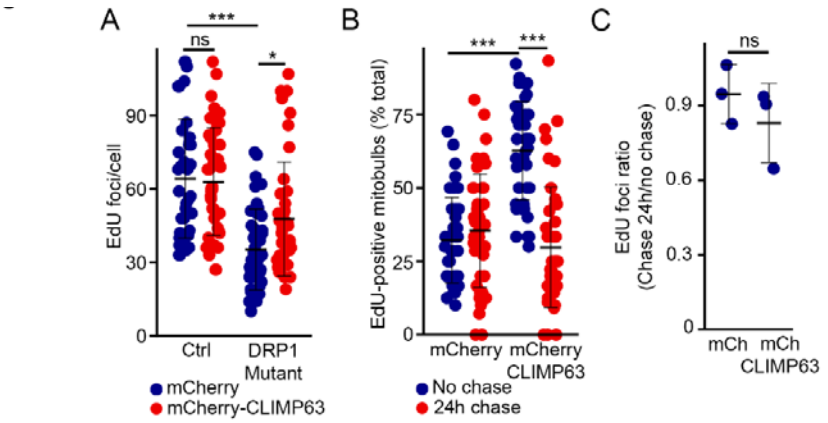

Figure 7. CLIMP63 expression rescues mtDNA replication and distribution in DRP1 mutant fibroblasts. (A) Quantification of EdU foci in control and DRP1 mutants expressing mCherry or mCherry-CLIMP63 in cells labelled with EdU for 4 hours. Each point represents one cell, with at least 43 cells quantified in 3 independent experiments. Bars show the average ± SD. One way ANOVA. * $p < 0.05$, *** $p < 0.001$, ns not significant. (B) Quantification of EdU-positive mitobulbs in EdU-labelled DRP1 mutants expressing mCherry or mCherry-CLIMP63. Cells were pulsed with EdU as in (A) then the EdU was chased for 24 hours where indicated. Each point represents one cell, with at least 44 cells quantified in 3 independent experiments. Bars show the average ± SD. One way ANOVA. *** $p < 0.001$. (C) EdU foci ratio (chase/no chase) from the experiments in (A-B). Each point represents one independent experiment ($n = 3$). Bars show the average ± SD. Two-sided t-test. ns not significant.

Discussion

mtDNA replication is intimately associated with mitochondrial dynamics, especially mitochondrial fusion which is required for mtDNA replication and integrity (11, 12). On the other hand, mitochondrial fission has been suggested to be associated with nucleoid segregation on the basis of the fact that defects in mitochondrial fission result in nucleoid aggregation within mitobulbs (13, 15, 16). With the help of Mitomate Tracker, an automated tool developed in our lab, we have shown that this alters overall nucleoid distribution along mitochondrial networks (14). Nevertheless, the mechanism by which DRP1 affects nucleoid distribution remains unclear. Here, we demonstrate that

DRP1 regulates mtDNA replication and distribution along mitochondrial network through modulating ER sheet structure, independently of mitochondrial fission.

It is well known that ER tubules regulate mtDNA replication (19). However, whether ER sheets also play a role in this process remains unclear. Nevertheless, our data shows that ER sheets directly interact with mitochondria and are present at the site of mitochondrial fission in the perinuclear region (Fig. 5). This is in consistent with the previous observation that ER sheets interact with mitochondria and regulate lipid metabolism in mouse liver cells (26), suggesting an important physiological role for this interaction. As we previously showed that, in DRP1 mutants, nucleoids aggregate around the perinuclear region where ER sheets are found (14), we further defined how DRP1 impacts this process. Our data demonstrates that DRP1 associates with ER sheets independently of mitochondria and that loss of DRP1 function alters ER sheet structure. Furthermore, DRP1 mutant cells showed increased interaction between ER sheets and mitochondria. Of note, we did not observe distinct changes in ER tubules in our cell models, possibly because ER tubular formation requires the variable domain of DRP1 (25) which is still intact in our mutant lines (mutation in the middle domain (G362D)) (28). Overall, these results indicate that DRP1 regulates ER sheet structure and their interaction with mitochondria.

The altered ER sheets present in DRP1 mutant cells also lead to the accumulation of mtDNA within mitobulbs. Importantly, modulating ER sheets by expressing CLIMP63 recovered nucleoid aggregation and nucleoid number in DRP1 mutants, supporting the idea that ER sheets regulate nucleoid distribution. In addition, our EdU data demonstrate that proper ER sheet structure is necessary to actively regulate mtDNA replication. Altogether, our data show that DRP1-regulated ER sheet structure is essential for both mtDNA replication and distribution, and that this occurs independently of DRP1-dependent mitochondrial fission.

While we demonstrated that ER sheets play an important role in mtDNA replication and distribution, ER tubules are still required. This was shown in a previous study

overexpressing CLIMP63 under conditions that caused the complete loss of ER tubules, which significantly reduced mitochondrial DNA replication in cells with wild-type DRP1 (19). In contrast, when we expressed CLIMP63 under conditions that do not affect tubular ER structure, it did not impact cells with wild-type DRP1.

Our study also provides novel insights into the defects present in DRP1 mutant patients. Reported human DRP1 mutations are mostly found in the middle and GTPase domains of DRP1, leading to peripheral neuropathy, epilepsy, optic atrophy, and encephalopathy in these patients (28, 29). Here, we have used patient fibroblasts with a dominant negative mutation in the middle domain of DRP1 (G362D), leading to refractory epilepsy (28). At the cellular level, conditional deletion of DRP1 in mice affects the movement of mitochondria to the nerve terminal, leading to the loss of dopamine neurons (30), while its postnatal deletion in CA1 hippocampal neurons results in functionally impaired mitochondria at the nerve terminals (31). Based on our key findings here, we speculate that the altered mtDNA replication and distribution could severely hamper the movement of functional mitochondria towards the synaptic nerve terminal in the patient neurons and thereby impairing neuronal signaling.

Altogether, our results demonstrate the importance of ER sheets in mtDNA maintenance and distribution and identify DRP1 as key regulator of ER sheets and their interaction with mitochondria. Alteration of this regulation following DRP1 mutation leads the perinuclear accumulation of mtDNA, which could explain the defects observed in these cells in the absence of overt metabolic alterations (28).

Materials and methods

Reagents

Cell culture reagents were obtained from Wisent. Other chemicals were purchased from Sigma-Aldrich, except where indicated.

Cell culture and live cell imaging

Primary human fibroblasts (controls and DRP1 mutants) were generated from skin biopsies, collected as part of an approved research protocol (Research Ethics Board of the Children's Hospital of Eastern Ontario (DRP1 mutants)), and written informed consent from participants was obtained. This study was performed in accordance with the Declaration of Helsinki. Biopsy samples were processed as described and cultured in Dulbecco's modified Eagle's medium (DMEM) containing 10% fetal bovine serum (FBS), supplemented with Penicillin/Streptomycin (100 IU/ml/100µL/mL) (28). Immortalized Mouse Embryonic Fibroblasts (MEFs) were cultured in DMEM supplemented with 10% fetal bovine serum. For live cell imaging, cells were seeded onto glass bottom dishes and allowed to adhere to the plate. Then cells were stained for 30 minutes with 250 nM TMRM (Thermo fisher Scientific, T668) and the DNA dye Picogreen (Thermo Fisher Scientific, P11495) (3 µL/mL). After staining, cells were washed 3 times with pre-warmed 1X phosphate buffered saline (PBS), and normal growth media was added prior to imaging.

Microscopy

Images were acquired with a Leica TSC SP8 confocal microscope fitted with a 63x/1.40 oil objective using the optimal resolution for the wavelength (determined using the Leica software).

siRNA treatment

MEFs were seeded onto 24 well dish and transfected with 15nM of DRP1 siRNA (Thermo Fisher Scientific, Silencer Select, 4390771) and negative siRNA (Thermo Fisher Scientific, Silencer Select, 4390843) using siLenFect lipid reagent (Bio-Rad,1703361). After 48 hrs, cells were treated again with siRNA for another 48 hours. The cells were collected for either western blotting or seeded onto the coverslips for immunofluorescence.

Transient transfection of primary cells

Primary cells were trypsinized and centrifuged at 577 X g for 10 minutes. Cell pellets were suspended in 10µl of the Neon transfection buffer R (ThermoFisher Scientific, MPK1096). Cells were transiently transfected with mCherry (gift from Michael Davidson, Addgene, 54517), mCherry-tagged CLIMP63 (gift from Gia Voeltz (32), Addgene, 136293), DRP1-GFP (gift from Thomas Cribbs (33)), mCherry-Cytochrome b5 (gift from Uri Manor) using the Neon transfection system (ThermoFisher Scientific, MPK5000) according to the manufacturer's protocol. To minimize effects on ER tubules, minimal concentrations (1µg) of mCherry and mCherry-CLIMP63 plasmids were used.

Immunofluorescence

Cells were seeded onto glass coverslips (Fisherbrand, 1254580) and allowed to adhere overnight. Mitochondria was stained using 50 nM Mitotracker Orange (Thermo fisher scientific, M7510) prior to fixing for certain experiment. Cells were fixed with 4% paraformaldehyde for 15 minutes at room temperature (RT). For antigen retrieval, cells were incubated in sodium citrate buffer (pH 6.0) for 10 minutes at 95°C. Then, cells were permeabilized with 1% BSA / 0.2% Triton X-100 in PBS followed by blocking with 1% BSA / 0.1% Triton X-100 in PBS. The following antibodies were used: CLIMP63 (Rb, Abcam, ab84712, 1:150), CLIMP63 (Mo, ENZO, ENZ-ABS669, 1: 200), RRBP1 (Rb, Novus Biologicals, NBP1-32813, 1:200), DRP1 (Mo, BD Transduction Laboratories, 611112, 1:100), TOM20 (Rb, Abcam, ab186735, 1:250), mtTFAM (Mo, Novusbio, NBP1-71648, 1:150), Calnexin (Mo, Millipore, MABF2067, 1:200), RTN4/NOGOA (Rb, Bio-Rad, AHP1799, 1:200), ATP5a (Mo, Abcam, ab14748, 1:150). Next, cells were incubated with fluorescent tagged secondary antibody (Jackson Immunoresearch, 1:500). To verify the interaction of DRP1 with organelles (ER sheets, mitochondria) or to detect the interaction between organelles (bulb-like mitochondria and ER sheets), line scan analysis was performed using the RGB profiler in Image J. To avoid bias during manually classification of ER structure, images were renamed to random numbers and both control and mutant images were shuffled together. The blindfolded ER sheet images were manually classified as structured or altered using reference images. In addition,

we segmented the ER sheet images in ImageJ (Filter/minimum (0.5), Filter/Median (1.0), then thresholding and adjusting the resulting image using Binary/Erode) and measured total area and the median size of individual ER sheets using the *Analyze Particle* function. Mitochondrial structures were manually quantified by binning them into the indicated categories (short, intermediate, elongated). To measure DRP1 association with mitochondria and ER sheets in fixed cell, DRP1 foci were identified in individual cell using ImageJ. The DRP1 channel was first segmented as for ER sheets. Total DRP1 foci were then measured using the *Analyze Particle* function. Selected DRP1 foci were then applied onto mitochondria and ER sheet channels and DRP1 distribution on each organelle was manually counted. For live cell experiment, the images were manually analyzed for the association of DRP1 with mitochondria, ER sheets or both at the fission sites. Further, ER sheets association with mitochondrial ends was tracked following fission event.

Proximity Ligation Assay (PLA)

Cells were grown on glass coverslips and fixed with 4% paraformaldehyde. Following antigen retrieval, cells were permeabilized with 1% BSA/0.2% Triton X-100 in PBS for 15 minutes at RT. The ER was marked with an antibody recognizing CLIMP63 or calnexin and mitochondria was marked with an antibody recognizing TOM20. The PLA assays were performed using Duolink In Situ green kit Mouse/ Rabbit (Sigma Aldrich) following the manufacturer's protocol. The primary antibodies were then labelled using fluorescent-tagged secondary antibodies. Total and mitobulb associated PLA foci were manually counted at the site of CLIMP63-TOM20 signal while overall calnexin-TOM20 foci were quantified using the analyze particles function in ImageJ.

Transmission Electron Microscopy (TEM)

Primary fibroblasts were seeded on Nunc Lab-Tek chamber slides (Thermo Fisher Scientific, 177437) and allowed to adhere overnight. Cells were washed with 0.1M sodium cacodylate buffer (pH 7.3) and fixed with 2.5% glutaraldehyde in 0.1M sodium cacodylate buffer (pH 7.3), overnight at 4°C. Fixed cells were further processed in

McGill's facility for electron microscopy research (FEMR). Images were acquired using a EMS208S electron microscope (Philips) by an independent trained operator in University of Quebec in Trois-Rivières' TEM facility. ER sheet-mitochondrial contact sites in the perinuclear region was manual quantified, considering only contact sites ± 30 nm based on a previous study (34). To measure changes in ER structure we considered rough ER as 'sheets' and smooth ER as 'tubules'. We manually measured ER surface area and luminal width for 10 randomly chosen ER sheets/tubules in each of the four quadrants per image of the cell. The width was measured across each individual ER sheets/tubules and averaged to obtain the luminal width of each individual ER tubules /sheets.

Western Blot

Cells were lysed in 10 mM Tris-HCl, pH 7.4, 1mM EDTA, 150 mM NaCl, 1% Triton X-100, 50 mM sodium fluoride, complemented with a protease inhibitor cocktail (Sigma-Aldrich), centrifuged at 15890 X g for 5 minutes and protein supernatants collected. Protein concentrations were estimated calorimetrically by DC protein assay kit (BioRad). For SDS-PAGE, 20 µg (siRNA treatment in MEFs)/25 µg (Mitochondrial and ER proteins in human fibroblasts) of proteins were mixed with 1X Lammeli buffer containing β-mercaptoethanol, then subjected to SDS-PAGE, transferred to nitrocellulose membranes and blotted with the indicated antibodies (DRP1 (BD Transduction Laboratories, 611112, 1:1000), CLIMP63 (Mo, ENZO, ENZ-ABS669, 1: 500), TOM20 (Rb, Abcam, ab186735, 1:1000), Calnexin (Mo, Millipore, MABF2067, 1:1000), RTN4/NOGOA (Rb, Bio-Rad, AHP1799, 1:1000), ATP5a (Mo, Abcam, ab14748, 1:1000), HRP-tagged Actin (1:10,000). Membranes were then incubated with a 1:5000 dilution of horseradish peroxidase-conjugated secondary antibodies (Jackson Immunoresearch) and visualized by enhanced chemiluminescence (Thermo Fisher scientific) using a Bio-Rad imaging system.

EdU Labeling

Primary fibroblasts (Control and DRP1 mutants) were incubated with 60μM EdU for 2 hours at 37°C. For the chase experiments, the EdU containing media was replaced with fresh media and incubated further for 24 hours. Cells were then fixed with 4% paraformaldehyde for 15 minutes at RT, permeabilized and EdU detected using Click-iT EdU imaging kit (Thermo Fisher Scientific, C10337). Cells were then immunolabelled for TOM20 (Abcam, ab186735, 1:250). EdU foci in mitobulbs and total EdU foci were manually counted.

Data analysis and statistics

All graphs and statistical analysis were done using R. Immunofluorescence data were quantified and images representative of at least three independent experiments shown (exact n are in the quantification figures). Data are represented as average ± SD as specified in figure legends. Statistical significance was determined using Student's t test (between 2 groups) or one-way ANOVA with a Tukey post hoc test (multiple comparisons).

Acknowledgements

This work was supported by grants from the Natural Sciences and Engineering Research Council of Canada and the Fondation de l'UQTR to MG. HSI was supported by a Queen Elizabeth II Diamond Jubilee Scholarship and a FRQ-NT scholarship.

References

1. J. B. Spinelli, M. C. Haigis, The multifaceted contributions of mitochondria to cellular metabolism. Nature Cell Biology 20, 745-754 (2018).

2. F. J. Bock, S. W. G. Tait, Mitochondria as multifaceted regulators of cell death. Nature Reviews Molecular Cell Biology 21, 85-100 (2019).

3. C. Giorgi, S. Marchi, P. Pinton, The machineries, regulation and cellular functions of mitochondrial calcium. Nature Reviews Molecular Cell Biology 19, 713-730 (2018).

4. Gerald S. Shadel, Tamas L. Horvath, Mitochondrial ROS Signaling in Organismal Homeostasis. Cell 163, 560-569 (2015).

5. P. Lisowski, P. Kannan, B. Mlody, A. Prigione, Mitochondria and the dynamic control of stem cell homeostasis. EMBO reports 19, (2018).

6. V. Tiku, M.-W. Tan, I. Dikic, Mitochondrial Functions in Infection and Immunity. Trends in Cell Biology 30, 263-275 (2020).

7. H. Otera et al., Mff is an essential factor for mitochondrial recruitment of Drp1 during mitochondrial fission in mammalian cells. Journal of Cell Biology 191, 1141-1158 (2010).

8. O. C. Losón, Z. Song, H. Chen, D. C. Chan, D. D. Newmeyer, Fis1, Mff, MiD49, and MiD51 mediate Drp1 recruitment in mitochondrial fission. Molecular Biology of the Cell 24, 659-667 (2013).

9. H. Chen et al., Mitofusins Mfn1 and Mfn2 coordinately regulate mitochondrial fusion and are essential for embryonic development. Journal of Cell Biology 160, 189-200 (2003).

10. S. Cipolat, O. M. de Brito, B. Dal Zilio, L. Scorrano, OPA1 requires mitofusin 1 to promote mitochondrial fusion. Proceedings of the National Academy of Sciences 101, 15927-15932 (2004).

11. E. Silva Ramos et al., Mitochondrial fusion is required for regulation of mitochondrial DNA replication. PLOS Genetics 15, (2019).

12. H. Chen et al., Mitochondrial Fusion Is Required for mtDNA Stability in Skeletal Muscle and Tolerance of mtDNA Mutations. Cell 141, 280-289 (2010).

13. R. Ban-Ishihara, T. Ishihara, N. Sasaki, K. Mihara, N. Ishihara, Dynamics of nucleoid structure regulated by mitochondrial fission contributes to cristae reformation and release of cytochrome c. Proceedings of the National Academy of Sciences 110, 11863-11868 (2013).

14. H. S. Ilamathi et al., A new automated tool to quantify nucleoid distribution within mitochondrial networks. Scientific reports 11, 22755 (2021).

15. T. Ishihara et al., Dynamics of Mitochondrial DNA Nucleoids Regulated by Mitochondrial Fission Is Essential for Maintenance of Homogeneously Active Mitochondria during Neonatal Heart Development. Molecular and Cellular Biology 35, 211-223 (2015).

16. N. Ishihara, T. Ishihara, A. Ota, Mitochondrial nucleoid morphology and respiratory function are altered in Drp1-deficient HeLa cells. The Journal of Biochemistry 167, 287-294 (2020).

17. R. G. Abrisch, S. C. Gumbin, B. T. Wisniewski, L. L. Lackner, G. K. Voeltz, Fission and fusion machineries converge at ER contact sites to regulate mitochondrial morphology. Journal of Cell Biology 219, (2020).

18. J. R. Friedman et al., ER Tubules Mark Sites of Mitochondrial Division. Science 334, 358-362 (2011).

19. S. C. Lewis, L. F. Uchiyama, J. Nunnari, ER-mitochondria contacts couple mtDNA synthesis with mitochondrial division in human cells. Science 353, (2016).

20. J. R. Friedman, G. K. Voeltz, The ER in 3D: a multifunctional dynamic membrane network. Trends in Cell Biology 21, 709-717 (2011).

21. D. S. Schwarz, M. D. Blower, The endoplasmic reticulum: structure, function and response to cellular signaling. Cellular and Molecular Life Sciences 73, 79-94 (2015).

22. Y. Shibata et al., Mechanisms Determining the Morphology of the Peripheral ER. Cell 143, 774-788 (2010).

23. H. Zhang, J. Hu, Shaping the Endoplasmic Reticulum into a Social Network. Trends in Cell Biology 26, 934-943 (2016).

24. W.-K. Ji et al., Receptor-mediated Drp1 oligomerization on endoplasmic reticulum. Journal of Cell Biology 216, 4123-4139 (2017).

25. Y. Adachi et al., Drp1 Tubulates the ER in a GTPase-Independent Manner. Molecular Cell 80, 621-632.e626 (2020).

26. I. Anastasia et al., Mitochondria-rough-ER contacts in the liver regulate systemic lipid homeostasis. Cell Reports 34, (2021).

27. E. Smirnova, L. Griparic, D.-L. Shurland, A. M. van der Bliek, T. D. Pollard, Dynamin-related Protein Drp1 Is Required for Mitochondrial Division in Mammalian Cells. Molecular Biology of the Cell 12, 2245-2256 (2001).

28. J. R. Vanstone et al., DNM1L-related mitochondrial fission defect presenting as refractory epilepsy. European Journal of Human Genetics 24, 1084-1088 (2015).

29. R. Banerjee, A. Mukherjee, S. Nagotu, Mitochondrial dynamics and its impact on human health and diseases: inside the DRP1 blackbox. Journal of Molecular Medicine, (2021).

30. A. Berthet et al., Loss of Mitochondrial Fission Depletes Axonal Mitochondria in Midbrain Dopamine Neurons. Journal of Neuroscience 34, 14304-14317 (2014).

31. L. Y. Shields et al., Dynamin-related protein 1 is required for normal mitochondrial bioenergetic and synaptic function in CA1 hippocampal neurons. Cell Death & Disease 6, e1725-e1725 (2015).

32. Y. Shibata et al., The reticulon and DP1/Yop1p proteins form immobile oligomers in the tubular endoplasmic reticulum. The Journal of biological chemistry 283, 18892-18904 (2008).

33. S. Strack, J. T. Cribbs, Allosteric Modulation of Drp1 Mechanoenzyme Assembly and Mitochondrial Fission by the Variable Domain. Journal of Biological Chemistry 287, 10990-11001 (2012).

34. G. r. Csordás et al., Structural and functional features and significance of the physical linkage between ER and mitochondria. Journal of Cell Biology 174, 915-921 (2006).

Supplementary Figures

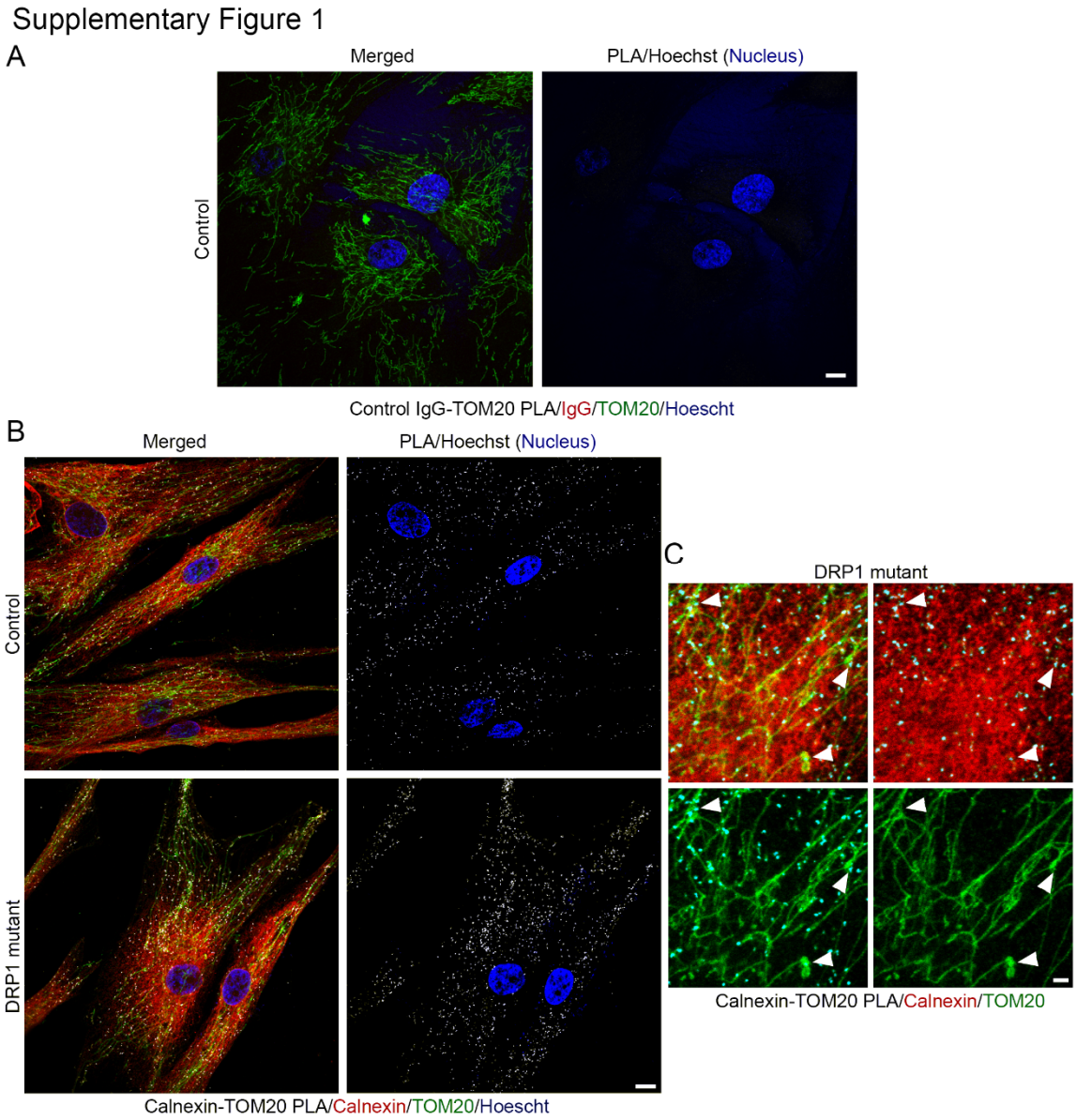

Sup. Figure S1. Calnexin-TOM20 PLA. (A) Representative image of PLA (IgG and TOM20; white) for the antibody control (IgG), along with IgG (red), TOM20 (green) and nuclei (Hoechst, Blue) in control fibroblasts. (B) Representative images of control and DRP1 mutant fibroblasts showing the PLA for Calnexin and TOM20 (white), along with Calnexin (red), TOM20 (Green) and nuclei (Hoechst, Blue). (C) Zoomed in image of DRP1 mutant. Arrowheads denote PLA foci on mitobulbs. Scale bar 10 µm, 2 µm for the zoomed images.

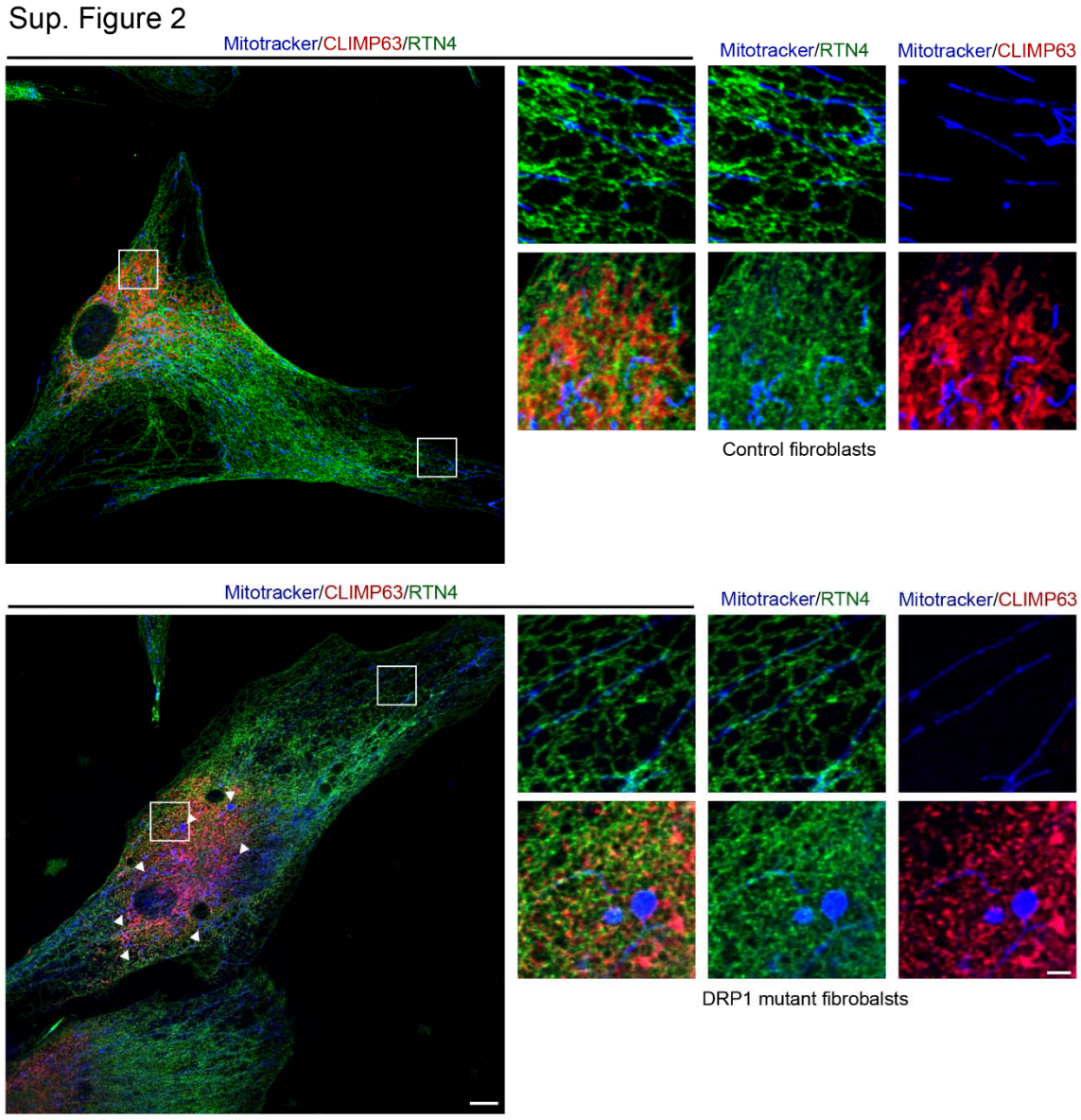

Sup. Figure S2. ER structure in DRP1 mutant fibroblasts. Representative images of control (Top) and DRP1 mutant (Bottom) human fibroblasts showing CLIMP63 (ER sheets, Red), RTN4 (ER, Green) and mitochondria (Mitotracker orange, Blue). The enlarged boxed areas show ER structure in the perinuclear area (CLIMP63-positive) and periphery of the cells. Scale bar 10 µm, 2 µm for the enlarged images.

Supplementary Figure 3

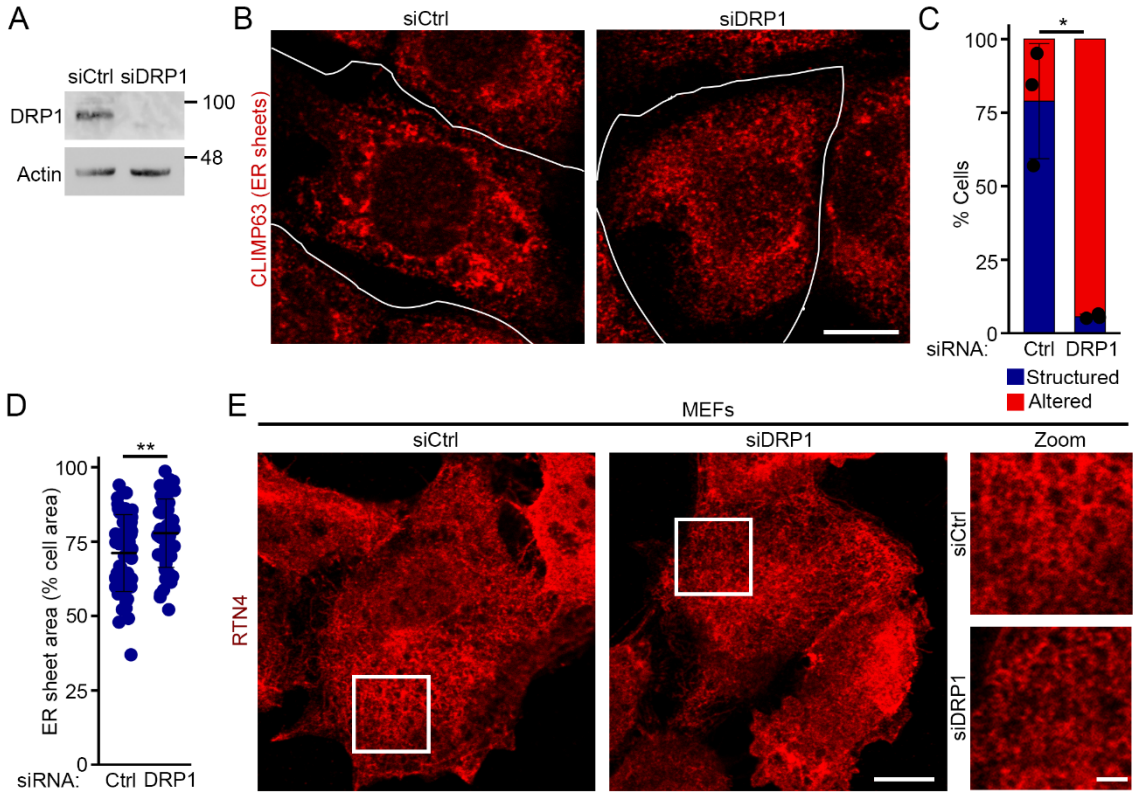

Sup. Figure S3. ER Structure following DRP1 knockdown in MEFs. (A) WB showing DRP1 expression in WT MEFs transfected with a control siRNA (siCtrl) or a siRNA against DRP1 (siDRP1). (B) Representative images showing CLIMP63 staining in MEFs transfected with control and DRP1 siRNAs. White lines represent the cell edge. Scale bar 10 µm (C) Quantification of ER sheet structure as Structured (Blue) or Altered (red; presence of punctate structures and thick ER sheet patches). Each point represents one independent experiment, with at least 20 cells quantified per experiment. Bars show the average ± SD. * $p < 0.05$, Two-sided t-test using the data for Structured ER. (D) Quantification of ER sheet surface area relative to the total cell area (determined by DIC). Each data point represents one cell. Bars represent the average of 54 cells in 3 independent experiments ± SD. ** $p < 0.01$ two-sided t-test. (E) Representative images showing RTN4 in control and DRP1 siRNAs. Scale bar 10 µm, 2 µm for the zoomed images.

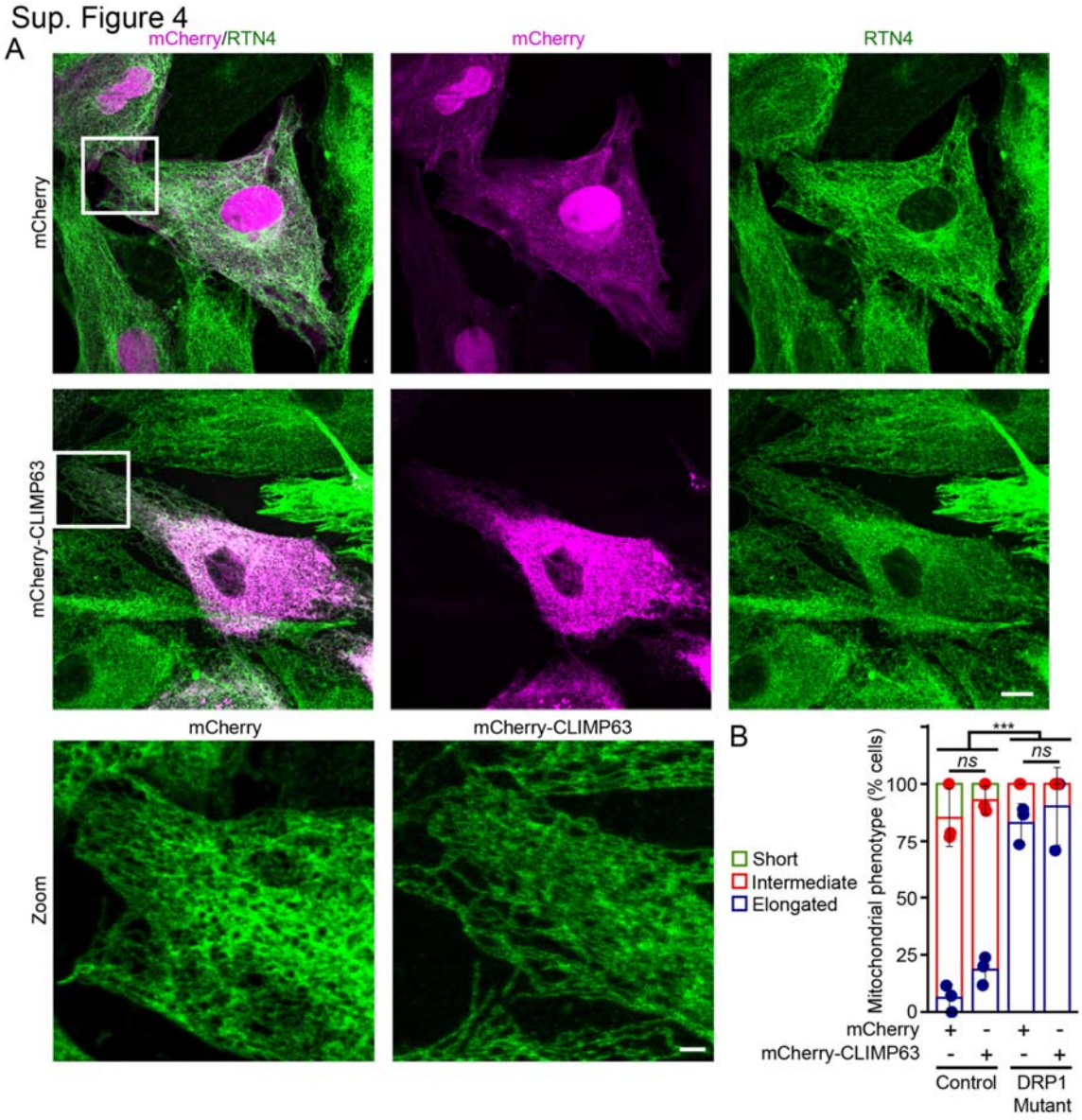

Sup. Figure S4. ER tubules are not affected by CLIMP63 expression. (A) Representative images of Control cells expressing mCherry and mCherry-CLIMP63 (Magenta) and immunolabelled for RTN4 (green). Scale bar 10 µm, 2 µm for the zoomed images. (B) Quantification of mitochondrial phenotypes (short (green), intermediate (red), elongated (blue)) in mCherry and mCherry-CLIMP63 expressing control and DRP1 mutant fibroblasts. Each point represents an independent experiment. Bars show the average± SD. Two-way ANOVA. *** $p < 0.001$, ns not significant.

Sup. Figure 5

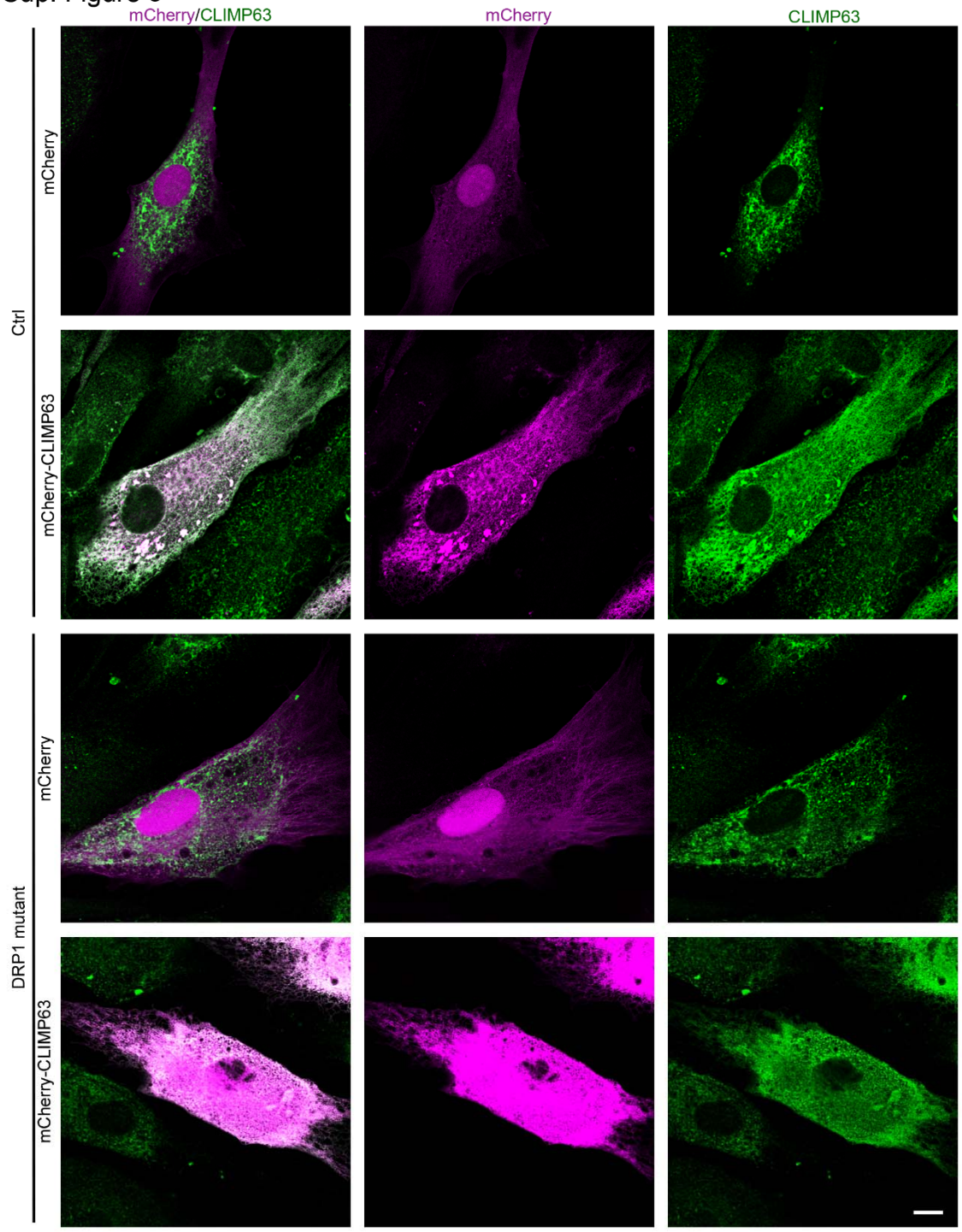

Sup. Figure S5. CLIMP63 expression alters ER sheet structure in control and DRP1 mutants. Representative images of control and DRP1 mutant fibroblasts expressing mCherry or mCherry-CLIMP63 (Magenta) and immunolabelled for CLIMP63 (ER sheets, green). Scale bar 10 µm.

Sup. Figure 6

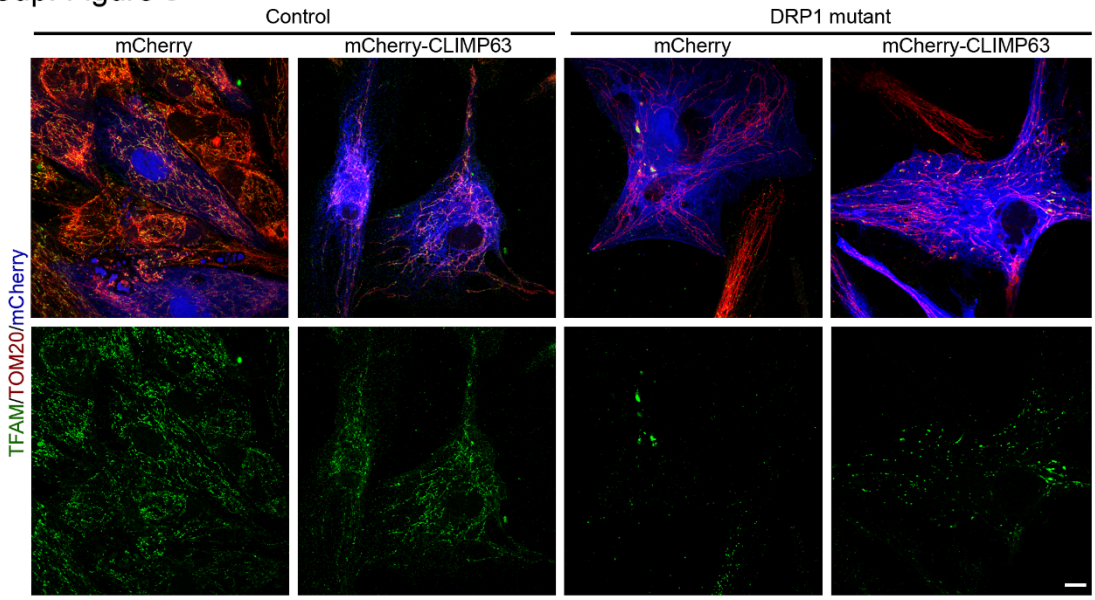

Sup. Figure S6. CLIMP63 expression rescues nucleoid aggregation in DRP1 mutants. Representative images of control and DRP1 mutant fibroblasts expressing mCherry or mCherry-CLIMP63 (blue) immunolabeled for TFAM (nucleoids, Green) and TOM20 (mitochondria, Red). Scale bar 10 µm.

CHAPTER IV

DISCUSSION AND CONCLUSION

mtDNA maintenance is essential for proper mitochondrial function and defects in mtDNA maintenance cause mitochondrial diseases. mtDNA maintenance is mainly regulated by nuclear-encoded mitochondrial genes, particularly those controlling mitochondrial dynamics. Defects in mitochondrial fission cause nucleoid enlargement, though the mechanism behind this is unclear. Using an automated tool that we developed, we demonstrated that the distribution of nucleoids within mitochondrial networks is non-random. Furthermore, we demonstrated that mitochondrial fission is essential for proper nucleoid distribution within mitochondrial networks. In particular, loss or defect in DRP1 results in alterations in ER sheet structure that are associated with nucleoid aggregation sites. Restructuring ER sheet structure rescues nucleoid aggregation in the DRP1 mutant. While our studies have some limitations, they have opened a potential arena for manipulating nucleoid distribution defects independently of mutant DRP1. This section will highlight different questions that resulted from our research work and possible ways to address them.

4.1 Factors regulating mtDNA-nucleoid distribution

Nucleoid distribution is an active process. Our data demonstrated that nucleoids are distributed in a non-random fashion. Under physiological conditions, nucleoids maintain a certain distance (~1-3μm) from neighboring nucleoids. Impairment in mitochondrial fission proteins alters this distribution pattern, causing the aggregation of nucleoids. This aggregation could be caused by one of the following reasons: (i) increased nucleoid trafficking and clustering within hyperfused mitochondrial networks due to loss of fission, (ii) impairment in nucleoid segregation following mitochondrial biogenesis (Figure 4.1).

Under physiological conditions, nucleoids move along mitochondrial networks. During this trafficking, they encounter neighboring nucleoids and undergo transient interactions, including the association and dissociation of a nucleoid from neighboring nucleoids (32). So, to test if nucleoid trafficking is impaired in the fission mutant, live cell imaging could be performed in control and DRP1 mutants using picogreen (DNA stain) and TMRM (mitochondria). Time-based images can be taken to track nucleoid movement and interactions. We showed that DRP1 mutant patient cells clearly have multiple replication competent mtDNA foci in nucleoid aggregates (Chapter III – Figure 6D, E). Based on this evidence, we speculate the presence of restrictive movement at the nucleoid aggregation site. In addition, this aggregation could be further enhanced by the association of neighboring nucleoids, which needs further investigation.

Nucleoid distribution could also be influenced by its trafficking machinery within mitochondrial networks. However, the mechanisms regulating nucleoid trafficking are unclear. The cytoskeleton could be involved in trafficking nucleoids within mitochondrial networks. There is evidence suggesting that mitochondria-associated actin could be regulating short range transport of nucleoids within mitochondrial networks. Previous studies suggest that a sub-population of β-actin is present within mitochondria and is associated with nucleoids. Loss of β-actin causes nucleoid aggregation, suggesting its potential role in nucleoid distribution (34, 244). To verify changes in β-actin structure, we could immunolabel control and DRP1 mutant cells for mitochondria (Tom20) and actin (β-actin) and image them by confocal microscopy. This experiment will help to address whether nucleoid aggregation could be linked with alterations in the mitochondrial associated β-actin structure (Figure 4.1). On the other hand, it is possible that nucleoids aggregate due to limited actin-mediated movement of nucleoids in DRP1 mutants. Especially, increased ER sheet-mitochondrial interaction could restrict nucleoid movements in DRP1 mutants (Figure 4.1). To demonstrate this, we could perform live cell imaging of control and DRP1 mutant fibroblasts transfected with fluorescent tagged β-actin and labelled for mitochondria (mitotracker dye) and nucleoids (picogreen). Tracking actin-associated nucleoid movement along mitochondrial networks will help us to address changes in nucleoid trafficking in DRP1 mutants. Further, to address the role

of ER sheets-mitochondria interaction in nucleoid movement, control and DRP1 mutants could be transfected with mch or mch-CLIMP and labelled for mitochondria (mitotracker dye) and nucleoids (picogreen). Time-based images could be taken in the live cell to verify nucleoid movement with changes in ER sheets-mitochondria interaction, particularly at mitobulb regions in DRP1 mutants, which can help us to validate our hypothesis. Altogether, these experiments will demonstrate the primary role of fission in nucleoid distribution and other key players regulating it.

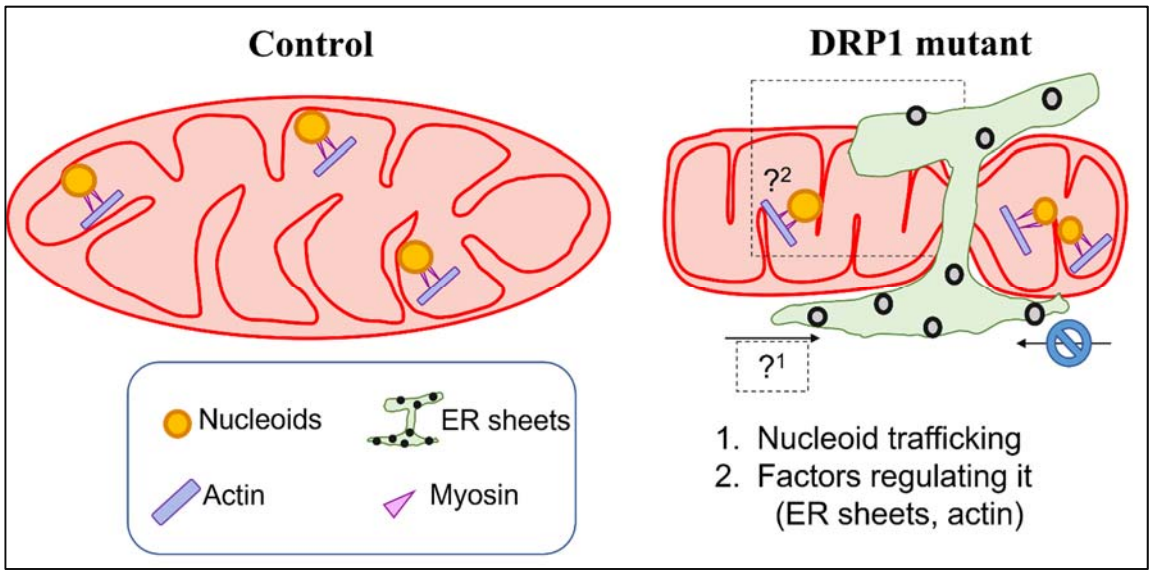

Figure 4.1 Nucleoid trafficking in the DRP1 mutant and factors regulating it.

4.2 mtDNA replication and nucleoid spatial localization

Intracellular positioning of cellular organelles varies in response to cellular metabolic cues. Basically, mitochondria are spatially distributed across the cell to perform different roles. For example, mitochondria are transported and docked near the plasma membrane to regulate Ca^{2+} dependent secretory pathways in polarized cells (245). Numerous studies have demonstrated that mitochondrial populations differ in their number, shape, movement, function, and dynamics based on their cellular spatial localization (246, 247). Furthermore, there are reports suggesting that mtDNA replication and translation are enriched in the perinuclear region (247-250). In contrast, a study

reported replicating mtDNA throughout the mitochondrial network (251). We speculate that newly divided mtDNA are distributed throughout the rest of the mitochondrial network with time. In support of this evidence, the microtubule motor protein kinesin 5B(KIF5B) has been shown to regulate the distribution of nucleoid-containing mitochondria to the periphery of the cell. KIF5B promotes MDT, a process where mitochondria are pulled out from pre-existing mitochondrial tubules in the perinuclear region to form a framework for the peripheral mitochondrial network (33, 252). During this process, nucleoids are pulled along with mitochondria. KIF5B is linked to mtDNA through the MICOS protein complex in the IMM and hence, uncoupling the mtDNA-MICOS-KIF5B interaction axis prevents distribution of nucleoids in the peripheral mitochondrial network through MDT (Figure 4.3) (252).

mtDNA replication occurs at sites of ER tubule-mitochondria contact (226). We have shown here that ER sheets in the perinuclear region also participate in mitochondrial fission and are essential for mtDNA replication and nucleoid distribution. Alterations in ER sheet structure affect nucleoid distribution, resulting in the aggregation of mtDNA in the perinuclear region and a decline in the total number of nucleoids within mitochondrial networks. As DRP1-defective cells nevertheless have ER tubules, this suggests that ER sheet associated mtDNA replication has a major influence on the peripheral distribution of nucleoids. Hence, we speculate that mtDNA replication occurs actively in the perinuclear region and spreads to the peripheral region by MDT (Figure 4.2). To demonstrate this, MICOS subunits could be knocked down in primary control cells. The intracellular spatial distribution of replicating mtDNA could then be determined using the nucleotide analog EdU. Further, live cell imaging could be performed in control and MICOS subunit knockdown primary fibroblasts transfected with fluorescently tagged DNA polymerase γ (mitochondrial DNA polymerase), along with mitochondrial labelling (TMRM) to monitor the spatial distribution of newly replicated nucleoids and MDT events associated with it. Overall, these experiments would help us to understand the intracellular spatial organization of mtDNA replication. Also, this would give us a deep insight into the importance of the differential spatial distribution of mitochondria within the cell.

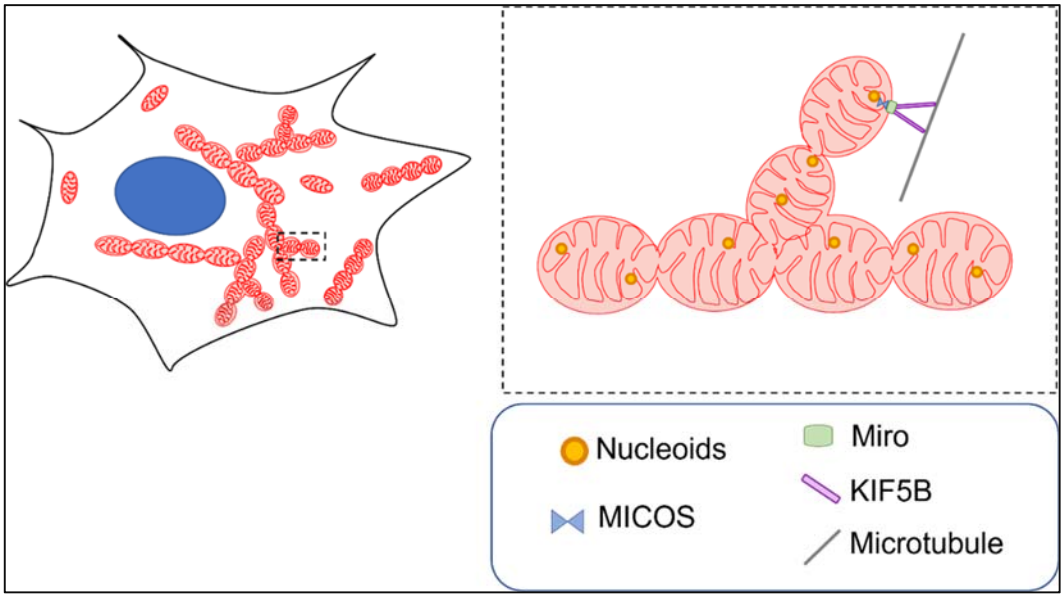

Figure 4.2 Role of KIF5B in the distribution of newly divided nucleoid by MDT.

4.3 DRP1 regulates ER sheet structure

Mitochondrial function and its dynamics are interlinked with each other. For instance, loss of mitochondrial fission results in mosaic functioning of the organelle (86, 91, 192). In addition to their role in mitochondrial division, evidence suggests that fission proteins are associated with the ER and could regulate its structure (206, 253). A recent study identified a population of DRP1 associated with the ER, independently of mitochondria and peroxisomes, that regulate ER tubule formation (206, 253). However, the association and effects of fission proteins on ER sheets is poorly understood. Previous work identified DRP1 in the ER fraction (tubules and sheets) of the cell (254). In our work, we observed a mitochondria-independent population of DRP1 associated with ER sheets. Though all this evidence demonstrates that DRP1 is associated with ER sheets, two important questions remain to be thoroughly investigated. (i) DRP1 lacks a protein domain required for direct interaction with ER membranes, so it is unclear how DRP1 is recruited on ER sheets. (ii) We have shown here that defects in DRP1 alter ER sheet structure. However, DRP1-mediated structural regulation of ER sheets is unclear. Here, we discuss potential ways to address these questions.

Unlike other dynamins, DRP1 lacks a pleckstrin homology domain to directly interact with the membrane. Hence, it depends on surface receptors to interact with an organelle. However, factors necessary for DRP1 recruitment on the ER are controversial and poorly understood. DRP1 has different receptors on mitochondria (MFF, MiD49/51, FIS1). Similarly, the ER has a mitochondria-independent population of MFF and FIS1 that recruits DRP1 on the ER. A previous in vitro study demonstrated that DRP1 can increase membrane curvature, thereby resulting in the formation of tubules. However, DRP1-mediated ER tubule formation occurs independently of MFF/Fis1(206, 253). This suggests the presence of other receptors on ER tubules that facilitate DRP1 recruitment.

Our data demonstrated that DRP1 mutation or knock down alters ER sheet structure. This results in nucleoid aggregation in mitobulbs. Similarly, other studies have shown that the loss of the DRP1 receptor MFF results in mitobulb formation (86). Overall, we speculate that defects in DRP1/MFF could affect DRP1 recruitment on ER sheets and thereby modify their structure. This could result in altered ER sheets-mitochondria interaction and thus improper nucleoid distribution along mitochondrial networks. Further, based on this evidence, we hypothesize that DRP1 regulates ER tubules (MFF independent) and sheets by different mechanisms. To demonstrate this, MFF could be knocked-out in MEFs/ HFs. Then, to monitor the effect of DRP1 on ER sheets, a rapamycin sensitive FRB-FKBP12 inducible system could be used to target MFF to the ER. Changes in ER sheet structure could be determined by immunofluorescence for ER sheets (RRBP1, CLIMP63) and imaged by confocal microscopy. Altogether, this will help us to understand the role of MFF-recruited DRP1 in ER sheet dynamics.

Based on high resolution imaging and theoretical models, the ER sheet structure is characterized by a stacked planar surface with curved edges that are connected to each other by helicoidal membranes (255, 256). In addition, ER sheet stacks are linked to their neighbors by short tubules, resulting in the formation of small fenestrations/holes on their surface (255, 257). These curved edges, helicoidal membranes and fenestrations are characterized by higher membrane curvatures than planar surfaces. However,

the mechanisms of the formation of ER sheets and proteins regulating this process are unclear. The dynamin family of proteins are known to constrict lipid membranes in a GTP-dependent manner, which is essential for fission of endocytic vesicles and organelles (mitochondria, peroxisomes) (258, 259). Further, in vitro liposomal studies suggest that DRP1 binds and maintains curved membrane structures. DRP1 can bind to these curved membranes and induce tubule formation independently of GTP, as noticed in ER tubules formation (206, 260). A study also reported that the variable domain of DRP1 is indispensable for this ER tubulation process (206). On the other hand, DRP1 mutants reported in our study have a major alteration in ER sheet structure. These mutants have a defect in the middle domain of DRP1, which is essential for its oligomerization (179). Altogether, this suggests that DRP1 could be regulating ER sheet structure independent of its ER tubulation activity. To verify this, DRP1 could be knocked out in MEFs/HFs. Then, to identify the DRP1 domain associated with ER sheet structure regulation, knockout cells can be transfected with constructs expressing DRP1 with mutations in the GTPase, middle, variable, or GED domain. Then, changes in ER sheet structure can be determined by immunofluorescence for ER sheets (RRBP1, CLIMP63). Further, to monitor the effect of DRP1 protein domains on ER sheet membrane curvature (curved edges, helicoidal membrane and fenestrations), these cells can be imaged by focused ion beam scanning electron microscopy, which reveals the three-dimensional structure of ER sheets. Thus, these experiments will address the role of DRP1 in regulating ER sheet structure.

4.4 ER sheets-mitochondria interactions and nucleoid distribution

Crosstalk between organelles is important for the exchange of materials and signaling molecules. This dynamic interaction between organelles is important for different cellular functions and to regulate organelle dynamics. ER sheets-mitochondria contact are involved in regulating lipid homeostasis and Ca^{2+} signaling (234, 236). Furthermore, our data demonstrates that ER sheets-mitochondria interactions regulate the distribution of nucleoids. However, the ER sheets-mediated signaling mechanism that regulates nucleoid distribution is still unclear. Our findings raise several questions about

the ER sheets-mitochondria contact sites associated with nucleoids. (i) Contact sites are generally established by tethering of proteins present on the outer membrane of the organelles. Different protein pairs tether at contact sites, and some of them have distinct functional roles. Therefore, it is important to identify the tethering protein complexes at nucleoid associated ER sheets-mitochondria contact sites. (ii) Contact sites are the hotspots for the transfer of messages between organelles in the form of signaling molecules. So, this raises the question of whether the signaling molecules transferred between the ER sheets associated with the OMM on the one hand, and the nucleoids attached to the IMM on the other hand (Figure 4.3).

Studies have shown that mtDNA maintenance is linked to IMM lipid content. mtDNA is docked to the IMM with the help of nucleoid associated proteins. This lipid-protein interaction at the IMM regulates mtDNA movement and segregation. The IMM is composed of different phospholipids, including cardiolipin and cholesterol. Evidence suggests that nucleoids interact with cardiolipin and cholesterol. Modulation of cardiolipin and cholesterol availability influences mtDNA maintenance (261-263). A study in yeast cells demonstrated that cardiolipin is essential for proper nucleoid segregation, especially under stress (263). Besides, replicating mtDNA is bound to cholesterol, and perturbation in cholesterol metabolism affects mtDNA distribution, causing enlargement of nucleoids (262, 264). It is known that ER-mitochondria contact sites are hotspots for lipid transfer and metabolism. Based on this evidence, we speculate that ER sheets-mitochondria contact sites could be regulating nucleoid distribution through modulating lipid metabolism and transfer. A recent study showed that the ER sheet protein RRBP1 plays a role in lipid metabolism at ER sheets-mitochondria contact sites (236). In addition, RRBP1 has been shown to interact with the OMM protein SYNJ2BP (235). Hence, it is possible that the SYNJ2BP-RRBP1 axis could be regulating nucleoid-associated ER sheets-mitochondria contact sites through modulating lipid metabolism (Figure 4.3). To initially check if there is an alteration in lipid composition, the IMM can be sub-fractioned from control and DRP1 mutant fibroblasts. Cholesterol and phospholipid levels in the IMM can be quantified using fluorescent-based assay kits and thin layer chromatography, respectively (264). Further, to understand the role of the

SYNJ2BP-RRBP1 complex in lipid metabolism and nucleoid distribution, SYNJ2BP or RRBP1 can be knocked out in control and DRP1 mutant fibroblasts. Then, cholesterol and phospholipid content can be measured as described earlier. Finally, to monitor the changes in nucleoid distribution, these knockout cells can be stained with TMRM (mitochondria) and picogreen (DNA) and imaged using confocal microscopy. Overall, these experiments will address the signaling events occurring at the nucleoid associated ER sheets-mitochondrial contact site.

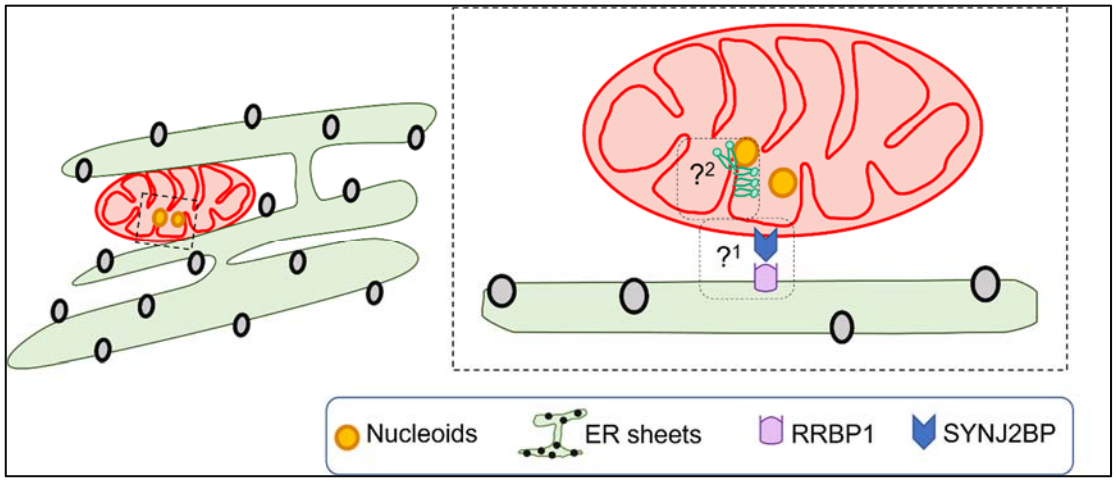

Figure 4.3 ER sheet-mitochondria interaction at a mtDNA replication site.

4.5 DRP1 effect on nucleoid distribution in neuronal cells

Mitochondria are essential for stimulating and transmitting signals across neuronal cells. Mitochondria are enriched at the synaptic site where the signal is passed from the axon of a neuron to the dendrites of the neighboring cell. Mitochondria help to maintain Ca^{2+} levels and supply the ATP necessary for this signal transmission. Neuronal cells have two populations of mitochondria, (i) tubulated mitochondria in the cell body and (ii) short mitochondria in the axons. Mitochondrial dynamics play an important role in the differential regulation of mitochondrial network structure in the cell body and axons of neurons. Especially, studies suggest that mitochondrial fission is essential for the proper distribution of mitochondria from cell body to the axons. Knockout of DRP1 in mice causes embryonic lethality and DRP1 knockout mice die a few days after birth. Clinically,

mitochondrial fission defects result in poor brain development and affect the proper functioning of the peripheral nervous system in patients. However, the cellular mechanisms that are altered in neuronal cells due to the DRP1 defect are still poorly understood.

Our results in fibroblast cells demonstrate that DRP1 is essential for proper nucleoid distribution and defects in DRP1 result in failure of mtDNA replication and nucleoid distribution. This results in mosaic functioning of the organelle. Based on our results, we speculate that fission defects result in improper distribution of nucleoids in neuronal cells, especially at the synapse. These defective mitochondria could affect the proper transmission of nerve signals. Further experiments are necessary to validate this hypothesis.

Development of a DRP1 Knockout (KO) mice model is challenging due to embryonic lethality. Conditional knockout of DRP1 in specific regions of the brain (hippocampal region) showed an alteration in synaptic transmission due to alterations in the mitochondrial structure (191, 192). However, whether nucleoid distribution affects signal transmission in neuronal cells is yet to be defined. Therefore, neuronal cells from conditional KO mice could be utilized to test our hypothesis. The nucleoid distribution can be verified by live cell imaging using mitochondrial (TMRM) and DNA (picogreen) staining. To address the effect of nucleoid distribution on synaptic transmission, a fluorescent based Ca^{2+} indictor can be utilized. Changes in the fluorescent intensity will be an indicator of synaptic defects in DRP1 KO neuronal cells.

Neuronal cells have a continuous ER network continuously distributed along dendrites, cell body, axon, and the nerve terminals. Rough ER/ ER sheets are mostly present in the cell body. Smooth ER extends from ER sheets in the cell body and predominantly distributed along axon and nerve terminals with the occasional presence of ER sheets. To confirm the fact that the changes observed in DRP1 mutants are associated with altered ER sheet structure and ER sheets- mitochondria interaction, CLIMP63, an ER sheet protein can be expressed in these cells and recovery of synaptic transmission could

be monitored by Ca^{2+} indicator. These experiments will help to better understand DRP1 mediated changes in neuronal cells that could be correlated to clinical pathology.

4.6 Conclusion

Mitochondrial function depends on the proper maintenance and distribution of mtDNA within mitochondrial networks. Defects in the genes regulating this process result in mitochondrial diseases. Limited knowledge of the processes of mtDNA maintenance and distribution restrain the development of treatments. Our work identified the global distribution pattern of nucleoids within mitochondrial networks and the importance of mitochondrial fission in regulating it. Based on our results, we propose a model of nucleoid distribution (Figure 4.4). Fission occurs at ER sheets-mitochondrial interaction sites. In DRP1 mutants, alterations in ER sheet structure increased ER sheets-mitochondria interaction. Hence, these sites are pre-licensed for the initiation of mtDNA replication. However, newly divided nucleoids failed to segregate and distribute in the absence of fission, resulting in nucleoid enlargement. This causes mosaic functioning of the organelle in cells with fission defects.

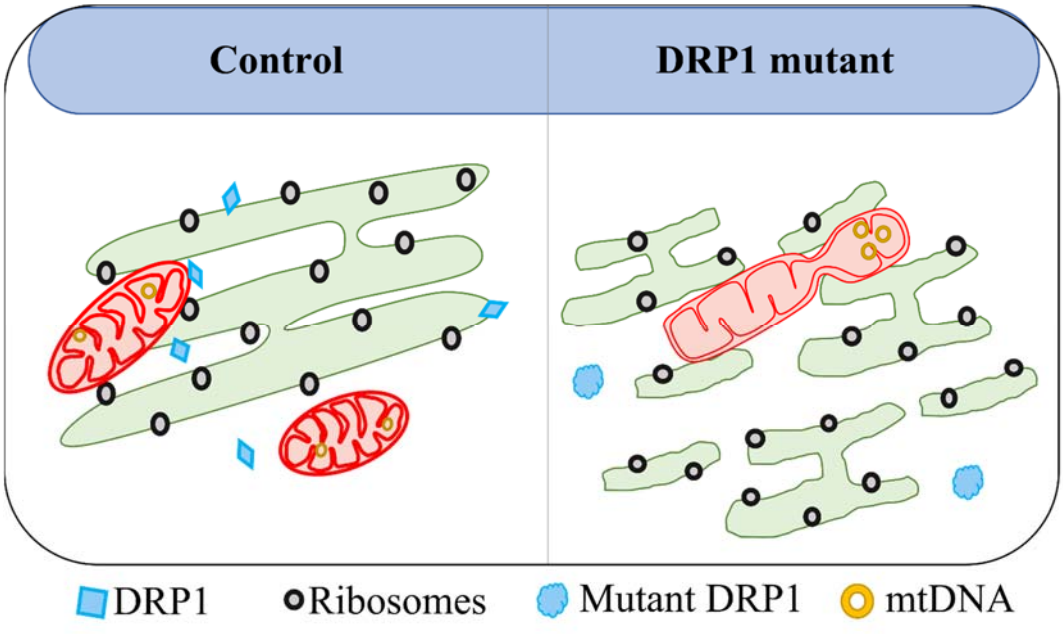

Figure 4.4 Model of ER sheet regulated nucleoid distribution.

Overall, our work identified the process of nucleoid segregation and distribution within the mitochondrial networks and key players involved in it. At the same time, our work brings up different questions as mentioned earlier in this chapter which need thorough investigation. In-depth knowledge on mtDNA maintenance and distribution processes will open an avenue to develop treatment for mitochondrial diseases associated with mtDNA maintenance defects in future.

REFERENCES

1. A. J. Roger, S. A. Muñoz-Gómez, R. Kamikawa, The Origin and Diversification of Mitochondria. Current Biology 27, R1177-R1192 (2017).

2. S. E. Calvo, V. K. Mootha, The Mitochondrial Proteome and Human Disease. Annual Review of Genomics and Human Genetics 11, 25-44 (2010).

3. T. Wai, T. Langer, Mitochondrial Dynamics and Metabolic Regulation. Trends in Endocrinology & Metabolism 27, 105-117 (2016).

4. J. B. Spinelli, M. C. Haigis, The multifaceted contributions of mitochondria to cellular metabolism. Nature Cell Biology 20, 745-754 (2018).

5. N. S. Chandel, Mitochondria as signaling organelles. BMC Biology 12 (2014).

6. Navdeep S. Chandel, Evolution of Mitochondria as Signaling Organelles. Cell Metabolism 22, 204-206 (2015).

7. J. C. Iovine, S. M. Claypool, N. N. Alder, Mitochondrial compartmentalization: emerging themes in structure and function. Trends in Biochemical Sciences 46, 902-917 (2021).

8. D. C. Logan, The mitochondrial compartment. Journal of Experimental Botany 57, 1225-1243 (2006).

9. R. P. Chakrabarty, N. S. Chandel, Mitochondria as Signaling Organelles Control Mammalian Stem Cell Fate. Cell Stem Cell 28, 394-408 (2021).

10. F. J. Iborra, H. Kimura, P. R. Cook, The functional organization of mitochondrial genomes in human cells. BMC Biology 2 (2004).

11. B. Glancy, Y. Kim, P. Katti, T. B. Willingham, The Functional Impact of Mitochondrial Structure Across Subcellular Scales. Frontiers in Physiology 11 (2020).

12. S. R. Lee, J. Han, Mitochondrial Nucleoid: Shield and Switch of the Mitochondrial Genome. Oxidative Medicine and Cellular Longevity 2017, 1-15 (2017).

13. C. Kukat et al., Super-resolution microscopy reveals that mammalian mitochondrial nucleoids have a uniform size and frequently contain a single copy of mtDNA. Proceedings of the National Academy of Sciences 108, 13534-13539 (2011).

14. B. A. Kaufman et al., The Mitochondrial Transcription Factor TFAM Coordinates the Assembly of Multiple DNA Molecules into Nucleoid-like Structures. Molecular Biology of the Cell 18, 3225-3236 (2007).

15. C. Brüser, J. Keller-Findeisen, S. Jakobs, The TFAM-to-mtDNA ratio defines inner-cellular nucleoid populations with distinct activity levels. Cell Reports 37 (2021).

16. Y. Wang, D. F. Bogenhagen, Human Mitochondrial DNA Nucleoids Are Linked to Protein Folding Machinery and Metabolic Enzymes at the Mitochondrial Inner Membrane. Journal of Biological Chemistry 281, 25791-25802 (2006).

17. N. Rajala, J. M. Gerhold, P. Martinsson, A. Klymov, J. N. Spelbrink, Replication factors transiently associate with mtDNA at the mitochondrial inner membrane to facilitate replication. Nucleic Acids Research 42, 952-967 (2013).

18. P. Kaur et al., Single-molecule level structural dynamics of DNA unwinding by human mitochondrial Twinkle helicase. Journal of Biological Chemistry 295, 5564-5576 (2020).

19. E. A. McKinney, M. T. Oliveira, Replicating animal mitochondrial DNA. Genetics and Molecular Biology 36, 308-315 (2013).

20. T. Yasukawa et al., Replication of vertebrate mitochondrial DNA entails transient ribonucleotide incorporation throughout the lagging strand. The EMBO Journal 25, 5358-5371 (2006).

21. A. Reyes et al., Mitochondrial DNA replication proceeds via a ‘bootlace’ mechanism involving the incorporation of processed transcripts. Nucleic Acids Research 41, 5837-5850 (2013).

22. I. J. Holt, H. E. Lorimer, H. T. Jacobs, Coupled Leading- and Lagging-Strand Synthesis of Mammalian Mitochondrial DNA. Cell 100, 515-524 (2000).

23. D. L. Robberson, H. Kasamatsu, J. Vinograd, Replication of Mitochondrial DNA. Circular Replicative Intermediates in Mouse L Cells. Proceedings of the National Academy of Sciences 69, 737-741 (1972).

24. T. Yasukawa, D. Kang, An overview of mammalian mitochondrial DNA replication mechanisms. The Journal of Biochemistry 164, 183-193 (2018).

25. T. J. Nicholls et al., Topoisomerase 3α Is Required for Decatenation and Segregation of Human mtDNA. Molecular Cell 69, 9-23.e26 (2018).

26. M. Falkenberg, Mitochondrial DNA replication in mammalian cells: overview of the pathway. Essays in Biochemistry 62, 287-296 (2018).

27. T. Rey et al., Mitochondrial RNA granules are fluid condensates positioned by membrane dynamics. Nature Cell Biology 22, 1180-1186 (2020).

28. V. J. Xavier, J.-C. Martinou, RNA Granules in the Mitochondria and Their Organization under Mitochondrial Stresses. International Journal of Molecular Sciences 22 (2021).

29. Aaron R. D'Souza, M. Minczuk, Mitochondrial transcription and translation: overview. Essays in Biochemistry 62, 309-320 (2018).

30. C. Osman, T. R. Noriega, V. Okreglak, J. C. Fung, P. Walter, Integrity of the yeast mitochondrial genome, but not its distribution and inheritance, relies on mitochondrial fission and fusion. Proceedings of the National Academy of Sciences 112, E947-E956 (2015).

31. J. Tauber et al., Distribution of mitochondrial nucleoids upon mitochondrial network fragmentation and network reintegration in HEPG2 cells. The International Journal of Biochemistry & Cell Biology 45, 593-603 (2013).

32. T. Sasaki, Y. Sato, T. Higashiyama, N. Sasaki, Live imaging reveals the dynamics and regulation of mitochondrial nucleoids during the cell cycle in Fucci2-HeLa cells. Scientific Reports 7 (2017).

33. J. Qin et al., ER-mitochondria contacts promote mtDNA nucleoids active transportation via mitochondrial dynamic tubulation. Nature Communications 11 (2020).

34. A. Reyes et al., Actin and myosin contribute to mammalian mitochondrial DNA maintenance. Nucleic Acids Research 39, 5098-5108 (2011).

35. C.-T. Chen, Y.-R. V. Shih, T. K. Kuo, O. K. Lee, Y.-H. Wei, Coordinated Changes of Mitochondrial Biogenesis and Antioxidant Enzymes During Osteogenic Differentiation of Human Mesenchymal Stem Cells. Stem Cells 26, 960-968 (2008).

36. W. Zhou et al., HIF1α induced switch from bivalent to exclusively glycolytic metabolism during ESC-to-EpiSC/hESC transition. The EMBO Journal 31, 2103-2116 (2012).

37. M. Khacho et al., Mitochondrial Dynamics Impacts Stem Cell Identity and Fate Decisions by Regulating a Nuclear Transcriptional Program. Cell Stem Cell 19, 232-247 (2016).

38. Z. Li, K.-I. Okamoto, Y. Hayashi, M. Sheng, The Importance of Dendritic Mitochondria in the Morphogenesis and Plasticity of Spines and Synapses. Cell 119, 873-887 (2004).

39. S. Campello et al., Orchestration of lymphocyte chemotaxis by mitochondrial dynamics. Journal of Experimental Medicine 203, 2879-2886 (2006).

40. H. M. Cho, W. Sun, Molecular cross talk among the components of the regulatory machinery of mitochondrial structure and quality control. Experimental & Molecular Medicine 52, 730-737 (2020).

41. M. Ouellet, G. Guillebaud, V. Gervais, D. Lupien St-Pierre, M. Germain, A novel algorithm identifies stress-induced alterations in mitochondrial connectivity and inner membrane structure from confocal images. PLOS Computational Biology 13 (2017).

42. H. Chen et al., Mitofusins Mfn1 and Mfn2 coordinately regulate mitochondrial fusion and are essential for embryonic development. The Journal of cell biology 160, 189-200 (2003).

43. Z. Song, H. Chen, M. Fiket, C. Alexander, D. C. Chan, OPA1 processing controls mitochondrial fusion and is regulated by mRNA splicing, membrane potential, and Yme1L. Journal of Cell Biology 178, 749-755 (2007).

44. L. C. Gomes, G. D. Benedetto, L. Scorrano, During autophagy mitochondria elongate, are spared from degradation and sustain cell viability. Nature Cell Biology 13, 589-598 (2011).

45. A. S. Rambold, B. Kostelecky, N. Elia, J. Lippincott-Schwartz, Tubular network formation protects mitochondria from autophagosomal degradation during nutrient starvation. Proceedings of the National Academy of Sciences 108, 10190-10195 (2011).

46. E. Smirnova, L. Griparic, D.-L. Shurland, A. M. van der Bliek, T. D. Pollard, Dynamin-related Protein Drp1 Is Required for Mitochondrial Division in Mammalian Cells. Molecular Biology of the Cell 12, 2245-2256 (2001).

47. T. Shutt, M. Geoffrion, R. Milne, H. M. McBride, The intracellular redox state is a core determinant of mitochondrial fusion. EMBO reports 13, 909-915 (2012).

48. R. Sabouny et al., The Keap1–Nrf2 Stress Response Pathway Promotes Mitochondrial Hyperfusion Through Degradation of the Mitochondrial Fission Protein Drp1. Antioxidants & Redox Signaling 27, 1447-1459 (2017).

49. D. Tondera et al., SLP-2 is required for stress-induced mitochondrial hyperfusion. The EMBO Journal 28, 1589-1600 (2009).

50. A. J. A. Molina et al., Mitochondrial Networking Protects β-Cells From Nutrient-Induced Apoptosis. Diabetes 58, 2303-2315 (2009).

51. J. Ježek, K. Cooper, R. Strich, Reactive Oxygen Species and Mitochondrial Dynamics: The Yin and Yang of Mitochondrial Dysfunction and Cancer Progression. Antioxidants 7 (2018).

52. R. Ban-Ishihara, T. Ishihara, N. Sasaki, K. Mihara, N. Ishihara, Dynamics of nucleoid structure regulated by mitochondrial fission contributes to cristae reformation and release of cytochrome c. Proceedings of the National Academy of Sciences of the United States of America 110, 11863-11868 (2013).

53. D. G. Breckenridge, M. Stojanovic, R. C. Marcellus, G. C. Shore, Caspase cleavage product of BAP31 induces mitochondrial fission through endoplasmic reticulum calcium signals, enhancing cytochrome c release to the cytosol. Journal of Cell Biology 160, 1115-1127 (2003).

54. M.-H. Schuler et al., Miro1-mediated mitochondrial positioning shapes intracellular energy gradients required for cell migration. Molecular Biology of the Cell 28, 2159-2169 (2017).

55. S. L. Mironov, ADP Regulates Movements of Mitochondria in Neurons. Biophysical Journal 92, 2944-2952 (2007).

56. A. F. MacAskill et al., Miro1 Is a Calcium Sensor for Glutamate Receptor-Dependent Localization of Mitochondria at Synapses. Neuron 61, 541-555 (2009).

57. T. L. Stephen et al., Miro1 Regulates Activity-Driven Positioning of Mitochondria within Astrocytic Processes Apposed to Synapses to Regulate Intracellular Calcium Signaling. Journal of Neuroscience 35, 15996-16011 (2015).

58. G. López-Doménech et al., Miro proteins coordinate microtubule- and actin-dependent mitochondrial transport and distribution. The EMBO Journal 37, 321-336 (2018).

59. M. van Spronsen et al., TRAK/Milton Motor-Adaptor Proteins Steer Mitochondrial Trafficking to Axons and Dendrites. Neuron 77, 485-502 (2013).

60. J.-S. Kang et al., Docking of Axonal Mitochondria by Syntaphilin Controls Their Mobility and Affects Short-Term Facilitation. Cell 132, 137-148 (2008).

61. N. Ohno et al., Mitochondrial immobilization mediated by syntaphilin facilitates survival of demyelinated axons. Proceedings of the National Academy of Sciences 111, 9953-9958 (2014).

62. M. Shah, L. A. Chacko, J. P. Joseph, V. Ananthanarayanan, Mitochondrial dynamics, positioning and function mediated by cytoskeletal interactions. Cellular and Molecular Life Sciences 78, 3969-3986 (2021).

63. I. R. Boldogh et al., Arp2/3 complex and actin dynamics are required for actin-based mitochondrial motility in yeast. Proceedings of the National Academy of Sciences 98, 3162-3167 (2001).

64. K. L. Fehrenbacher, H.-C. Yang, A. C. Gay, T. M. Huckaba, L. A. Pon, Live Cell Imaging of Mitochondrial Movement along Actin Cables in Budding Yeast. Current Biology 14, 1996-2004 (2004).

65. O. A. Quintero et al., Human Myo19 Is a Novel Myosin that Associates with Mitochondria. Current Biology 19, 2008-2013 (2009).

66. J. L. Bocanegra et al., The MyMOMA domain of MYO19 encodes for distinct Miro-dependent and Miro-independent mechanisms of interaction with mitochondrial membranes. Cytoskeleton 77, 149-166 (2020).

67. B. I. Shneyer, M. Usaj, A. Henn, Myo19 is an Outer Mitochondrial Membrane Motor and Effector of Starvation Induced Filopodia. Journal of Cell Science (2015).

68. D. Pathak, K. J. Sepp, P. J. Hollenbeck, Evidence That Myosin Activity Opposes Microtubule-Based Axonal Transport of Mitochondria. Journal of Neuroscience 30, 8984-8992 (2010).

69. S. Li et al., Transient assembly of F-actin on the outer mitochondrial membrane contributes to mitochondrial fission. Journal of Cell Biology 208, 109-123 (2015).

70. A. Pagliuso et al., A role for septin 2 in Drp1-mediated mitochondrial fission. EMBO reports 17, 858-873 (2016).

71. K. Rehklau et al., Cofilin1-dependent actin dynamics control DRP1-mediated mitochondrial fission. Cell Death & Disease 8, e3063-e3063 (2017).

72. Ho L. Tang et al., Vimentin supports mitochondrial morphology and organization. Biochemical Journal 410, 141-146 (2008).

73. D. J. Milner, M. Mavroidis, N. Weisleder, Y. Capetanaki, Desmin cytoskeleton linked to muscle mitochondrial distribution and respiratory function. The Journal of cell biology 150, 1283-1298 (2000).

74. S. Reipert, Association of Mitochondria with Plectin and Desmin Intermediate Filaments in Striated Muscle. Experimental Cell Research 252, 479-491 (1999).

75. T. Yardeni et al., High content image analysis reveals function of miR-124 upstream of Vimentin in regulating motor neuron mitochondria. Scientific Reports 8 (2018).

76. B. J. Gentil et al., Normal role of the low-molecular-weight neurofilament protein in mitochondrial dynamics and disruption in Charcot-Marie-Tooth disease. The FASEB Journal 26, 1194-1203 (2011).

77. W. Bernhard, C. Rouiller, Close Topographical Relationship between Mitochondria and Ergastoplasm of Liver Cells in a Definite Phase of Cellular Activity. The Journal of Biophysical and Biochemical Cytology 2, 73-78 (1956).

78. X. Huang, C. Jiang, L. Yu, A. Yang, Current and Emerging Approaches for Studying Inter-Organelle Membrane Contact Sites. Frontiers in Cell and Developmental Biology 8 (2020).

79. M. Rossini, P. Pizzo, R. Filadi, Better to keep in touch: investigating inter-organelle cross-talk. The FEBS Journal 288, 740-755 (2020).

80. R. G. Abrisch, S. C. Gumbin, B. T. Wisniewski, L. L. Lackner, G. K. Voeltz, Fission and fusion machineries converge at ER contact sites to regulate mitochondrial morphology. Journal of Cell Biology 219 (2020).

81. Y. C. Wong, D. Ysselstein, D. Krainc, Mitochondria-lysosome contacts regulate mitochondrial fission via RAB7 GTP hydrolysis. Nature 554, 382-386 (2018).

82. T. Kleele et al., Distinct fission signatures predict mitochondrial degradation or biogenesis. Nature 593, 435-439 (2021).

83. S. Nagashima et al., Golgi-derived PI (4) P-containing vesicles drive late steps of mitochondrial division. Science 367, 1366-1371 (2020).

84. A. Misko, S. Jiang, I. Wegorzewska, J. Milbrandt, R. H. Baloh, Mitofusin 2 Is Necessary for Transport of Axonal Mitochondria and Interacts with the Miro/Milton Complex. Journal of Neuroscience 30, 4232-4240 (2010).

85. X. Liu, D. Weaver, O. Shirihai, G. Hajnóczky, Mitochondrial 'kiss-and-run': interplay between mitochondrial motility and fusion–fission dynamics. The EMBO Journal 28, 3074-3089 (2009).

86. T. Ishihara et al., Dynamics of mitochondrial DNA nucleoids regulated by mitochondrial fission is essential for maintenance of homogeneously active mitochondria during neonatal heart development. Molecular and cellular biology 35, 211-223 (2015).

87. H. Chen, J. M. McCaffery, D. C. Chan, Mitochondrial fusion protects against neurodegeneration in the cerebellum. Cell 130, 548-562 (2007).

88. H. Chen et al., Mitochondrial Fusion Is Required for mtDNA Stability in Skeletal Muscle and Tolerance of mtDNA Mutations. Cell 141, 280-289 (2010).

89. E. Silva Ramos et al., Mitochondrial fusion is required for regulation of mitochondrial DNA replication. PLOS Genetics 15 (2019).

90. R. Ban-Ishihara, T. Ishihara, N. Sasaki, K. Mihara, N. Ishihara, Dynamics of nucleoid structure regulated by mitochondrial fission contributes to cristae reformation and release of cytochrome c. Proceedings of the National Academy of Sciences 110, 11863-11868 (2013).

91. N. Ishihara, T. Ishihara, A. Ota, Mitochondrial nucleoid morphology and respiratory function are altered in Drp1-deficient HeLa cells. The Journal of Biochemistry 167, 287-294 (2020).

92. C. T. Chu, Mechanisms of selective autophagy and mitophagy: Implications for neurodegenerative diseases. Neurobiology of disease 122, 23-34 (2019).

93. A. Tanaka et al., Proteasome and p97 mediate mitophagy and degradation of mitofusins induced by Parkin. The Journal of cell biology 191, 1367-1380 (2010).

94. N. C. Chan et al., Broad activation of the ubiquitin-proteasome system by Parkin is critical for mitophagy. Hum Mol Genet 20, 1726-1737 (2011).

95. E. Ziviani, R. N. Tao, A. J. Whitworth, Drosophila parkin requires PINK1 for mitochondrial translocation and ubiquitinates mitofusin. Proceedings of the National Academy of Sciences of the United States of America 107, 5018-5023 (2010).

96. G. Twig et al., Fission and selective fusion govern mitochondrial segregation and elimination by autophagy. EMBO J 27, 433-446 (2008).

97. N. Ishihara, Y. Fujita, T. Oka, K. Mihara, Regulation of mitochondrial morphology through proteolytic cleavage of OPA1. EMBO J 25, 2966-2977 (2006).

98. S. Hoppins et al., The Soluble Form of Bax Regulates Mitochondrial Fusion via MFN2 Homotypic Complexes. Molecular Cell 41, 150-160 (2011).

99. T. Koshiba et al., Structural Basis of Mitochondrial Tethering by Mitofusin Complexes. Science 305, 858-862 (2004).

100. T. Brandt, L. Cavellini, W. Kühlbrandt, M. M. Cohen, A mitofusin-dependent docking ring complex triggers mitochondrial fusion in vitro. eLife 5 (2016).

101. F. Daste et al., The heptad repeat domain 1 of Mitofusin has membrane destabilization function in mitochondrial fusion. EMBO reports 19 (2018).

102. S. Mattie, J. Riemer, J. G. Wideman, H. M. McBride, A new mitofusin topology places the redox-regulated C terminus in the mitochondrial intermembrane space. Journal of Cell Biology 217, 507-515 (2018).

103. C. Delettre et al., Mutation spectrum and splicing variants in the OPA1 gene. Human Genetics 109, 584-591 (2001).

104. A. Olichon et al., The human dynamin-related protein OPA1 is anchored to the mitochondrial inner membrane facing the inter-membrane space. FEBS Letters 523, 171-176 (2002).

105. B. Head, L. Griparic, M. Amiri, S. Gandre-Babbe, A. M. van der Bliek, Inducible proteolytic inactivation of OPA1 mediated by the OMA1 protease in mammalian cells. Journal of Cell Biology 187, 959-966 (2009).

106. S. Ehses et al., Regulation of OPA1 processing and mitochondrial fusion by m-AAA protease isoenzymes and OMA1. Journal of Cell Biology 187, 1023-1036 (2009).

107. L. Griparic, T. Kanazawa, A. M. van der Bliek, Regulation of the mitochondrial dynamin-like protein Opa1 by proteolytic cleavage. Journal of Cell Biology 178, 757-764 (2007).

108. R. Anand et al., The i-AAA protease YME1L and OMA1 cleave OPA1 to balance mitochondrial fusion and fission. Journal of Cell Biology 204, 919-929 (2014).

109. Z. Song et al., Mitofusins and OPA1 Mediate Sequential Steps in Mitochondrial Membrane Fusion. Molecular Biology of the Cell 20, 3525-3532 (2009).

110. T. Ban et al., Molecular basis of selective mitochondrial fusion by heterotypic action between OPA1 and cardiolipin. Nature Cell Biology 19, 856-863 (2017).

111. K. Pfeiffer et al., Cardiolipin Stabilizes Respiratory Chain Supercomplexes. Journal of Biological Chemistry 278, 52873-52880 (2003).

112. H. Rampelt et al., Assembly of the Mitochondrial Cristae Organizer Mic10 Is Regulated by Mic26–Mic27 Antagonism and Cardiolipin. Journal of Molecular Biology 430, 1883-1890 (2018).

113. D. Ardail et al., Mitochondrial contact sites. Lipid composition and dynamics. Journal of Biological Chemistry 265, 18797-18802 (1990).

114. S. Cogliati et al., Mitochondrial Cristae Shape Determines Respiratory Chain Supercomplexes Assembly and Respiratory Efficiency. Cell 155, 160-171 (2013).

115. C. Fröhlich et al., Structural insights into oligomerization and mitochondrial remodelling of dynamin 1-like protein. The EMBO Journal 32, 1280-1292 (2013).

116. S. Gandre-Babbe, A. M. van der Bliek, J. Shaw, The Novel Tail-anchored Membrane Protein Mff Controls Mitochondrial and Peroxisomal Fission in Mammalian Cells. Molecular Biology of the Cell 19, 2402-2412 (2008).

117. C. S. Palmer et al., MiD49 and MiD51, new components of the mitochondrial fission machinery. EMBO reports 12, 565-573 (2011).

118. C. S. Palmer et al., Adaptor Proteins MiD49 and MiD51 Can Act Independently of Mff and Fis1 in Drp1 Recruitment and Are Specific for Mitochondrial Fission. Journal of Biological Chemistry 288, 27584-27593 (2013).

119. O. C. Losón, Z. Song, H. Chen, D. C. Chan, D. D. Newmeyer, Fis1, Mff, MiD49, and MiD51 mediate Drp1 recruitment in mitochondrial fission. Molecular Biology of the Cell 24, 659-667 (2013).

120. H. Otera et al., Mff is an essential factor for mitochondrial recruitment of Drp1 during mitochondrial fission in mammalian cells. Journal of Cell Biology 191, 1141-1158 (2010).

121. L. D. Osellame et al., Cooperative and independent roles of Drp1 adaptors Mff and MiD49/51 in mitochondrial fission. Journal of Cell Science (2016).

122. J. Zhao et al., Human MIEF1 recruits Drp1 to mitochondrial outer membranes and promotes mitochondrial fusion rather than fission. The EMBO Journal 30, 2762-2778 (2011).

123. R. Kalia et al., Structural basis of mitochondrial receptor binding and constriction by DRP1. Nature 558, 401-405 (2018).

124. R. Yu, S. B. Jin, U. Lendahl, M. Nistér, J. Zhao, Human Fis1 regulates mitochondrial dynamics through inhibition of the fusion machinery. The EMBO Journal 38 (2019).

125. L. C. Gomes, L. Scorrano, High levels of Fis1, a pro-fission mitochondrial protein, trigger autophagy. Biochimica et Biophysica Acta (BBA) - Bioenergetics 1777, 860-866 (2008).

126. X. Qi et al., Aberrant mitochondrial fission in neurons induced by protein kinase Cδ under oxidative stress conditions in vivo. Molecular Biology of the Cell 22, 256-265 (2011).

127. X.-J. Han et al., CaM kinase Iα–induced phosphorylation of Drp1 regulates mitochondrial morphology. Journal of Cell Biology 182, 573-585 (2008).

128. Jennifer A. Kashatus et al., Erk2 Phosphorylation of Drp1 Promotes Mitochondrial Fission and MAPK-Driven Tumor Growth. Molecular Cell 57, 537-551 (2015).

129. N. Taguchi, N. Ishihara, A. Jofuku, T. Oka, K. Mihara, Mitotic Phosphorylation of Dynamin-related GTPase Drp1 Participates in Mitochondrial Fission. Journal of Biological Chemistry 282, 11521-11529 (2007).

130. C.-R. Chang, C. Blackstone, Cyclic AMP-dependent Protein Kinase Phosphorylation of Drp1 Regulates Its GTPase Activity and Mitochondrial Morphology. Journal of Biological Chemistry 282, 21583-21587 (2007).

131. D. Chandra et al., GSK3beta-Mediated Drp1 Phosphorylation Induced Elongated Mitochondrial Morphology against Oxidative Stress. PLoS ONE 7 (2012).

132. R. Yonashiro et al., A novel mitochondrial ubiquitin ligase plays a critical role in mitochondrial dynamics. The EMBO Journal 25, 3618-3626 (2006).

133. M. Karbowski, A. Neutzner, R. J. Youle, The mitochondrial E3 ubiquitin ligase MARCH5 is required for Drp1 dependent mitochondrial division. Journal of Cell Biology 178, 71-84 (2007).

134. Y.-Y. Park et al., Loss of MARCH5 mitochondrial E3 ubiquitin ligase induces cellular senescence through dynamin-related protein 1 and mitofusin 1. Journal of Cell Science 123, 619-626 (2010).

135. S. Wasiak, R. Zunino, H. M. McBride, Bax/Bak promote sumoylation of DRP1 and its stable association with mitochondria during apoptotic cell death. Journal of Cell Biology 177, 439-450 (2007).

136. E. Braschi, R. Zunino, H. M. McBride, MAPL is a new mitochondrial SUMO E3 ligase that regulates mitochondrial fission. EMBO reports 10, 748-754 (2009).

137. Z. Harder, R. Zunino, H. McBride, Sumo1 Conjugates Mitochondrial Substrates and Participates in Mitochondrial Fission. Current Biology 14, 340-345 (2004).

138. R. Zunino, A. Schauss, P. Rippstein, M. Andrade-Navarro, H. M. McBride, The SUMO protease SENP5 is required to maintain mitochondrial morphology and function. Journal of Cell Science 120, 1178-1188 (2007).

139. T. Gawlowski et al., Modulation of Dynamin-related Protein 1 (DRP1) Function by Increased O-linked-β-N-acetylglucosamine Modification (O-GlcNAc) in Cardiac Myocytes. Journal of Biological Chemistry 287, 30024-30034 (2012).

140. D.-H. Cho et al., S-Nitrosylation of Drp1 Mediates β-Amyloid-Related Mitochondrial Fission and Neuronal Injury. Science 324, 102-105 (2009).

141. J. R. Friedman et al., ER Tubules Mark Sites of Mitochondrial Division. Science 334, 358-362 (2011).

142. F. Korobova, V. Ramabhadran, H. N. Higgs, An Actin-Dependent Step in Mitochondrial Fission Mediated by the ER-Associated Formin INF2. Science 339, 464-467 (2013).

143. U. Manor et al., A mitochondria-anchored isoform of the actin-nucleating spire protein regulates mitochondrial division. eLife 4 (2015).

144. D. Mahecic et al., Mitochondrial membrane tension governs fission. Cell Reports 35 (2021).

145. M. Vicente-Manzanares, X. Ma, R. S. Adelstein, A. R. Horwitz, Non-muscle myosin II takes centre stage in cell adhesion and migration. Nature reviews. Molecular cell biology 10, 778-790 (2009).

146. F. Korobova, Timothy J. Gauvin, Henry N. Higgs, A Role for Myosin II in Mammalian Mitochondrial Fission. Current Biology 24, 409-414 (2014).

147. W. Almutawa et al., The R941L mutation in MYH14 disrupts mitochondrial fission and associates with peripheral neuropathy. EBioMedicine 45, 379-392 (2019).

148. Y. C. Wong, D. Ysselstein, D. Krainc, Mitochondria–lysosome contacts regulate mitochondrial fission via RAB7 GTP hydrolysis. Nature 554, 382-386 (2018).

149. B. Cho et al., Constriction of the mitochondrial inner compartment is a priming event for mitochondrial division. Nature Communications 8 (2017).

150. R. Chakrabarti et al., INF2-mediated actin polymerization at the ER stimulates mitochondrial calcium uptake, inner membrane constriction, and division. Journal of Cell Biology 217, 251-268 (2018).

151. S. C. Kamerkar, F. Kraus, A. J. Sharpe, T. J. Pucadyil, M. T. Ryan, Dynamin-related protein 1 has membrane constricting and severing abilities sufficient for mitochondrial and peroxisomal fission. Nature Communications 9 (2018).

152. J. R. Jimah, J. E. Hinshaw, Structural Insights into the Mechanism of Dynamin Superfamily Proteins. Trends in Cell Biology 29, 257-273 (2019).

153. J. E. Lee, L. M. Westrate, H. Wu, C. Page, G. K. Voeltz, Multiple dynamin family members collaborate to drive mitochondrial division. Nature 540, 139-143 (2016).

154. T. B. Fonseca, Á. Sánchez-Guerrero, I. Milosevic, N. Raimundo, Mitochondrial fission requires DRP1 but not dynamins. Nature 570, E34-E42 (2019).

155. A. Godi et al., ARF mediates recruitment of PtdIns-4-OH kinase-β and stimulates synthesis of PtdIns(4,5)P2 on the Golgi complex. Nature Cell Biology 1, 280-287 (1999).

156. E. Rosivatz, R. Woscholski, Removal or masking of phosphatidylinositol(4,5)bisphosphate from the outer mitochondrial membrane causes mitochondrial fragmentation. Cellular Signalling 23, 478-486 (2011).

157. L.-C. Tábara, J. L. Morris, J. Prudent, The Complex Dance of Organelles during Mitochondrial Division. Trends in Cell Biology 31, 241-253 (2021).

158. C. Delettre et al., Nuclear gene OPA1, encoding a mitochondrial dynamin-related protein, is mutated in dominant optic atrophy. Nature Genetics 26, 207-210 (2000).

159. C. Alexander et al., OPA1, encoding a dynamin-related GTPase, is mutated in autosomal dominant optic atrophy linked to chromosome 3q28. Nature Genetics 26, 211-215 (2000).

160. G. Hudson et al., Mutation of OPA1 causes dominant optic atrophy with external ophthalmoplegia, ataxia, deafness and multiple mitochondrial DNA deletions: a novel disorder of mtDNA maintenance. Brain 131, 329-337 (2008).

161. P. Amati-Bonneau et al., OPA1 mutations induce mitochondrial DNA instability and optic atrophy 'plus' phenotypes. Brain 131, 338-351 (2008).

162. K. Kijima et al., Mitochondrial GTPase mitofusin 2 mutation in Charcot?Marie?Tooth neuropathy type 2A. Human Genetics 116, 23-27 (2004).

163. S. Züchner et al., Mutations in the mitochondrial GTPase mitofusin 2 cause Charcot-Marie-Tooth neuropathy type 2A. Nature Genetics 36, 449-451 (2004).

164. C. Rouzier et al., The MFN2 gene is responsible for mitochondrial DNA instability and optic atrophy 'plus' phenotype. Brain 135, 23-34 (2011).

165. S. Vielhaber et al., Mitofusin 2 mutations affect mitochondrial function by mitochondrial DNA depletion. Acta Neuropathologica 125, 245-256 (2012).

166. R. H. Baloh, R. E. Schmidt, A. Pestronk, J. Milbrandt, Altered Axonal Mitochondrial Transport in the Pathogenesis of Charcot-Marie-Tooth Disease from Mitofusin 2 Mutations. Journal of Neuroscience 27, 422-430 (2007).

167. M. N. Serasinghe, J. E. Chipuk, in Pharmacology of Mitochondria. (2016), Chapter 38, pp. 159-188.

168. N. Keller et al., De novo DNM1L variant presenting with severe muscular atrophy, dystonia and sensory neuropathy. European Journal of Medical Genetics 64 (2021).

169. B. N. Whitley et al., Aberrant Drp1-mediated mitochondrial division presents in humans with variable outcomes. Human Molecular Genetics 27, 3710-3719 (2018).

170. F. Longo et al., Impaired turnover of hyperfused mitochondria in severe axonal neuropathy due to a novel DRP1 mutation. Human Molecular Genetics 29, 177-188 (2020).

171. D. Verrigni et al., Clinical-genetic features and peculiar muscle histopathology in infantile DNM1L-related mitochondrial epileptic encephalopathy. Human Mutation 40, 601-618 (2019).

172. K. A. Hogarth, S. R. Costford, G. Yoon, N. Sondheimer, J. T. Maynes, DNM1L Variant Alters Baseline Mitochondrial Function and Response to Stress in a Patient with Severe Neurological Dysfunction. Biochemical Genetics 56, 56-77 (2017).

173. S. Gerber et al., Mutations in DNM1L, as in OPA1, result in dominant optic atrophy despite opposite effects on mitochondrial fusion and fission. Brain 140, 2586-2596 (2017).

174. A. Nasca et al., Biallelic Mutations in DNM1L are Associated with a Slowly Progressive Infantile Encephalopathy. Human Mutation 37, 898-903 (2016).

175. G. Yoon et al., Lethal Disorder of Mitochondrial Fission Caused by Mutations in DNM1L. The Journal of Pediatrics 171, 313-316.e312 (2016).

176. Y.-H. Chao et al., Missense variants in the middle domain ofDNM1Lin cases of infantile encephalopathy alter peroxisomes and mitochondria when assayed inDrosophila. Human Molecular Genetics 25, 1846-1856 (2016).

177. K. Zaha et al., DNM1L -related encephalopathy in infancy with Leigh syndrome-like phenotype and suppression-burst. Clinical Genetics 90, 472-474 (2016).

178. J. A. Fahrner, R. Liu, M. S. Perry, J. Klein, D. C. Chan, A novel de novo dominant negative mutation inDNM1Limpairs mitochondrial fission and presents as childhood epileptic encephalopathy. American Journal of Medical Genetics Part A 170, 2002-2011 (2016).

179. J. R. Vanstone et al., DNM1L-related mitochondrial fission defect presenting as refractory epilepsy. European Journal of Human Genetics 24, 1084-1088 (2015).

180. H. Díez et al., Severe infantile parkinsonism because of a de novo mutation on DLP1 mitochondrial-peroxisomal protein. Movement Disorders 32, 1108-1110 (2017).

181. R. Sheffer et al., Postnatal microcephaly and pain insensitivity due to a de novo heterozygousDNM1Lmutation causing impaired mitochondrial fission and function. American Journal of Medical Genetics Part A 170, 1603-1607 (2016).

182. Y. Wei, M. Qian, Case Report: A Novel de novo Mutation in DNM1L Presenting With Developmental Delay, Ataxia, and Peripheral Neuropathy. Frontiers in Pediatrics 9 (2021).

183. N. Assia Batzir et al., De novo missense variant in the GTPase effector domain (GED) of DNM1L leads to static encephalopathy and seizures. Molecular Case Studies 5 (2019).

184. A. Nasca et al., Clinical and Biochemical Features in a Patient With Mitochondrial Fission Factor Gene Alteration. Frontiers in Genetics 9 (2018).

185. H. E. Shamseldin et al., Genomic analysis of mitochondrial diseases in a consanguineous population reveals novel candidate disease genes. Journal of Medical Genetics 49, 234-241 (2012).

186. J. Koch et al., Disturbed mitochondrial and peroxisomal dynamics due to loss of MFF causes Leigh-like encephalopathy, optic atrophy and peripheral neuropathy. Journal of Medical Genetics 53, 270-278 (2016).

187. I. Panda et al., Encephalopathy due to defective mitochondrial and peroxisomal fission 2 caused by a novel MFF gene mutation in a young child. Clinical Genetics 97, 933-937 (2020).

188. M. Charif et al., Dominant mutations in MIEF1 affect mitochondrial dynamics and cause a singular late onset optic neuropathy. Molecular Neurodegeneration 16 (2021).

189. F. Donaudy et al., Nonmuscle Myosin Heavy-Chain Gene MYH14 Is Expressed in Cochlea and Mutated in Patients Affected by Autosomal Dominant Hearing Impairment (DFNA4). The American Journal of Human Genetics 74, 770-776 (2004).

190. K.-Y. Kim, M. Kovács, S. Kawamoto, J. R. Sellers, R. S. Adelstein, Disease-associated Mutations and Alternative Splicing Alter the Enzymatic and Motile Activity of Nonmuscle Myosins II-B and II-C. Journal of Biological Chemistry 280, 22769-22775 (2005).

191. J. Wakabayashi et al., The dynamin-related GTPase Drp1 is required for embryonic and brain development in mice. Journal of Cell Biology 186, 805-816 (2009).

192. N. Ishihara et al., Mitochondrial fission factor Drp1 is essential for embryonic development and synapse formation in mice. Nature Cell Biology 11, 958-966 (2009).

193. Y. Kageyama et al., Mitochondrial division ensures the survival of postmitotic neurons by suppressing oxidative damage. Journal of Cell Biology 197, 535-551 (2012).

194. M. Suntharalingam, S. R. Wente, Peering through the Pore: Nuclear Pore Complex Structure, Assembly, and Function. Developmental Cell 4, 775-789 (2003).

195. Y. Shibata et al., Mechanisms Determining the Morphology of the Peripheral ER. Cell 143, 774-788 (2010).

196. M. Puhka, H. Vihinen, M. Joensuu, E. Jokitalo, Endoplasmic reticulum remains continuous and undergoes sheet-to-tubule transformation during cell division in mammalian cells. Journal of Cell Biology 179, 895-909 (2007).

197. P. Benyamini, P. Webster, D. I. Meyer, J. E. Gruenberg, Knockdown of p180 Eliminates the Terminal Differentiation of a Secretory Cell Line. Molecular Biology of the Cell 20, 732-744 (2009).

198. G. K. Voeltz, W. A. Prinz, Y. Shibata, J. M. Rist, T. A. Rapoport, A Class of Membrane Proteins Shaping the Tubular Endoplasmic Reticulum. Cell 124, 573-586 (2006).

199. E. Kiseleva, K. N. Morozova, G. K. Voeltz, T. D. Allen, M. W. Goldberg, Reticulon 4a/NogoA locates to regions of high membrane curvature and may have a role in nuclear envelope growth. Journal of Structural Biology 160, 224-235 (2007).

200. M. West, N. Zurek, A. Hoenger, G. K. Voeltz, A 3D analysis of yeast ER structure reveals how ER domains are organized by membrane curvature. Journal of Cell Biology 193, 333-346 (2011).

201. J. Hu et al., Membrane Proteins of the Endoplasmic Reticulum Induce High-Curvature Tubules. Science 319, 1247-1250 (2008).

202. G. Orso et al., Homotypic fusion of ER membranes requires the dynamin-like GTPase Atlastin. Nature 460, 978-983 (2009).

203. L. J. Byrnes et al., Structural basis for conformational switching and GTP loading of the large G protein atlastin. The EMBO Journal 32, 369-384 (2013).

204. S. Wang, H. Tukachinsky, F. B. Romano, T. A. Rapoport, Cooperation of the ER-shaping proteins atlastin, lunapark, and reticulons to generate a tubular membrane network. eLife 5 (2016).

205. S. Chen, P. Novick, S. Ferro-Novick, ER network formation requires a balance of the dynamin-like GTPase Sey1p and the Lunapark family member Lnp1p. Nature Cell Biology 14, 707-716 (2012).

206. Y. Adachi et al., Drp1 Tubulates the ER in a GTPase-Independent Manner. Molecular Cell 80, 621-632.e626 (2020).

207. C. M. Waterman-Storer, E. D. Salmon, Endoplasmic reticulum membrane tubules are distributed by microtubules in living cells using three distinct mechanisms. Current Biology 8, 798-807 (1998).

208. I. Grigoriev et al., STIM1 Is a MT-Plus-End-Tracking Protein Involved in Remodeling of the ER. Current Biology 18, 177-182 (2008).

209. M. J. Woźniak et al., Role of kinesin-1 and cytoplasmic dynein in endoplasmic reticulum movement in VERO cells. Journal of Cell Science 122, 1979-1989 (2009).

210. C. Lee, L. B. Chen, Dynamic behavior of endoplasmic reticulum in living cells. Cell 54, 37-46 (1988).

211. A. R. English, G. K. Voeltz, Rab10 GTPase regulates ER dynamics and morphology. Nature Cell Biology 15, 169-178 (2012).

212. W. K. Subczynski, M. Pasenkiewicz-Gierula, J. Widomska, L. Mainali, M. Raguz, High Cholesterol/Low Cholesterol: Effects in Biological Membranes: A Review. Cell Biochemistry and Biophysics 75, 369-385 (2017).

213. R. Galmes et al., ORP5/ORP8 localize to endoplasmic reticulum–mitochondria contacts and are involved in mitochondrial function. EMBO reports 17, 800-810 (2016).

214. A. Janer et al., SLC25A46 is required for mitochondrial lipid homeostasis and cristae maintenance and is responsible for Leigh syndrome. EMBO Molecular Medicine 8, 1019-1038 (2016).

215. J. E. Vance, Phospholipid synthesis in a membrane fraction associated with mitochondria. The Journal of biological chemistry 265, 7248-7256 (1990).

216. C. Osman, D. R. Voelker, T. Langer, Making heads or tails of phospholipids in mitochondria. Journal of Cell Biology 192, 7-16 (2011).

217. M. Fujimoto, T. Hayashi, T.-P. Su, The role of cholesterol in the association of endoplasmic reticulum membranes with mitochondria. Biochemical and Biophysical Research Communications 417, 635-639 (2012).

218. A. Sala-Vila et al., Interplay between hepatic mitochondria-associated membranes, lipid metabolism and caveolin-1 in mice. Scientific Reports 6 (2016).

219. R. M. Denton, Regulation of mitochondrial dehydrogenases by calcium ions. Biochimica et Biophysica Acta (BBA) - Bioenergetics 1787, 1309-1316 (2009).

220. M. Giacomello et al., Ca2+ Hot Spots on the Mitochondrial Surface Are Generated by Ca2+ Mobilization from Stores, but Not by Activation of Store-Operated Ca2+ Channels. Molecular Cell 38, 280-290 (2010).

221. E. Rapizzi et al., Recombinant expression of the voltage-dependent anion channel enhances the transfer of Ca2+ microdomains to mitochondria. Journal of Cell Biology 159, 613-624 (2002).

222. J. M. Baughman et al., Integrative genomics identifies MCU as an essential component of the mitochondrial calcium uniporter. Nature 476, 341-345 (2011).

223. D. De Stefani, A. Raffaello, E. Teardo, I. Szabò, R. Rizzuto, A forty-kilodalton protein of the inner membrane is the mitochondrial calcium uniporter. Nature 476, 336-340 (2011).

224. D. De Stefani et al., VDAC1 selectively transfers apoptotic Ca2+ signals to mitochondria. Cell Death & Differentiation 19, 267-273 (2011).

225. C. C. P. Mendes et al., The Type III Inositol 1,4,5-Trisphosphate Receptor Preferentially Transmits Apoptotic Ca2+ Signals into Mitochondria. Journal of Biological Chemistry 280, 40892-40900 (2005).

226. S. C. Lewis, L. F. Uchiyama, J. Nunnari, ER-mitochondria contacts couple mtDNA synthesis with mitochondrial division in human cells. Science 353 (2016).

227. O. M. de Brito, L. Scorrano, Mitofusin 2 tethers endoplasmic reticulum to mitochondria. Nature 456, 605-610 (2008).

228. N. S. Leal et al., Mitofusin-2 knockdown increases ER-mitochondria contact and decreases amyloid β-peptide production. Journal of Cellular and Molecular Medicine 20, 1686-1695 (2016).

229. D. Naon et al., Critical reappraisal confirms that Mitofusin 2 is an endoplasmic reticulum–mitochondria tether. Proceedings of the National Academy of Sciences 113, 11249-11254 (2016).

230. D. F. Montisano, J. Cascarano, C. B. Pickett, T. W. James, Association between mitochondria and rough endoplasmic reticulum in rat liver. The Anatomical Record 203, 441-450 (1982).

231. G. r. Csordás et al., Structural and functional features and significance of the physical linkage between ER and mitochondria. Journal of Cell Biology 174, 915-921 (2006).

232. P. T. C. Wang et al., Distinct mechanisms controlling rough and smooth endoplasmic reticulum-mitochondria contacts. Journal of Cell Science (2015).

233. V. Zinzalla, D. Stracka, W. Oppliger, Michael N. Hall, Activation of mTORC2 by Association with the Ribosome. Cell 144, 757-768 (2011).

234. C. Betz et al., mTOR complex 2-Akt signaling at mitochondria-associated endoplasmic reticulum membranes (MAM) regulates mitochondrial physiology. Proceedings of the National Academy of Sciences 110, 12526-12534 (2013).

235. V. Hung et al., Proteomic mapping of cytosol-facing outer mitochondrial and ER membranes in living human cells by proximity biotinylation. eLife 6 (2017).

236. I. Anastasia et al., Mitochondria-rough-ER contacts in the liver regulate systemic lipid homeostasis. Cell Reports 34 (2021).

237. S. Fang et al., The tumor autocrine motility factor receptor, gp78, is a ubiquitin protein ligase implicated in degradation from the endoplasmic reticulum. Proceedings of the National Academy of Sciences 98, 14422-14427 (2001).

238. M. Fu et al., Regulation of mitophagy by the Gp78 E3 ubiquitin ligase. Molecular Biology of the Cell 24, 1153-1162 (2013).

239. J. Shankar et al., Raft endocytosis of autocrine motility factor regulates mitochondrial dynamics via rac1 signaling and the gp78 ubiquitin ligase. Journal of Cell Science (2013).

240. R. Filadi et al., Mitofusin 2 ablation increases endoplasmic reticulum–mitochondria coupling. Proceedings of the National Academy of Sciences 112, E2174-E2181 (2015).

241. F. G. van der Goot, P. Cosson, A. Marchetti, M. Ravazzola, L. Orci, Mitofusin-2 Independent Juxtaposition of Endoplasmic Reticulum and Mitochondria: An Ultrastructural Study. PLoS ONE 7 (2012).

242. A. K. K. Lakkaraju et al., Palmitoylated calnexin is a key component of the ribosome-translocon complex. The EMBO Journal 31, 1823-1835 (2012).

243. E. M. Lynes et al., Palmitoylated TMX and calnexin target to the mitochondria-associated membrane. The EMBO Journal 31, 457-470 (2012).

244. X. Xie, T. Venit, N. Drou, P. Percipalle, In Mitochondria β-Actin Regulates mtDNA Transcription and Is Required for Mitochondrial Quality Control. iScience 3, 226-237 (2018).

245. J. Villanueva et al., The distribution of mitochondria and endoplasmic reticulum in relation with secretory sites in chromaffin cells. Journal of Cell Science (2014).

246. T. J. Collins, Mitochondria are morphologically and functionally heterogeneous within cells. The EMBO Journal 21, 1616-1627 (2002).

247. X. Lu, P. N. Thai, S. Lu, J. Pu, D. M. Bers, Intrafibrillar and perinuclear mitochondrial heterogeneity in adult cardiac myocytes. Journal of Molecular and Cellular Cardiology 136, 72-84 (2019).

248. A. F. Davis, D. A. Clayton, In situ localization of mitochondrial DNA replication in intact mammalian cells. Journal of Cell Biology 135, 883-893 (1996).

249. R. A. Schultz et al., Differential Expression of Mitochondrial DNA Replication Factors in Mammalian Tissues. Journal of Biological Chemistry 273, 3447-3451 (1998).

250. C. A. Albus et al., Mitochondrial Translation Occurs Preferentially in the Peri-Nuclear Mitochondrial Network of Cultured Human Cells. Biology 10 (2021).

251. J. Magnusson, Replication of mitochondrial DNA occurs throughout the mitochondria of cultured human cells. Experimental Cell Research 289, 133-142 (2003).

252. C. Wang et al., Dynamic tubulation of mitochondria drives mitochondrial network formation. Cell Research 25, 1108-1120 (2015).

253. W.-K. Ji et al., Receptor-mediated Drp1 oligomerization on endoplasmic reticulum. Journal of Cell Biology 216, 4123-4139 (2017).

254. Y. Yoon, K. R. Pitts, S. Dahan, M. A. McNiven, A Novel Dynamin-like Protein Associates with Cytoplasmic Vesicles and Tubules of the Endoplasmic Reticulum in Mammalian Cells. Journal of Cell Biology 140, 779-793 (1998).

255. T. Shemesh et al., A model for the generation and interconversion of ER morphologies. Proceedings of the National Academy of Sciences 111 (2014).

256. M. Terasaki et al., Stacked Endoplasmic Reticulum Sheets Are Connected by Helicoidal Membrane Motifs. Cell 154, 285-296 (2013).

257. M. Puhka et al., Progressive sheet-to-tubule transformation is a general mechanism for endoplasmic reticulum partitioning in dividing mammalian cells. Molecular Biology of the Cell 23, 2424-2432 (2012).

258. P. V. Bashkirov et al., GTPase Cycle of Dynamin Is Coupled to Membrane Squeeze and Release, Leading to Spontaneous Fission. Cell 135, 1276-1286 (2008).

259. B. Marks et al., GTPase activity of dynamin and resulting conformation change are essential for endocytosis. Nature 410, 231-235 (2001).

260. B. Ugarte-Uribe, H.-M. Müller, M. Otsuki, W. Nickel, A. J. García-Sáez, Dynamin-related Protein 1 (Drp1) Promotes Structural Intermediates of Membrane Division. Journal of Biological Chemistry 289, 30645-30656 (2014).

261. S. Peralta et al., ATAD3 controls mitochondrial cristae structure, influencing mtDNA replication and cholesterol levels in muscle. Journal of Cell Science (2018).

262. R. Desai et al., ATAD3 gene cluster deletions cause cerebellar dysfunction associated with altered mitochondrial DNA and cholesterol metabolism. Brain 140, 1595-1610 (2017).

263. L. A. Luévano-Martínez, M. F. Forni, V. T. dos Santos, N. C. Souza-Pinto, A. J. Kowaltowski, Cardiolipin is a key determinant for mtDNA stability and segregation during mitochondrial stress. Biochimica et Biophysica Acta (BBA) - Bioenergetics 1847, 587-598 (2015).

264. J. M. Gerhold et al., Human Mitochondrial DNA-Protein Complexes Attach to a Cholesterol-Rich Membrane Structure. Scientific Reports 5 (2015).